

ES - 2106

ORNL-5129

The Reactions of Atmospheric Vapors with Lunar Soil

**E. L. Fuller, Jr.
P. A. Agron**

MASTER

BLANK PAGE

Printed in the United States of America. Available from
National Technical Information Service
U.S. Department of Commerce
5285 Port Royal Road, Springfield, Virginia 22161
Price: Printed Copy \$5.00; Microfiche \$2.25

This report was prepared as an account of work sponsored by the United States Government. Neither the United States nor the Energy Research and Development Administration, nor any of their employees, nor any of their contractors, subcontractors, or their employees, makes any warranty, express or implied, or assumes any legal liability or responsibility for the accuracy, completeness or usefulness of any information, apparatus, product or process disclosed, or represents that its use would not infringe privately owned rights.

ORNL-5129
UC-34b

Contract No. W-7405-eng-26

THE REACTIONS OF ATMOSPHERIC VAPORS WITH LUNAR SOIL*

E. L. Fuller, Jr. and P. A. Agron

**Chemistry Division
Oak Ridge National Laboratory
Oak Ridge, Tennessee 37830**

***Research sponsored by NASA under Union Carbide contract with the
Energy Research and Development Administration.**

**By acceptance of this article, the publisher or recipient acknowledges
the U. S. Government's right to retain a non-exclusive, royalty-free
license in and to any copyright covering the article.**

MARCH 1976

**OAK RIDGE NATIONAL LABORATORY
Oak Ridge, Tennessee 37830
operated by
UNION CARBIDE CORPORATION
for the
ENERGY RESEARCH AND DEVELOPMENT ADMINISTRATION**

CONTENTS

	Page
Abstract	1
Part I Reactions of an Apollo 14 Sample	2
A. Introduction	2
B. Experimental Approach	3
C. Results and Discussion	3
C.1 Vapor Sorption on Original Samples	3
C.2 Reaction with Sorbed Water	6
C.3 Nitrogen Adsorption	14
C.4 Weight Loss on Outgassing and Sintering	23
C.5 Interrelation	23
D. Conclusion	28
E. Summary	32
F. References	34
Part II Geochemical Aspects of Lunar Soil Weathering	36
References	43
Part III Simulated Weathering of Volcanic Soil	53
References	73
Acknowledgements	74

v

LIST OF FIGURES

PART I

	Page
Figure 1 Adsorption on 14003.....	4
Figure 2 Vapor Sorption on Original 14003 Sample.....	5
Figure 3 Vapor Sorption on 14003 at -196°C.....	7
Figure 4 Adsorption Energy Related to Polarizability (14003)..	8
Figure 4a Polarization Effects of 14003.....	9
Figure 5 Sorption Energy Relations for 14003.....	10
Figure 6 Water Sorption by 14003 at 22.00°C.....	11
Figure 7 Retention of H ₂ O on 14003 at 22.00°C.....	12
Figure 8 H ₂ O Sorption on 14003 at 22.00°C.....	13
Figure 9 Nitrogen Sorption by 14003 at -196°C.....	15
Figure 10 Nitrogen Sorption (77°K) by 14003.....	16
Figure 11 Nitrogen Sorption on 14003 at -196°C.....	18
Figure 12 Nitrogen Sorption on 14003 at -196°C.....	19
Figure 13 Nitrogen Sorption on 14003 at -196°C.....	20
Figure 14 Nitrogen Sorption on 14003 at -196°C.....	21
Figure 15 Nitrogen Sorption on 14003 at -196°C.....	22
Figure 16 Vacuum Weight of 14003.....	24
Figure 17 Surface Properties of 14003.....	25
Figure 18 Dehydration of 14003.....	26
Figure 19 Surface Properties of 14003.....	27
Figure 20 Surface Properties of 14003 (Rehydration at 22.00°C)..	31
Figure 21 Temperature Effects for Lunar and Analogous Materials	33

PART III

Figure 1 Vapor Displacement by Aluminum Billet.....	54
Figure 2 Nitrogen on Aluminum Pellet.....	56
Figure 3 Helium Displacement.....	57
Figure 4 Helium on BSG33 at -196°C.....	58
Figure 5 Nitrogen Vapor on 63321 at -196°C.....	60
Figure 6 Nitrogen Interaction with BSG33 at -196°C (after H ₂ O).....	61
Figure 7 Nitrogen Sorption by BSG33 at -196°C.....	62
Figure 8 Nitrogen Adsorption on BSG33 at -196°C.....	63
Figure 9 Nitrogen Sorption by BSG33.....	65
Figure 10 Nitrogen Sorption on BSG33.....	66
Figure 11 Steady State Vacuum Weight of BSG33.....	67
Figure 12 Sorptive Properties of BSG33.....	68
Figure 13 H ₂ O (No. 11) on BSG33 at 22.00°C.....	69
Figure 14 Slow Sorption of H ₂ O by BSG33 at 22.00°C.....	71
Figure 15 Kinetic Parameters for Water Sorption on BSG33.....	72

ABSTRACT

Detailed experimental data have been acquired for the hydration of the surfaces of lunar fines. Inert vapor adsorption has been employed to measure the surface properties (surface energy, surface area, porosity, etc.) and changes wrought in the hydration-dehydration processes. Plausible mechanisms have been considered and the predominant process involves hydration of the metamict metallosilicate surfaces to form a hydrated lamina structure akin to terrestrial clays. Additional credence for this interpretation is obtained by comparison to existing geochemical literature concerning terrestrial weathering of primary metallosilicates. The surface properties of the hydrated lunar fines is compared favorably to those of terrestrial clay minerals. In addition, experimental results are given to show that fresh disordered surfaces of volcanic sand react with water vapor in a manner virtually identical to the majority of the lunar fines. The results show that ion track etching and/or grain boundary attack are minor contributions in the weathering of lunar fines in the realm of our microgravimetric experimental conditions.

BLANK PAGE

PART I REACTIONS OF AN APOLLO 14 SAMPLE

A. INTRODUCTION

Lunar materials react with the water and carbon dioxide of the terrestrial atmosphere^(1,2). The mechanism is somewhat ill-defined at present. This study was undertaken to obtain more details concerning the nature of the hydration processes which occur as the metamict surfaces are attacked. Specifically, we hoped to delineate between the three plausible mechanisms of (1) ion track etching⁽¹⁾, (2) metallosilicate hydration⁽²⁾ and/or (3) grain boundary attack⁽³⁾.

Mechanism (1) has been postulated as induced by water migration along the small channels of ion tracks, with subsequent countercurrent etching of larger chambers in the inner reaches of the bulk material, forming an "ink bottle" shaped pore. Presumably the "leached" material migrates to the surface and is rather uniformly distributed thereupon. The entrance channels are presumably blocked by bound water which can exclude inert vapors from the inner chambers. This bound water can be removed by stringent outgassing to permit access to inert vapors.

Mechanism (2) has been forwarded as being akin to the hydration of primary terrestrial minerals (metallosilicates) to form laminar (clay like) hydrated metallosilicates from the edges, amorphous outer surfaces of the particles. The pores are envisioned as the voids between the laminae which are formed as the hydration water is removed at elevated temperatures.

Mechanism (3) was presented as involving the grain boundaries inherent in the particles. Water presumably migrates down these boundaries allowing the primary sub-units (crystallites) to separate with a simultaneous release of strain energy. It is difficult to associate this mechanism with the observation that the bound water reversibly excludes inert vapors from the inner reaches of the sample as noted previously^(1,2) and in this work. Pores formed by this process should be "open" (orifices greater than inner dimensions).

We chose an Apollo 14 sample (14003-60) as being generally characteristic of lunar fine samples in terms of its chemical composition, mineralogy, glass sphere content, color, etc. Due to the paucity of material we have chosen to perform extensive, controlled microgravimetric analyses. The goal was to study the interrelationship of hydration and carbonation reactions and surface structural analyses (inert vapor adsorption). A detailed analysis of surface area, porosity, surface energy, etc., and changes therein should help measure the relative contributions of the three aforementioned mechanisms.

B. EXPERIMENTAL APPROACH

An aliquot of lunar fines was placed on a microbalance in an adsorption chamber described previously^(4,5) and subjected to the conditions described in the subsequent section. It was used as received, the fraction of a soil sample which passed through a 1 mm sieve. Optical microscopy showed that it was predominantly composed of angular dark fragments 1 to 10 μ m in size. A few translucent spheres of ca 5 to 10 μ m were dispersed in the sample.

Throughout the experimental sequence we have verified steady state data by allowing the sample to equilibrate at given temperatures and pressures for days to weeks when necessary. In the cases where slow processes were in play, we were able to determine the kinetics of the reactions. Various gases were adsorbed on the original material before extensive degassing and/or reaction with water vapor to evaluate the surface properties of the original material. The sample was then subjected to varying degrees of hydration via multiple exposures to water vapor. The gravimetric technique has proven to be quite informative in simultaneously monitoring several pertinent surface properties as anticipated by previous evaluations⁽⁵⁾.

C. RESULTS AND DISCUSSION

C.1 Vapor Sorption on Original Sample

Figure 1 is a graphical presentation of the sorption isotherms (-196°C for all but H_2O which was constructed with a sample temperature of 22.00°C). The general sigmoidal shape is noted in each. Only a small amount of hysteresis is noted at 0.5 to 1.0 P., characteristic of capillary condensation in mesopores whose orifices are smaller or equal to their internal dimensions ($> 20 \text{ \AA}$).

Figure 2 is a more detailed presentation of the same data on a molecular basis. The apparent monolayer is formed more readily (lower P/P.) in the sequence: $\text{H}_2\text{O} > \text{CO} > \text{N}_2 > \text{Ar} > \text{O}_2$. This trend is generally consistent with theories⁽⁶⁾ where the energy of adsorption is related to the polarizability, dipole moment, etc., of the adsorbate. BET analyses⁽⁷⁾ of the data gives apparent monolayer capacities as noted for each sorbate. The mean value, 5.15 μ moles per gram of sample, shows a mean deviation for each of the sorbates of $\approx 0.07 \mu$ moles/gm. However, this constant value is inconsistent for molecules whose theoretical cross-sectional area⁽⁸⁾ ranges from 10.6 \AA^2 /molecule (H_2O) to 16.2 \AA^2 /molecule (N_2). It seems that the amount of adsorption required to form a monolayer (in terms of number of molecules adsorbed) is independent of the chemical or physical properties of the adsorbate. Such behavior is consistent with the concept of site adsorption where the lattice parameters of the substrate are equal to or greater than the dimensions of the adsorbed molecules.

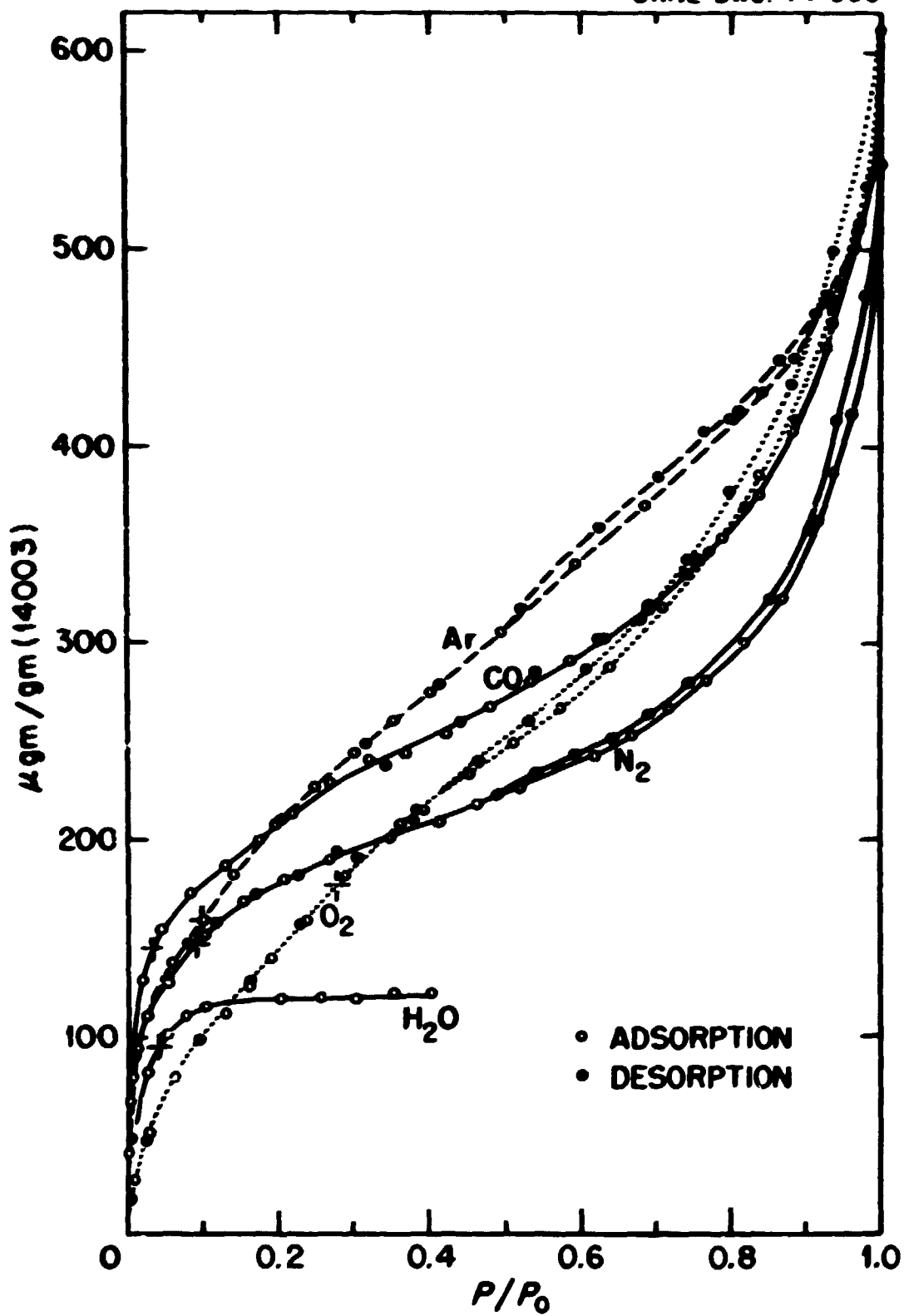


Fig. 1. Adsorption on 14003.

ORNL-DWG. 74-994

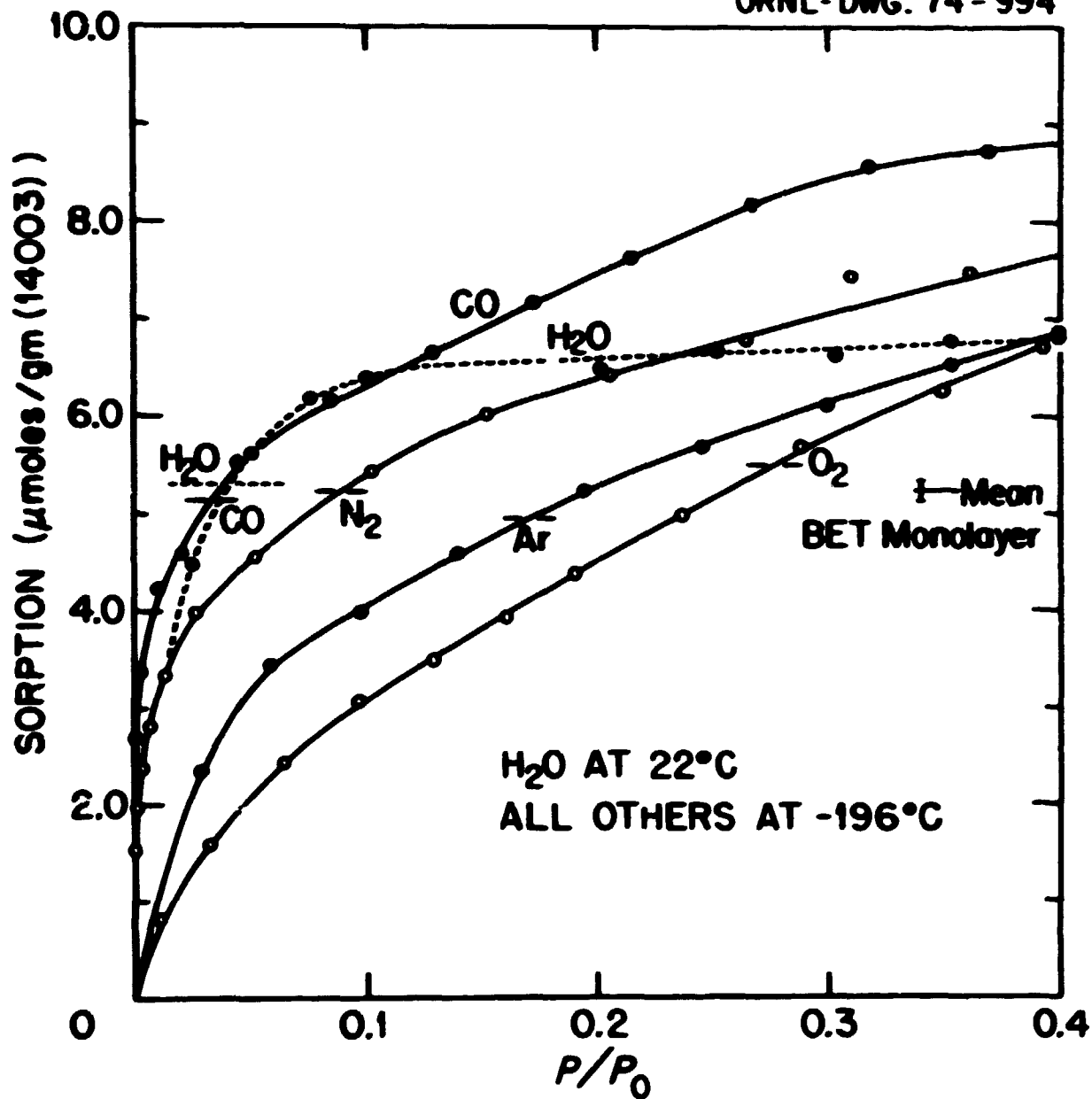


Fig. 2. Vapor sorption on original 14003 sample.

In our attempts to more fully understand the processes we have analyzed our data in terms of several theories of adsorption^(9,10). Figure 3 presents our most successful attempt to linearize our data over the classical "monolayer" region. This expresses the amount of adsorption in terms of the adsorption potential, ϵ as defined by Palonye⁽¹¹⁾

$$\epsilon = - RT \ln F/P. . \quad (1)$$

The functional behavior is given as

$$\epsilon = \epsilon^{\circ} e^{-\delta \Gamma} , \quad (2)$$

with ϵ° as a characteristic free energy for the adsorption of the first molecules on an essentially bare surface. Γ is defined as the surface concentration of adsorbate. The intercepts at $\Gamma = 0$ (Figure 3) allows us to calculate this ϵ° for each sorbate. Equation 2 was originally derived⁽¹²⁾ in terms of the theory of polarization of adsorbate by the electrostatic field that exists at the substrate surface. Each subsequent molecule is adsorbed with a lesser free energy in accordance with the distribution function (Eq. 2). Indeed ϵ° is linearly related to the polarizability⁽¹³⁾ of the sorbate as shown in Figure 4. An equally intriguing relationship relates the free energy term ϵ° to the enthalpy of vaporization of the respective liquid sorbate linearly as shown in Figure 5.

C.2 Reaction with Sorbed Water

Representative water vapor isotherms are given in Figure 6.^(1,2) Initial adsorption at pressures up to 0.4 P_o are characteristically somewhat limited with respect to apparent monolayer capacity and multi-layer formation. Each desorption boundary curve shows hysteresis in the capillary range (0.3 to 1.0 P_o) and marked low pressure and vacuum retention. Each of these isotherms are presented with respect to the vacuum weight of the sample upon completion of the preceding desorption cycle. These incremental vacuum retentions are cumulatively defined as "bound water", $\Gamma (B, H_2O)$ in subsequent discussions. Steady state weights were achieved in ca 5 minutes for pressures less than ca 0.85 P_o. Above this pressure slow, first order processes become predominant and relatively large amounts were adsorbed for each pressure increment.

Excursions to these higher pressures resulted in increasingly greater enhancement of the bound component, $\Gamma (B, H_2O)$ and apparent monolayer capacity, $\Gamma (m, H_2O)$. The nature of the irreversible retention for each of these larger excursions is seen more clearly in Figure 7. Here we have deduced the amount adsorbed, $\Gamma (A)$, from the amount remaining on desorption $\Gamma (D)$ to evaluate the retention $\Delta (P)$ at each pressure. From this we can evaluate the hysteretic concentration, $\Delta (h)$ and retention increment $\Delta (B)$ [$\Gamma (B) = \sum \Delta B$ for successive cycles].

A direct correlation between $\Gamma (m, H_2O)$ and $\Gamma (B, H_2O)$ is noted in Figure 8. The initial adsorption (1 a) is greater than the desorption $\Gamma (m)$ due to the increment of $\Gamma (B)$ involved. Thereafter each desorption

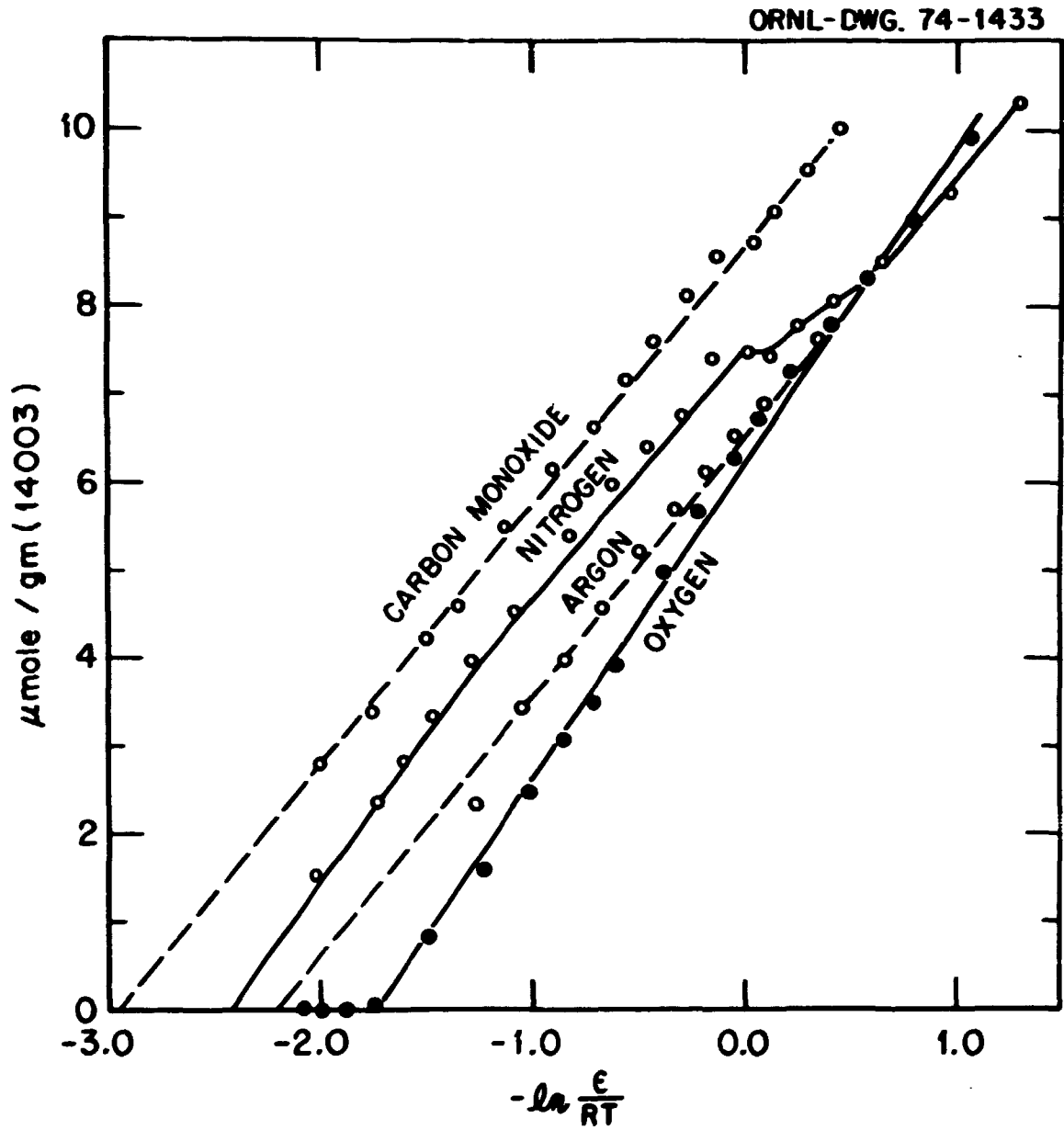


Fig. 3. Vapor sorption on 14003 at -196°C .

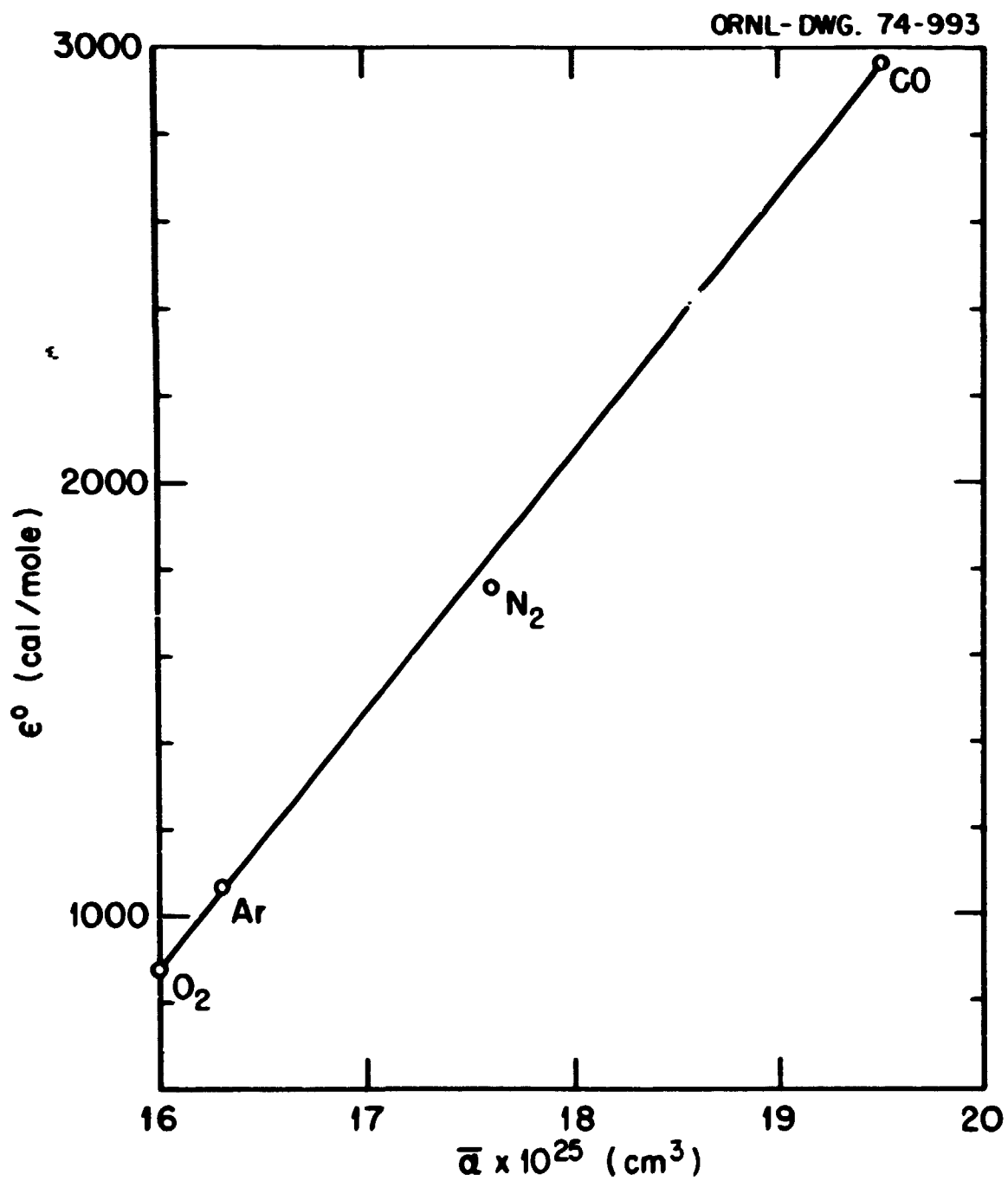


Fig. 4. Adsorption energy related to polarizability (14003).

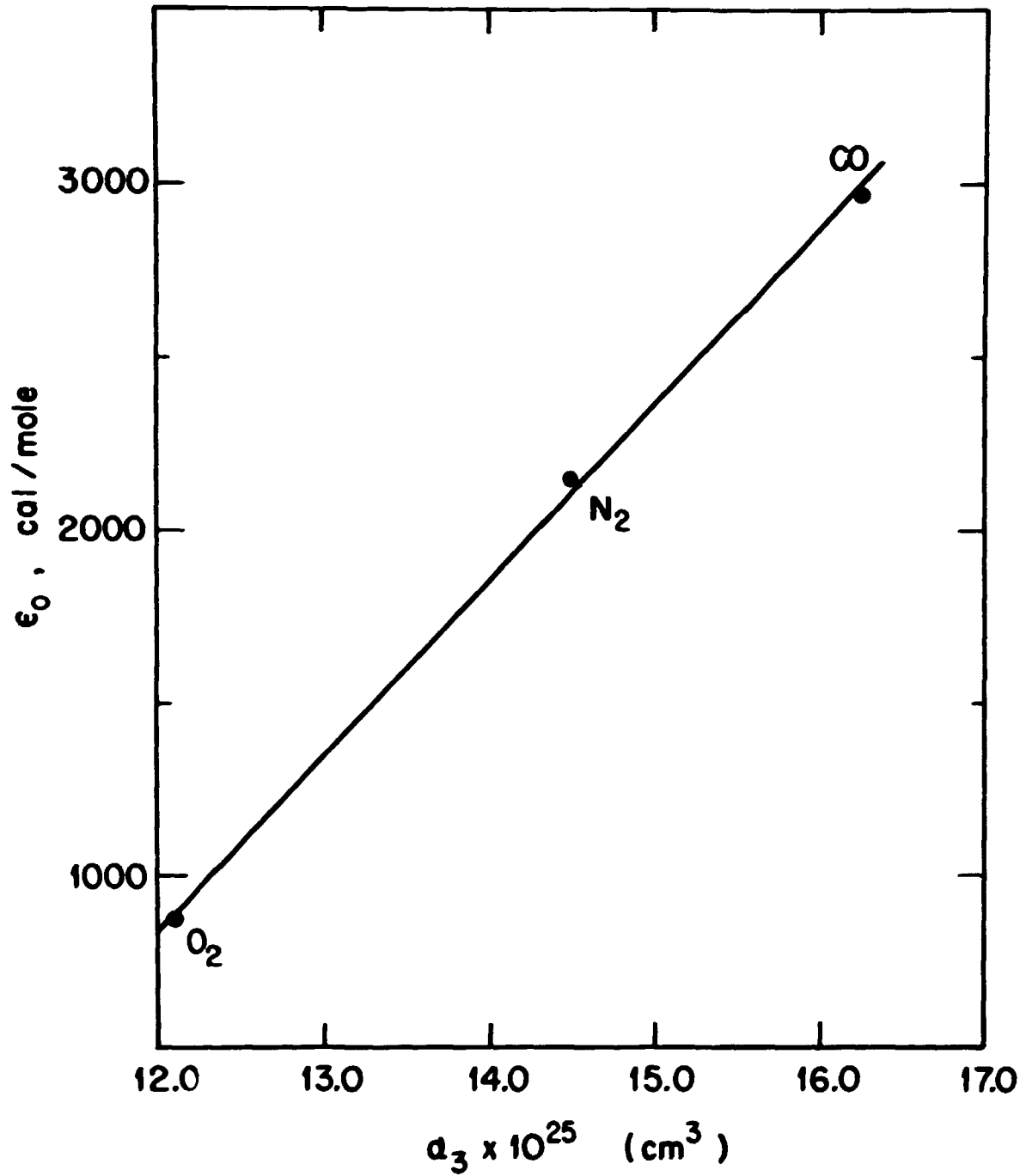


Fig. 4a. Polarization effects of 14003.

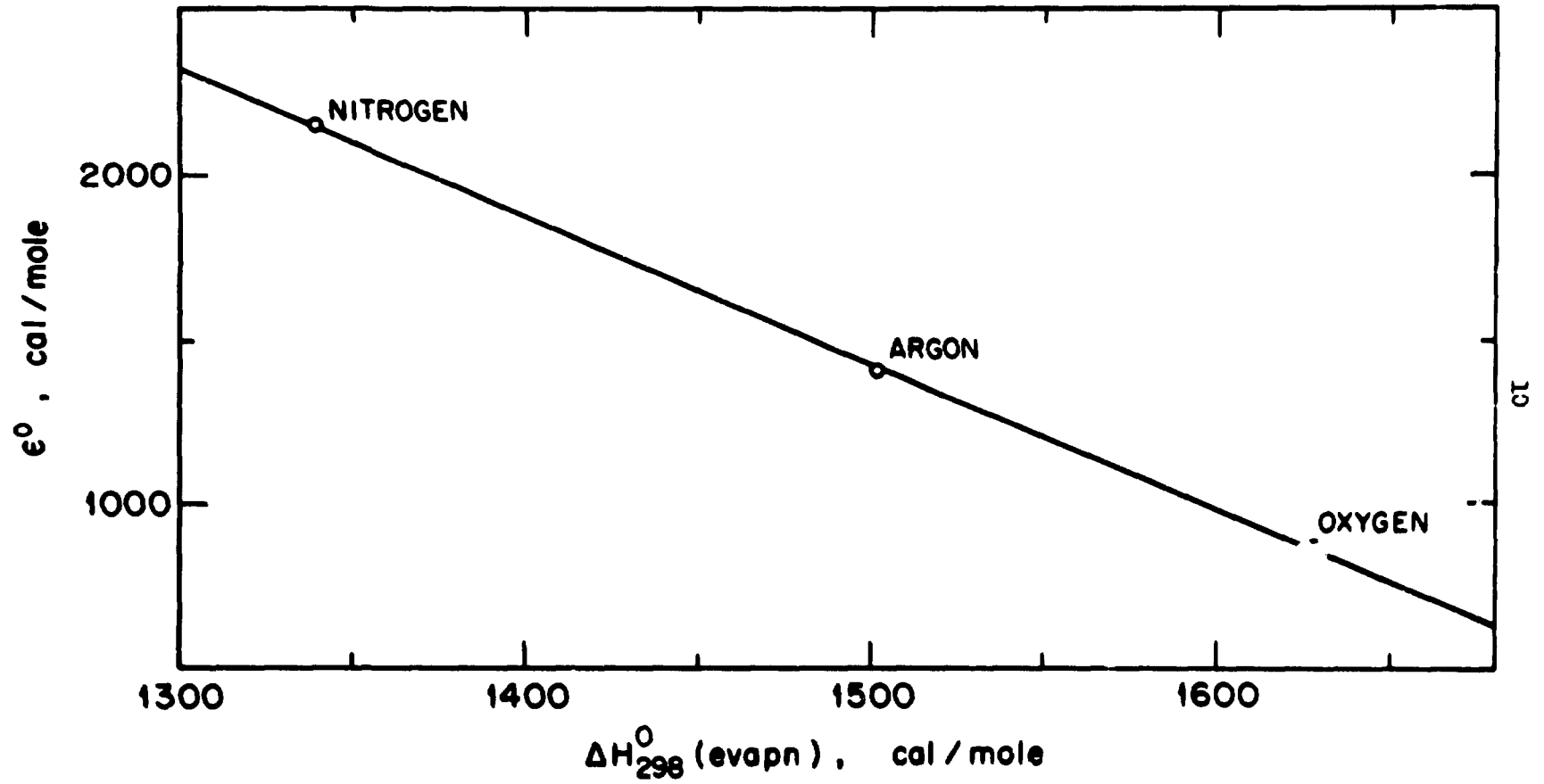


Fig. 5. Sorption energy relations for 14003.

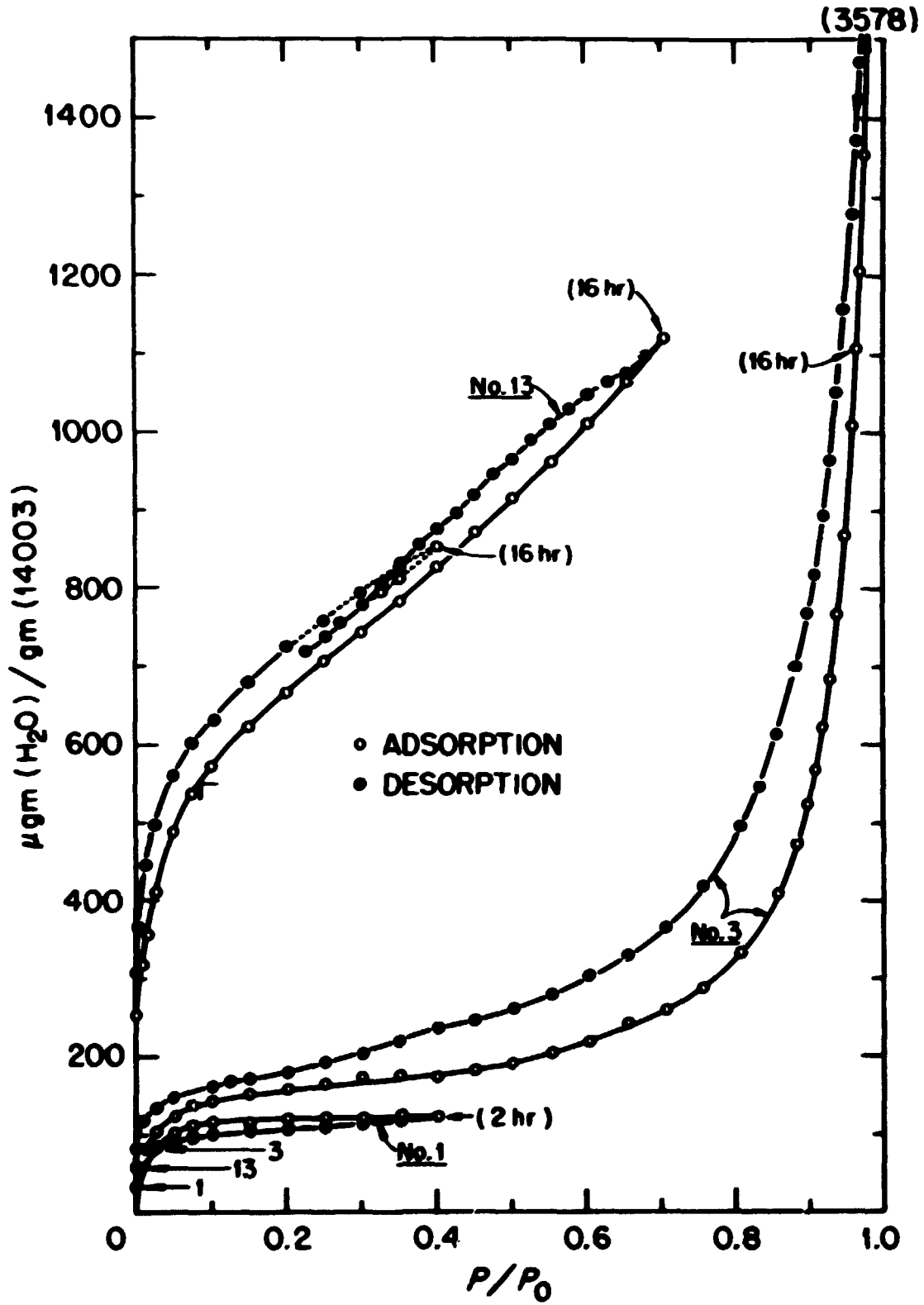
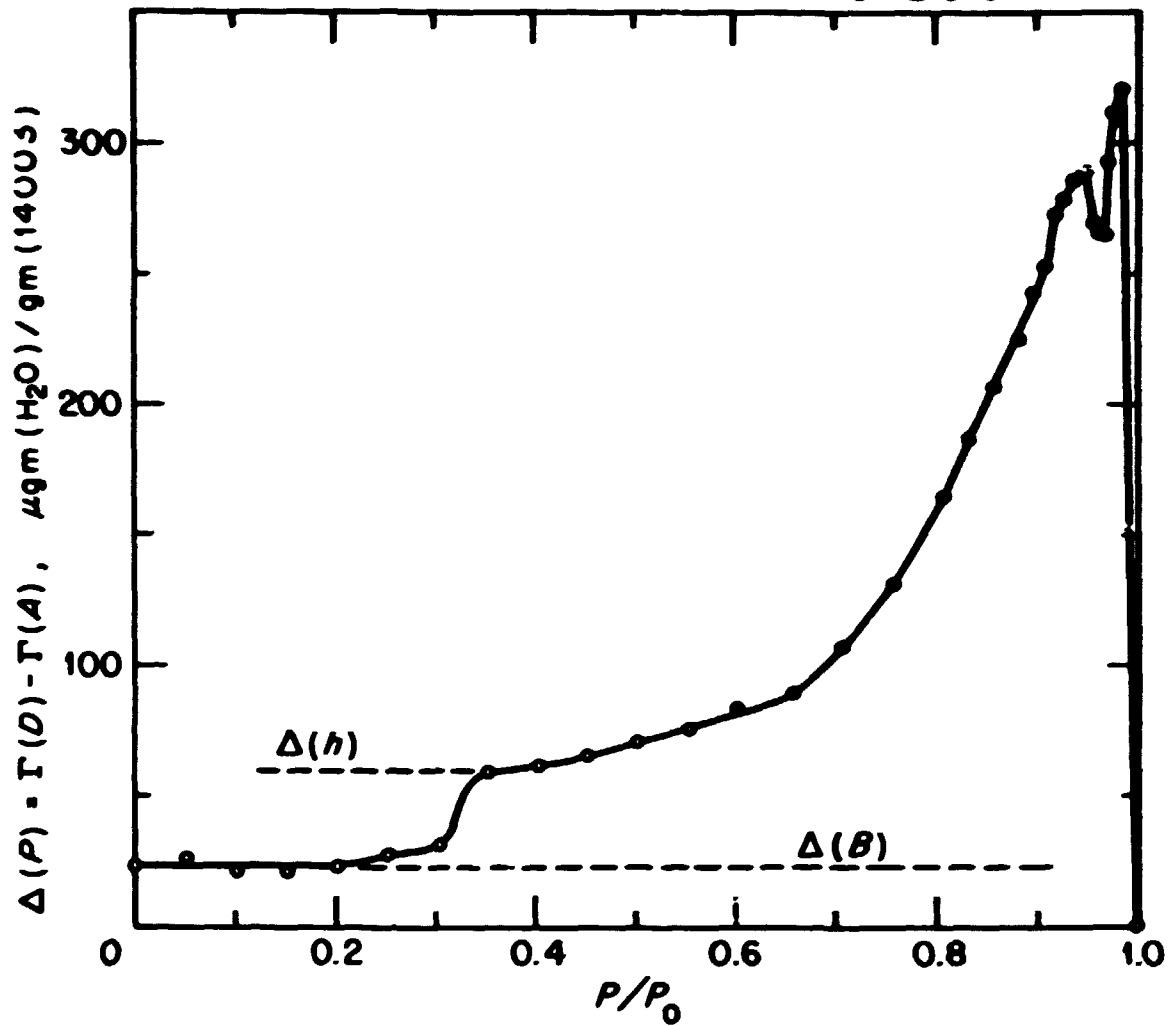


Fig. 6. Water sorption by 14003 at 22.00°C.

ORNL-DWG. 74-999

Fig. 7. Retention of H_2O on 14003 at 22.00°C.

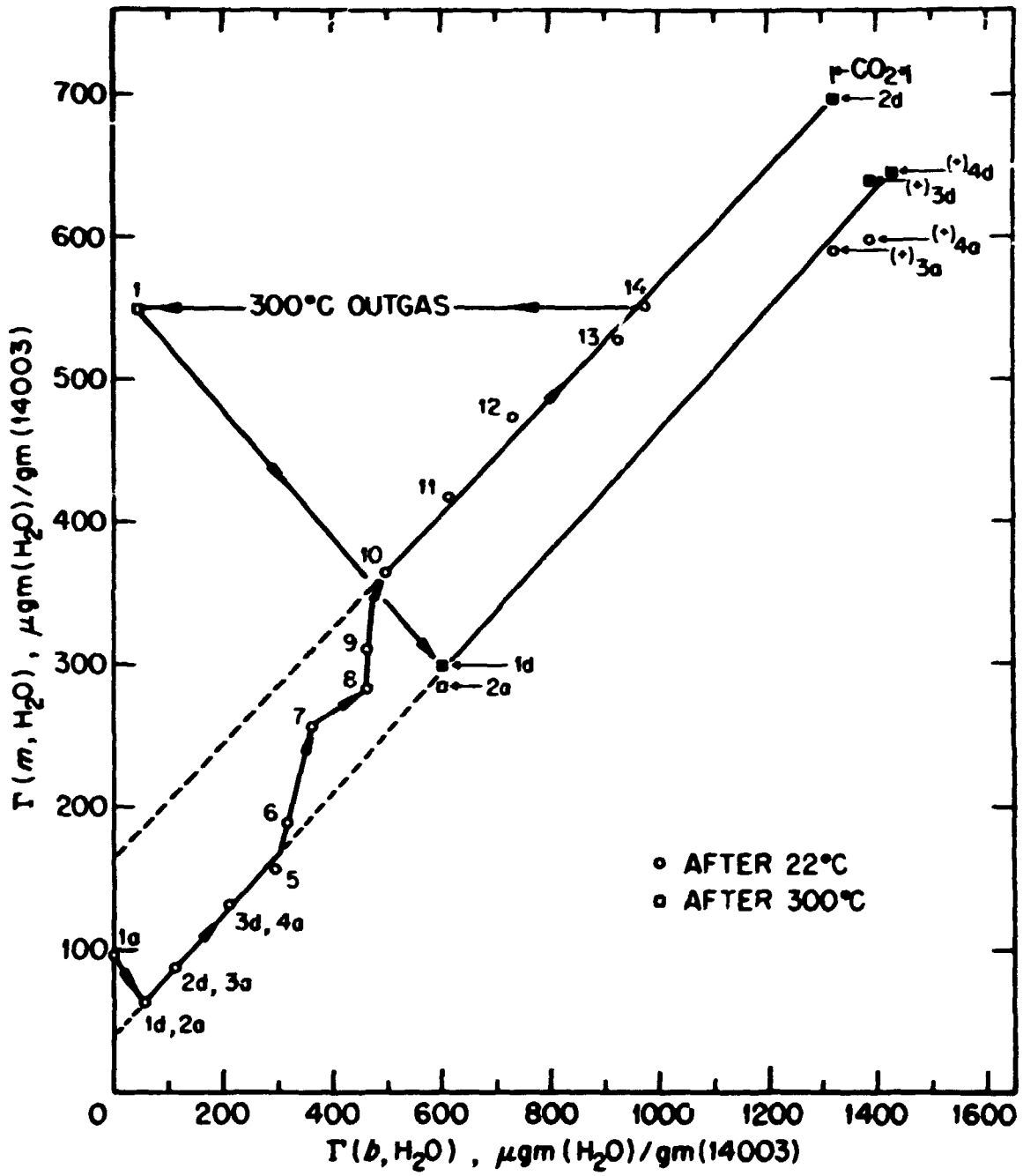


Fig. 8. H₂O sorption on 14003 at 22.00°C.

$\bar{\Gamma}$ (m) and subsequent adsorption $\bar{\Gamma}$ (m) were identical, for each is referred to the same vacuum weight [sample weight plus the respective $\bar{\Gamma}$ (B, H₂O)]. This trend continued for 5 cycles where data was acquired in the closed system mode⁽⁵⁾ (balance chamber connected to a liquid water reservoir whose vapor pressure (temperature) was precisely controlled). In view of the displacement phenomena noted previously⁽²⁾ we subsequently changed to the open mode of isotherm construction. Here we introduced and extracted (discarded) aliquots of water vapor as needed to produce the desired pressure cycles 6 thru 13. Cycle 14 was obtained in the closed mode of operation. The original trend [$\bar{\Gamma}$ (m) increasing with increasing $\bar{\Gamma}$ (B)] is enhanced initially and returns to the original relationship (cycles 10 - 14). Apparently the displaced species (CO₂?) is removed (cycles 6 - 10) and decreases the increments of apparent $\bar{\Gamma}$ (B, H₂O) proportionally until the original (concentration of bound $\bar{\Gamma}$ (B, CO₂) is removed. This conclusion is based on the CO₂ readsorption experiments described below.

Noting a continued increase in both $\bar{\Gamma}$ (B, H₂O) and $\bar{\Gamma}$ (m, H₂O) without any signs of approaching an upper limit we then outgassed the sample at 300°C with a nearly complete loss of the $\bar{\Gamma}$ (B, H₂O) complement. Subsequently, readsorption of water vapor (1 a) appears to occur on an area equivalent to the preceding maximal value. Considerable retention follows with the desorption (1 d) data commensurate with the original behavior. Excursion to 1.0 P_o in the next cycle reverted to the behavior (2 d) noted for the decarbonated sample. The sample was then exposed to CO₂ (700 torr) with a concomitant retention noted by the double arrow. Subsequent H₂O data is readily related to the original carbonated sample when $\bar{\Gamma}$ (B, H₂O) is corrected for $\bar{\Gamma}$ (B, CO₂) as noted in Figure 8.

C.3 Nitrogen Adsorption

During the course of the preceding experiment we constructed nitrogen isotherms as a measure of surface properties of the sample. Sample results are shown in Figure 9. We see that the initial water sorption (cycles 1 thru 14) enhanced $\bar{\Gamma}$ (m, N₂) and induced some porosity, which in turn gave rise to the hysteresis loop (curve B). Removal of the bound water by 300°C outgassing markedly increased both area and porosity (curve C). A small amount of retention was noted for the 300°C outgassed sample as noted in Figure 9. Rehydration and reoutgassing did not remove this disparity (0.0 to 0.5 P_o) at -196°C. However, the original vacuum weight was obtained in both cases by warming the sample to 22.00°C. We suspect that this phenomena is due to the existence of "hot spots" on the sample [defects or reduced states (i.e., metallic iron)]. We were able to oxidize the sample at 300°C and 100 torr (O₂) and then measure isotherm C of Figure 10. Nitrogen adsorption may well be an excellent way of measuring the concentration of such active sites on lunar samples.

Evaluation of surface areas from the nitrogen isotherms is fraught with the classical problems. As noted in section III A there

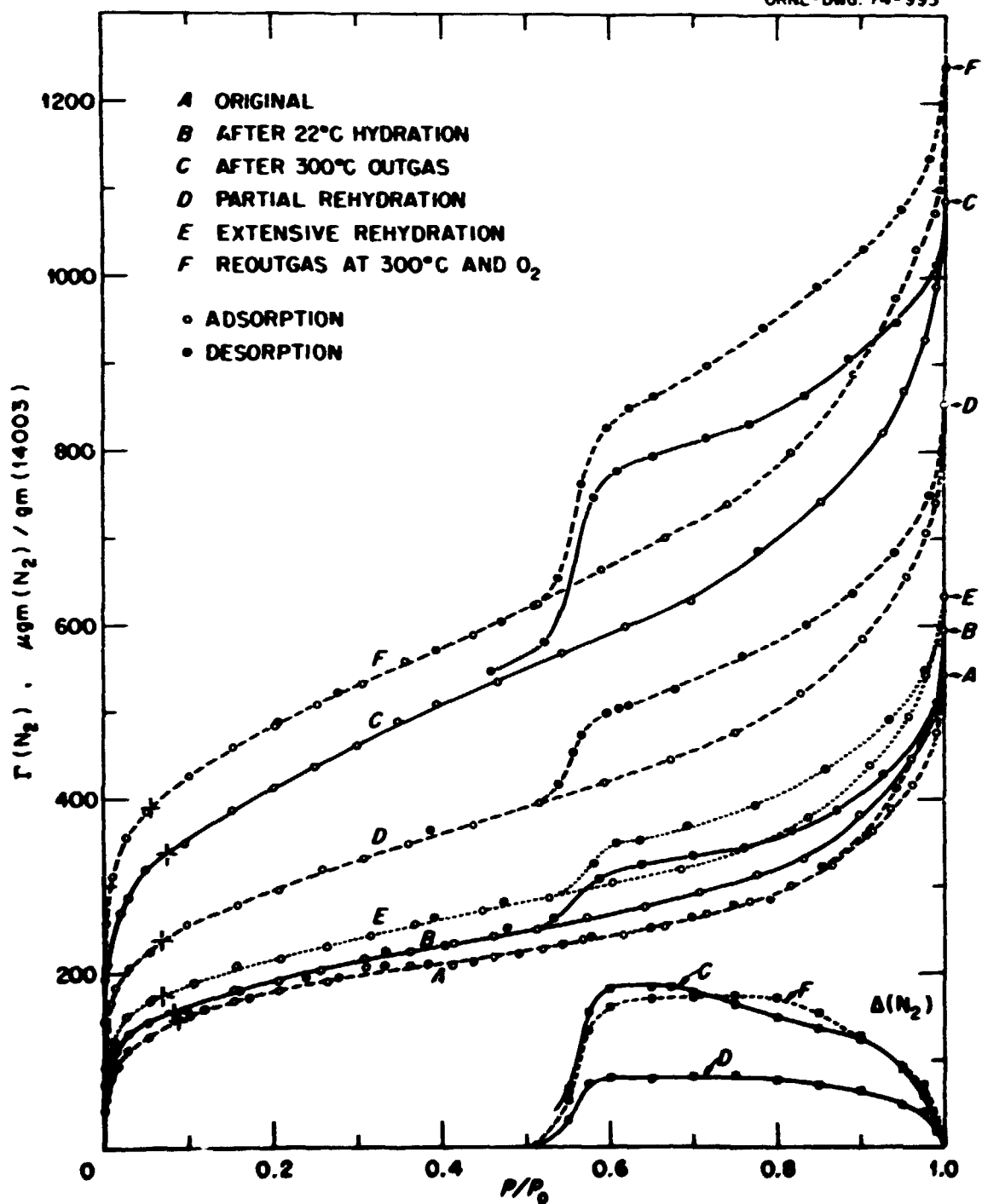


Fig. 9. Nitrogen sorption by 14003 at -196°C .

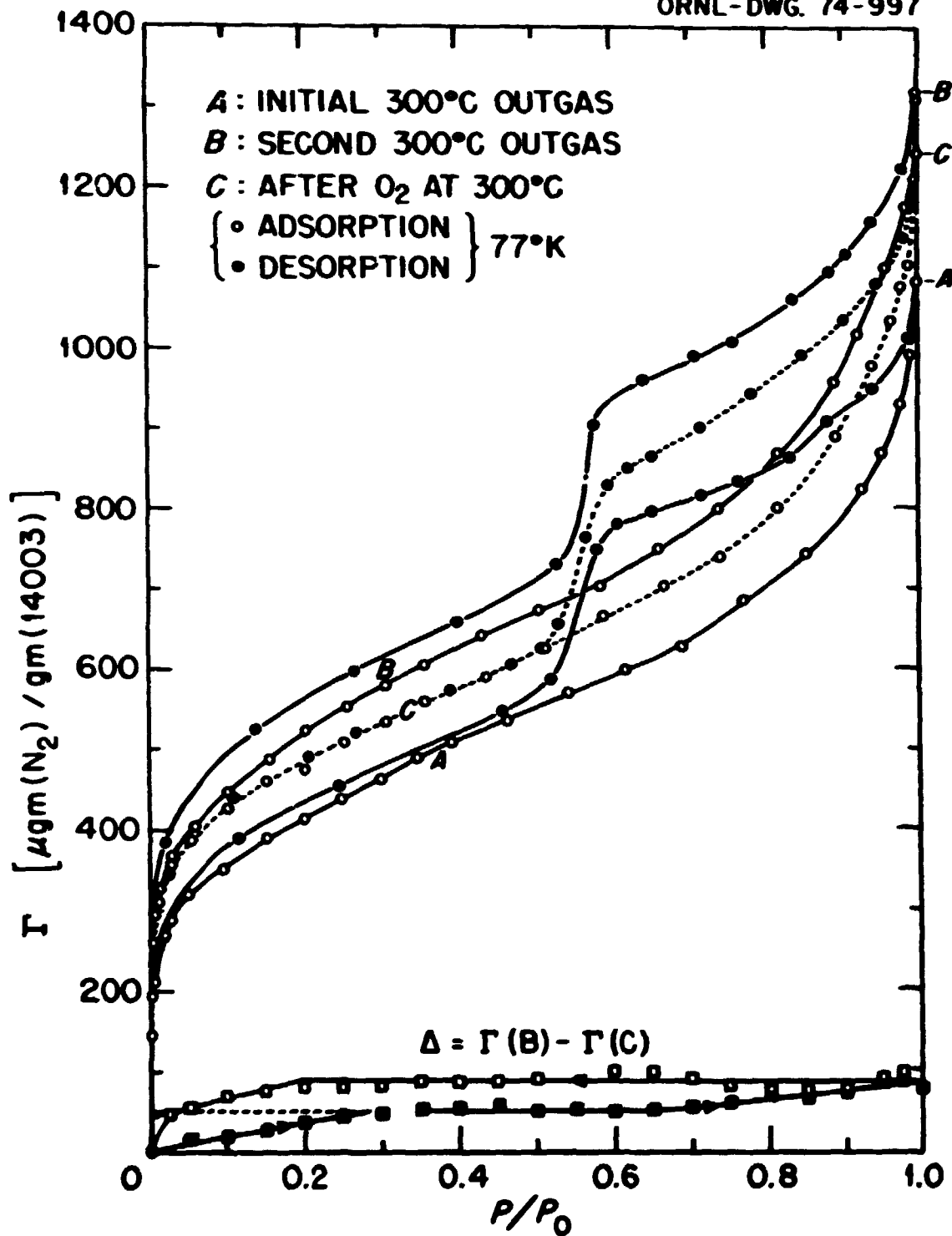


Fig. 10. Nitrogen sorption (77°K) by 14003.

is some question as to the area occupied by a sorbed nitrogen molecule in monolayer formation. We have adopted the classical⁽⁹⁾ convention of assumed $0.1627 \text{ nm}^2/\text{molecule}$ which allows us to calculate 3.482 square meters for each milligram of sorbed nitrogen in the classical BET monolayer. The data all gave linear BET plots in the range of 0.02 P.-0.32 P.. Such a convention may not be an accurate absolute measure of surface area but is assuredly a valid process relative to other work.

The nitrogen data is useful as a measure of surface properties and changes wrought by reaction with reactive vapors. We have chosen three nitrogen parameters for this purpose: $\Gamma(m, N_2)$, the BET monolayer capacity (+ in Figure 9); $\Gamma(h, N_2)$, the hysteretic retention (maximum of the $\Delta(N_2)$ curve in Figure 9); and $\Gamma(s)$, the amount adsorbed at 1.0 P. (annotated on right margin of Figure 9). The latter was evaluated as described previously⁽⁵⁾ as the reproducible maximum obtained when several aliquots of N_2 were introduced to assure condensation of liquid on the walls adjacent to the sample.

Figure 11 shows the variation of $\Gamma(m, N_2)$ and $\Gamma(h, N_2)$ for the initial outgassing (following 14 water cycles) for the range 22 to 300°C. In addition we have included the more comprehensive picture in Figure 12 where $\Gamma(m, N_2)$ variations are shown for hydration, dehydration, rehydration, dehydration, oxidation and sintering sequentially.

The data of Figure 10 suggest a linear relationship between $\Gamma(h, N_2)$ and $\Gamma(m, N_2)$. Pursuant to this topic we present a more comprehensive picture for the above sequence in Figure 13. In each case, dehydration or rehydration, the data extrapolate to $\Gamma(m, N_2)$ equal to ca $114.5 \mu\text{gm}(N_2)/\text{gm}(14003)$ when $\Gamma(h, N_2)$ is zero. This seems to be a measure of the external surface ($0.399 \text{ m}^2/\text{gm}$) which is virtually unaltered during these cycles. The 700 and 800°C data also indicate that the sintering process is primarily intraparticulate. Furthermore, the linear relationships between $\Gamma(h)$ and $\Gamma(m)$ is significant. If the internal dimensions of these pores is much greater than the orifices, the volume capacity [$\Gamma(h)$] will be considerably greater than the surface capacity [$\Gamma(m)$].

Furthermore, the correlation of $\Gamma(s, N_2)$ and $\Gamma(m, N_2)$ (Figure 14) shows that multilayer sorption is proportionally enhanced, virtually without limit, as more adsorption sites are exposed on dehydration. We can measure the internal area of this sample based on the above results in terms of adsorption capacities:

$$\Gamma(I, N_2) = \Gamma(m, N_2) - \Gamma(E, N_2) = \Gamma(m, N_2) - 114.5 .$$

Here $\Gamma(I, N_2)$, $\Gamma(m, N_2)$ and $\Gamma(E, N_2)$ are the internal [calculated], total [measured] and external [$114.5 \mu\text{gm } N_2/\text{gm}(14003)$] monolayer capacities, respectively. Figure 15 is a graph of $\Gamma(s, N_2)$ vs $\Gamma(I, N_2)$ and further shows that multilayer formation on the internal sites is in direct proportion to the number of sites upon which monolayer formation occurs. This data also shows that approximately $500 \mu\text{gm}(N_2)/\text{gm}(14003)$

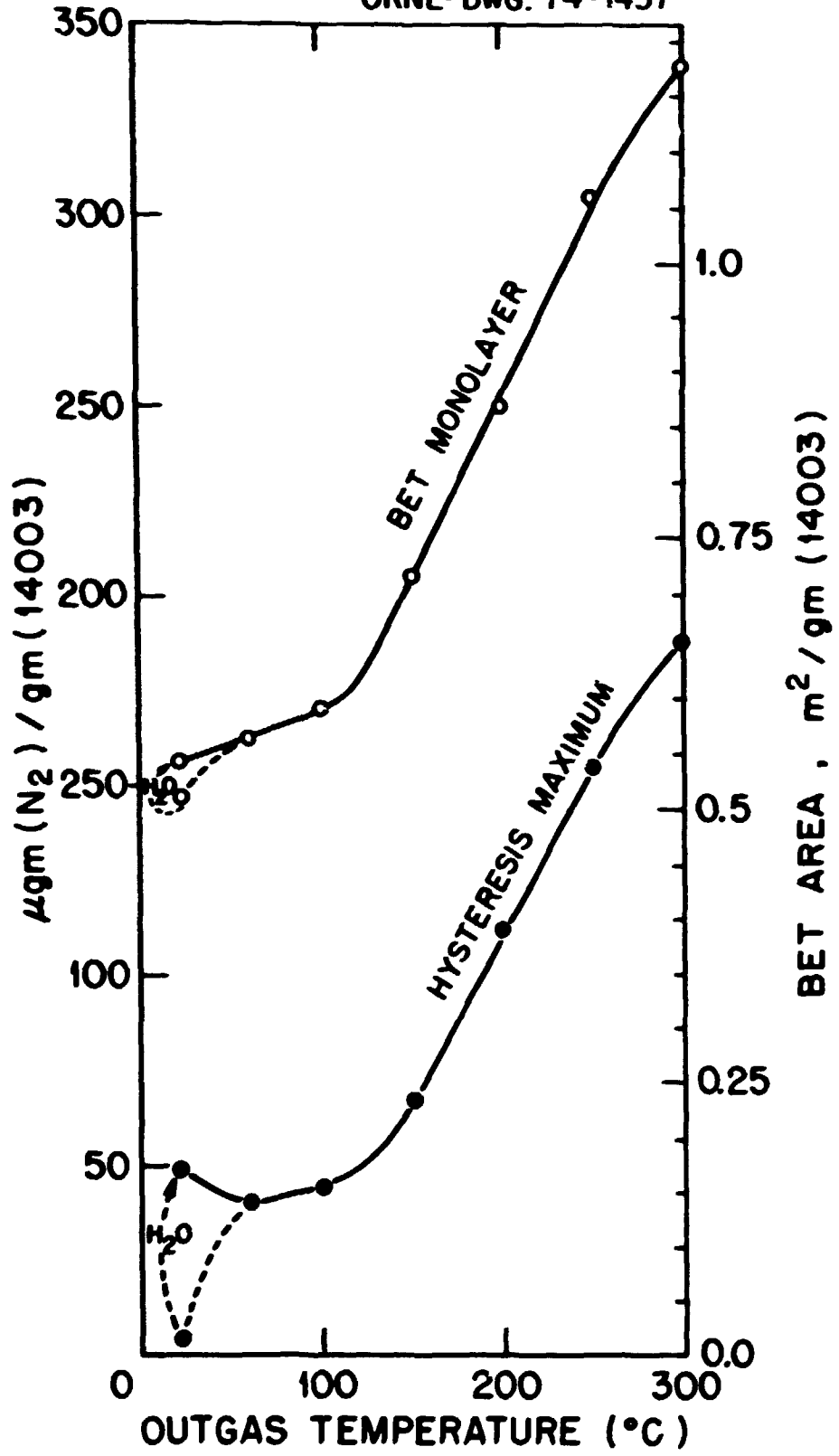


Fig. 11. Nitrogen sorption on 14003 at -196°C .

ORNL - DWG. 74 - 1435

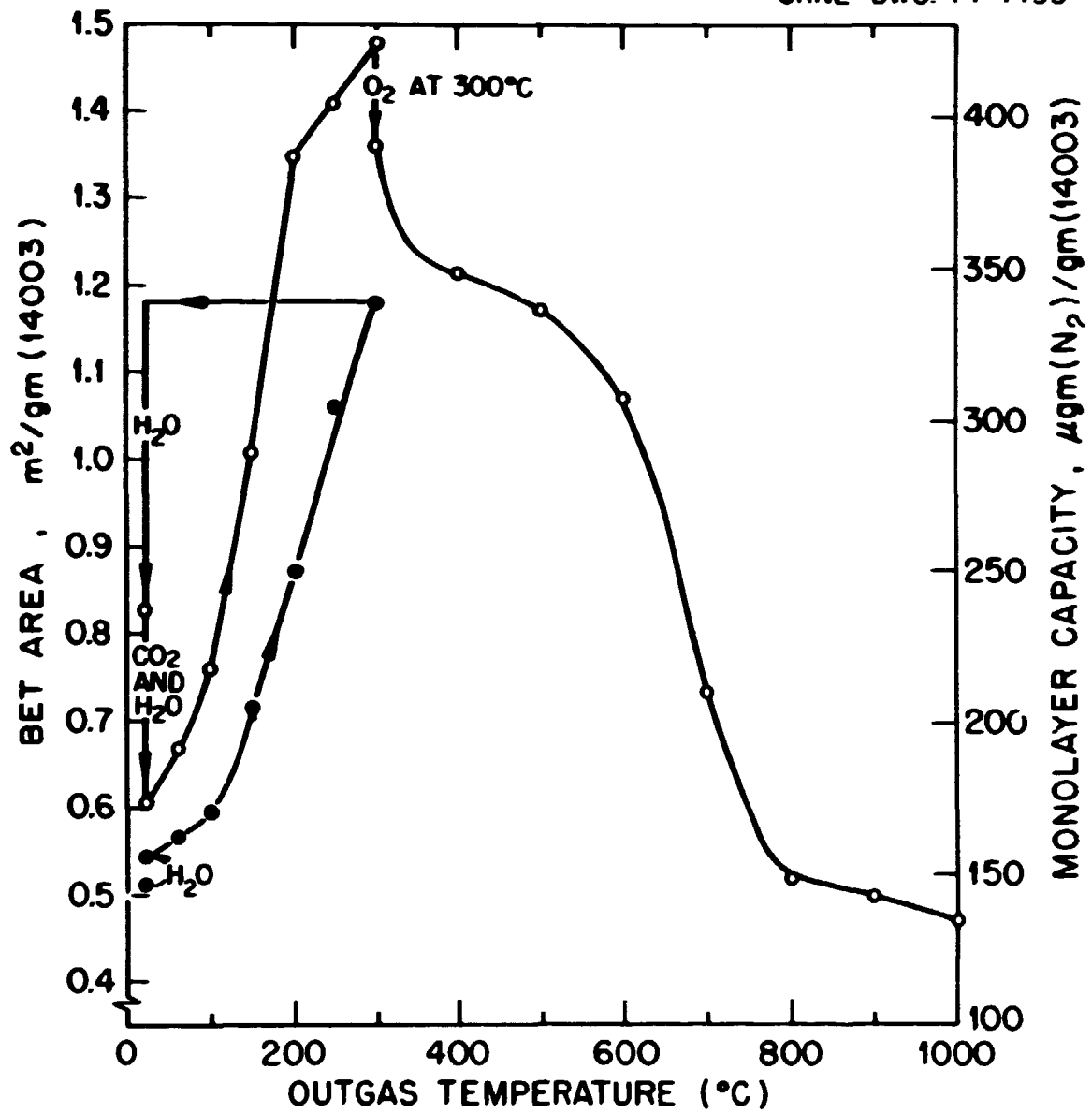


Fig. 12. Nitrogen sorption on 14003 at -196°C.

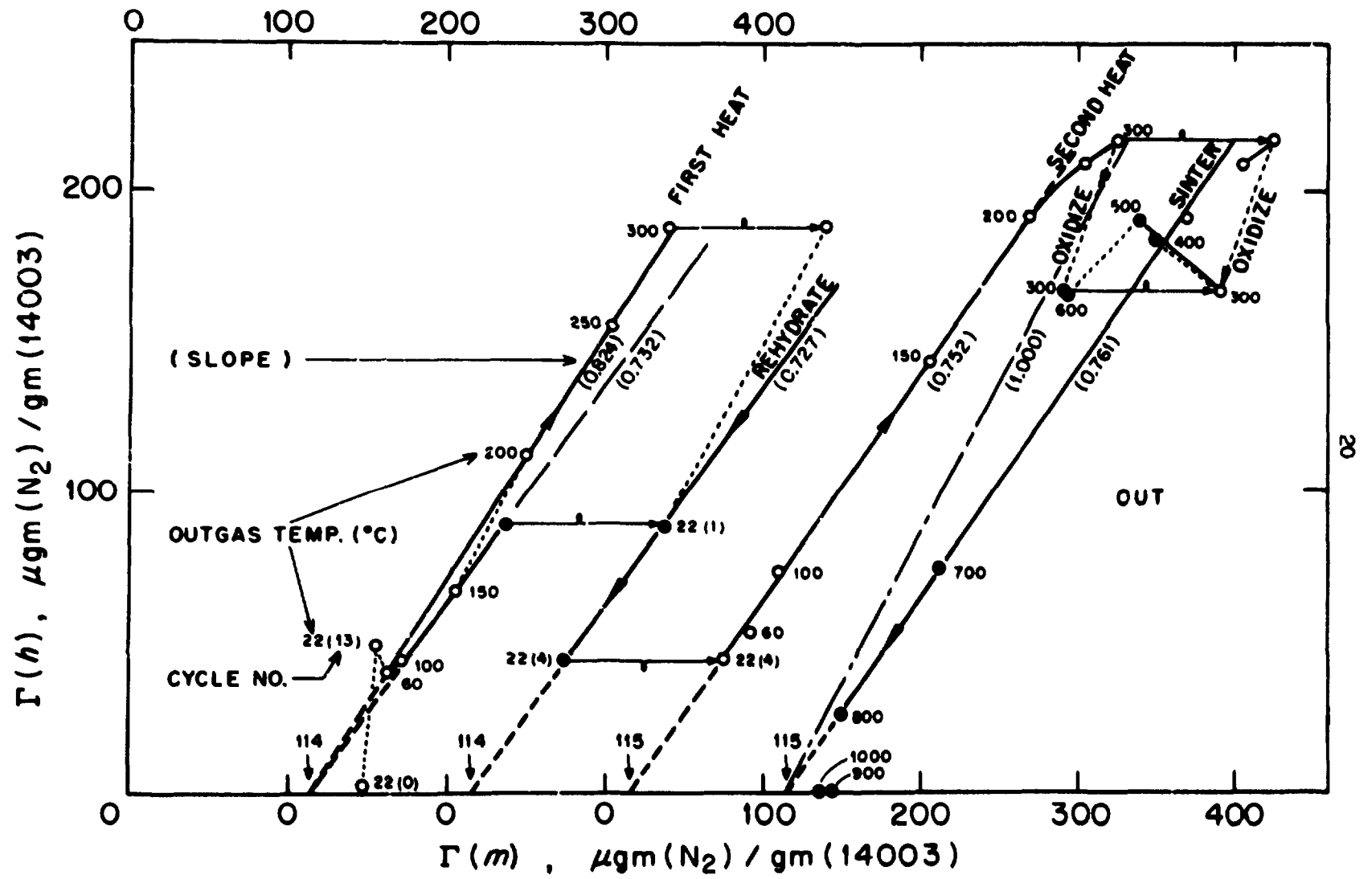


Fig. 13. Nitrogen sorption on 14003 at -196°C.

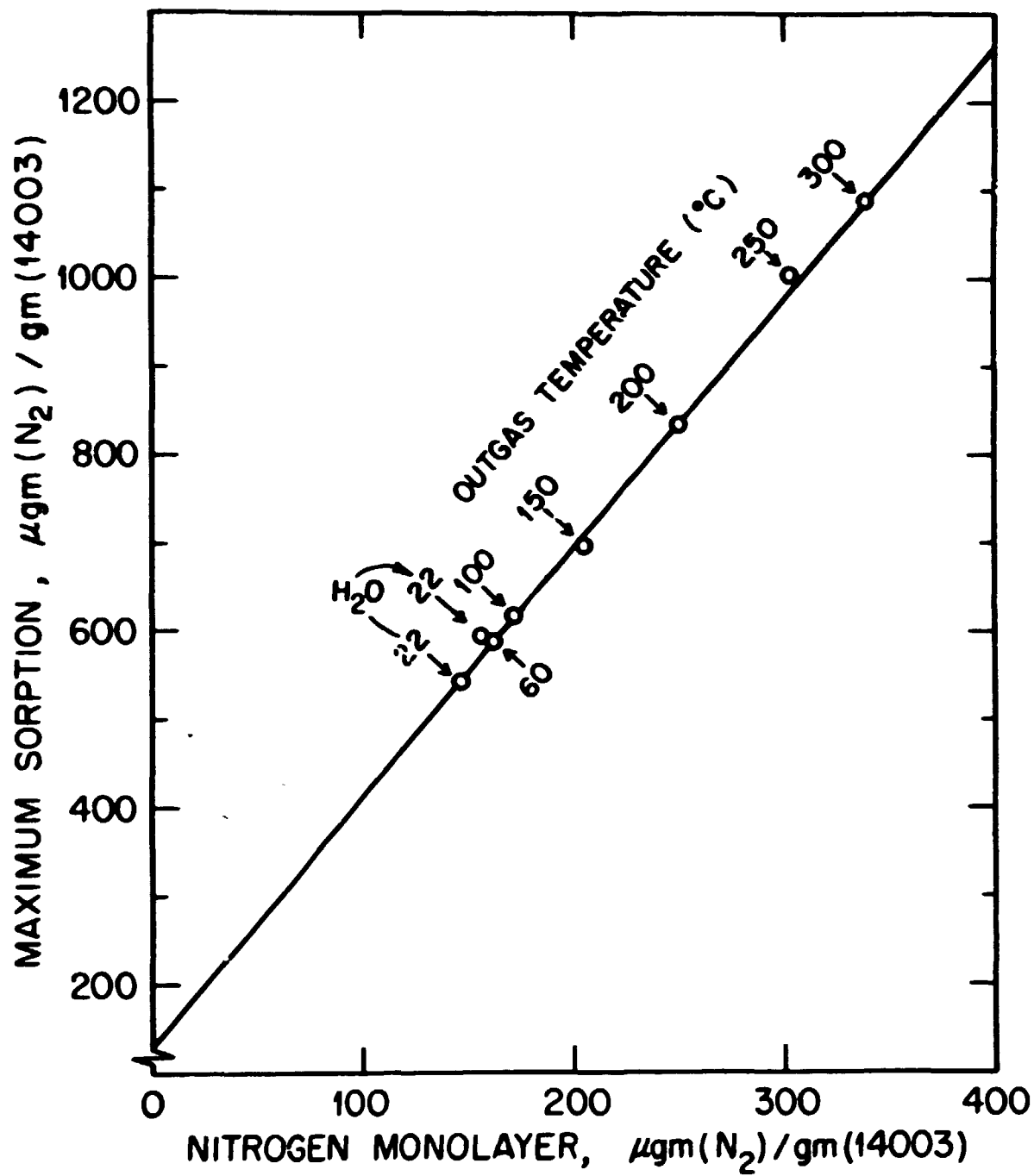


Fig. 14. Nitrogen sorption on 14003 at -196°C.

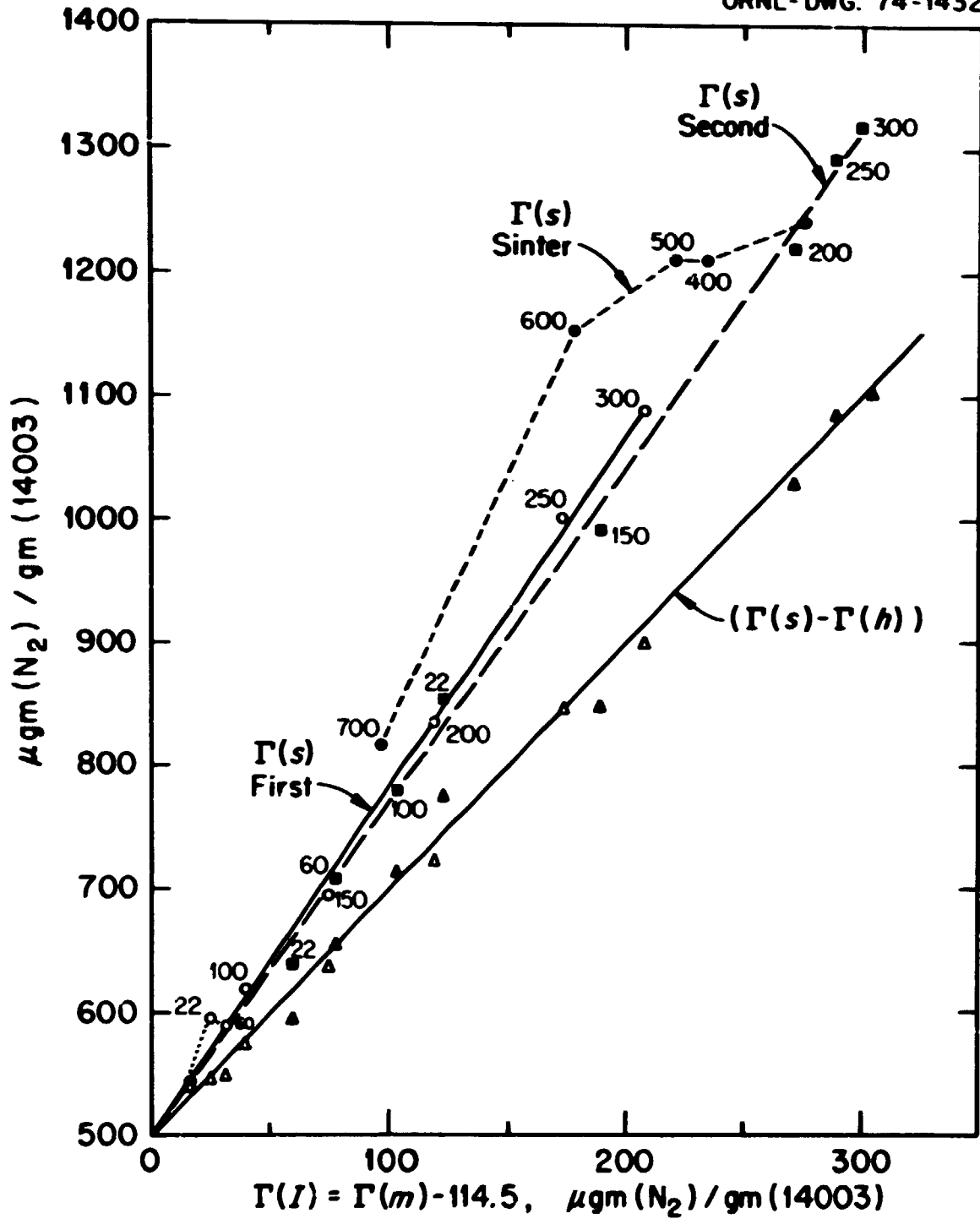


Fig. 15. Nitrogen sorption on 14003 at -196°C .

is characteristic of the saturation, $\Gamma (S, N_2)$, on the external surface. This corresponds to ca 4.4 layers ($500/114$) which is less than normally observed⁽¹⁴⁾ for the oxide samples. Temper this analyses with the radiation effect noted by others for gravimetric analyses at -196°C .⁽¹⁵⁾

C.4 Weight Loss on Outgassing and Sintering

We have monitored the sample weight throughout the sequence as shown in Figure 16. The initial weight gain for the 14 water cycles at 22.00°C is obvious. This is followed by a nearly linear weight loss on outgassing to 300°C . Rehydration and carbonation leads to an appreciable increase in $\bar{\Gamma} (B)$ which only partially is removed at 300°C in vacuum. The magnitude of the weight gain due to oxidation is shown at 300°C . Higher temperatures drive off more hydration species to ca 800°C . Rather massive slow weight loss is noted at 1000°C as volatile species are expelled from the inner reaches of the sample as noted for previous samples⁽²⁾.

C.5 Intercorrelation

In view of the aforementioned results where the reaction with sorbed water generates and fills porous internal area we have considered the variation of nitrogen sorption capacity, $\bar{\Gamma} (m, N_2)$ as the bound water, $\bar{\Gamma} (B, H_2O)$, is removed by degassing. Figure 17 shows the interrelationship where the chronology is represented by the arrows. Apparently it would have been possible to bring the hydration reaction to a state of completion where the nitrogen capacity is that of the external surface, $\bar{\Gamma} (E, N_2) = 114 \mu\text{gm/gm}$ (14003). This conclusion is based on the two desorption sequences (shown in expanded form in Figure 18). The data indicate that if our hydration process were to have been carried to $\bar{\Gamma} (B, H_2O) = 1852 \mu\text{gm/gm}$ (14003) we would have found nitrogen adsorption limited to the external area only. Figure 19 correlates equally well to show that no hysteretic capillary condensation would have occurred had we continued the hydration experiments to the noted extent.

Both sets of data (Figures 17 and 19) show that at least 2 dehydration mechanisms are in play as witnessed the increased nitrogen capacity at lower water concentrations (higher outgas temperatures). The intraparticulate sintering is quite evident for the higher temperature (500 to 800°C) data.

The original sample had been exposed to the laboratory atmosphere ($25 \pm 2^\circ\text{C}$ and $50 \pm 10\%$ relative humidity) prior to these analyses. Figure 20 is presented as an aid in discerning the surface properties of a pristine sample. The data indicate that if we could have measured water sorption on the fresh (unhydrated, nonporous) external surface that we would have not sensed any physical sorption in the monolayer region (i.e., $\bar{\Gamma} (m, H_2O) = 0$). This limiting case, characteristic of the lunar (vacuum) atmosphere, is complete hydrophobicity. Although we have not observed this phenomena directly, it is quite common oxide

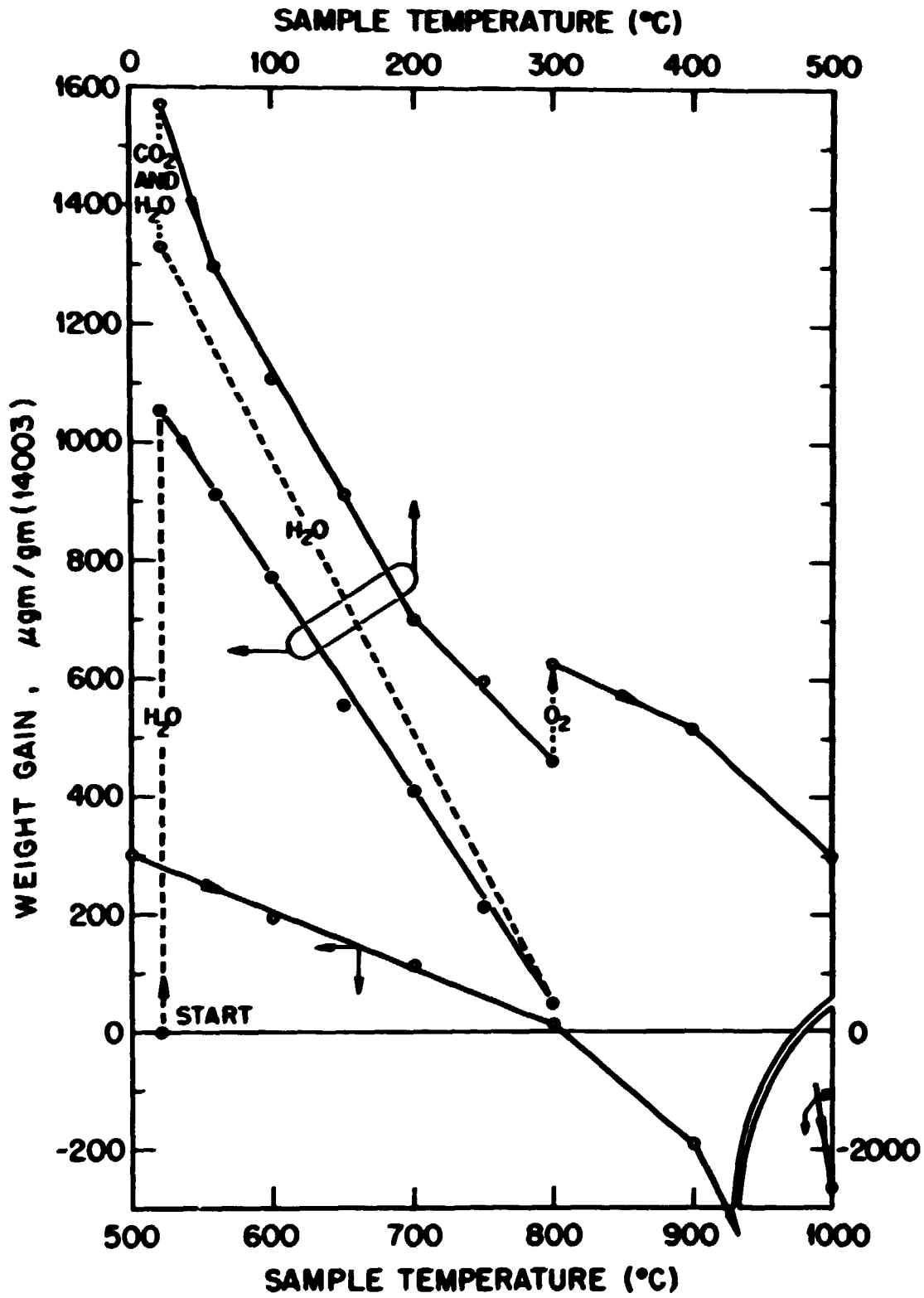


Fig. 16. Vacuum weight of 14003.

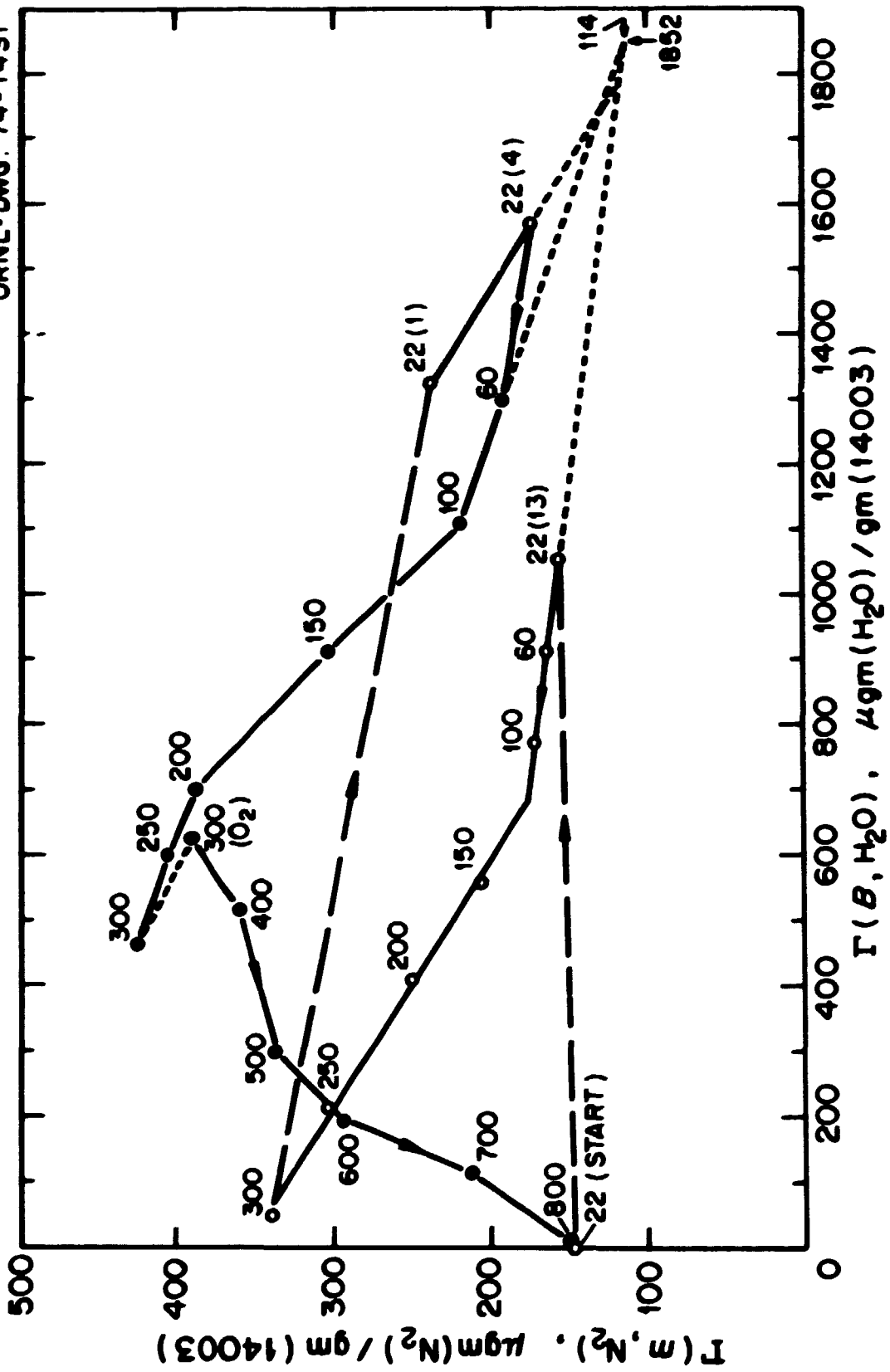


Fig. 17. Surface properties of 14003.

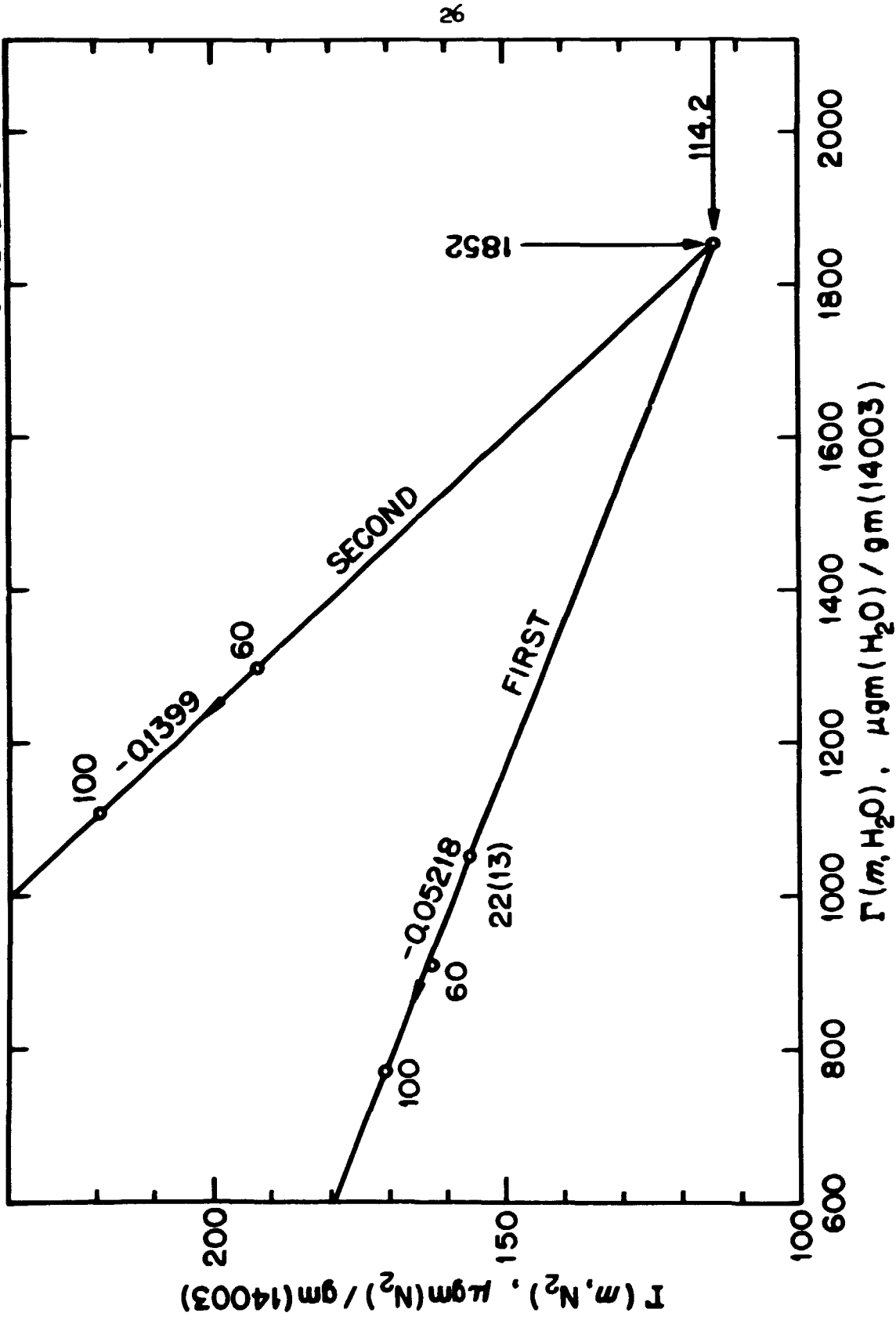


Fig. 18. Dehydration of 14003.

ORNL-DWG. 74-1001

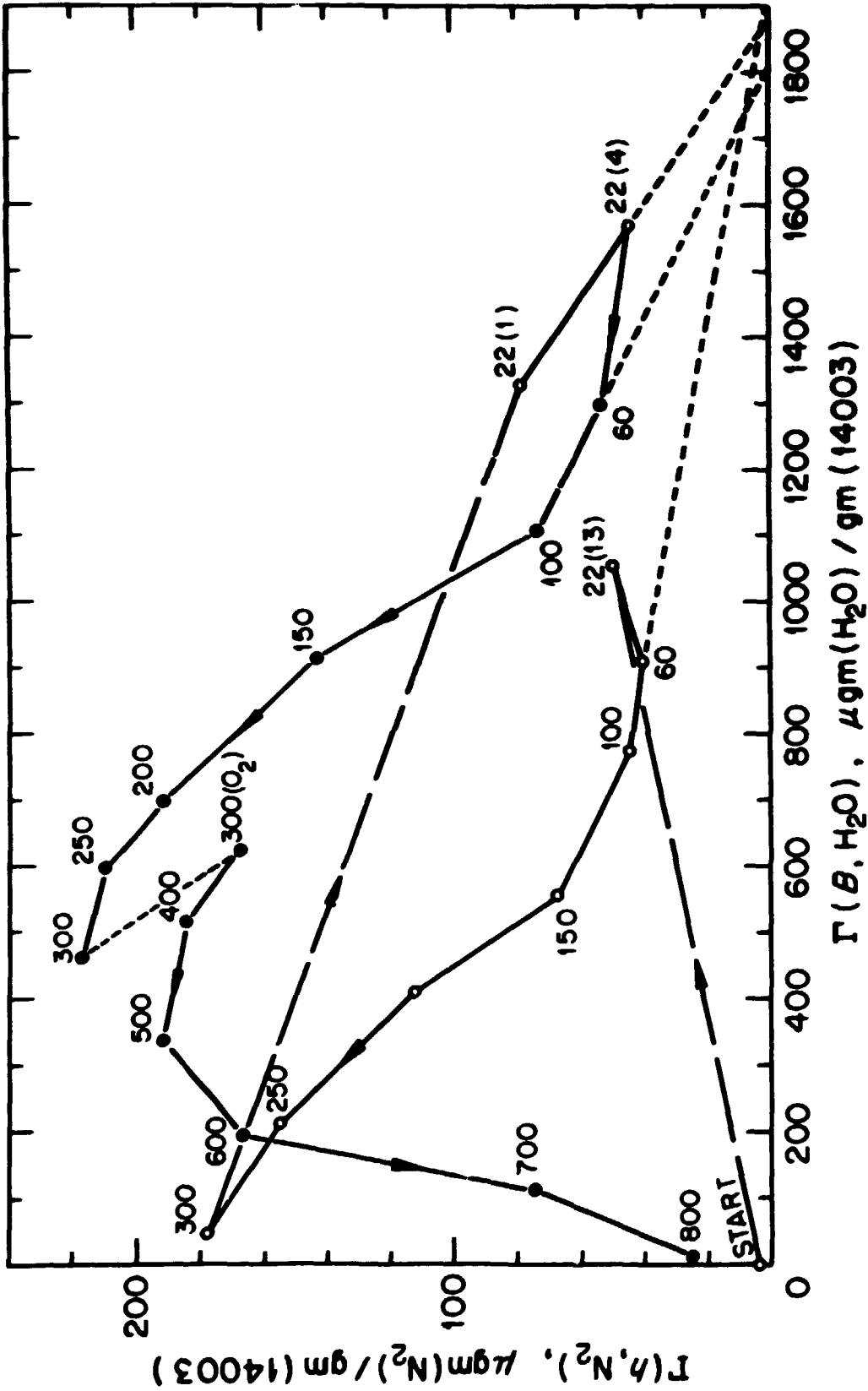


Fig. 19. Surface properties of 14003.

samples which have been extensively dehydrated⁽¹⁶⁾.

D. CONCLUSION

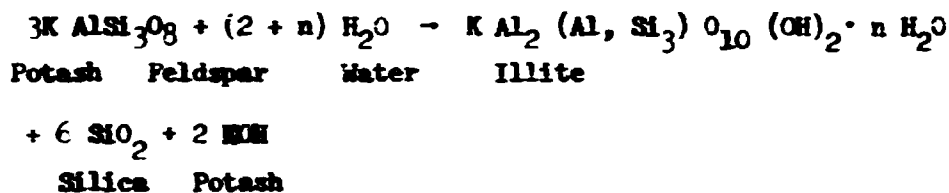
This sample has reacted in a very similar manner as have the majority of other lunar samples⁽²⁾. Water vapor has attacked the material to form and fill a porous structure. The new surfaces are accessible to inert vapors only after the bound water is recovered in vacuum at elevated temperatures. Rehydration reversibly fills the inner reaches to the exclusion of inert vapors. The hydration process requires multiple exposures to relatively high humidity. The cycling to and from vacuum is required to facilitate the hydration reaction whereas prolonged exposures at high humidity does not lead to appreciable further reaction. Water vapor physical adsorption is enhanced in proportion to the degree of hydration even in the presence of the bound water (in contrast to inert vapor (N_2) physical adsorption prohibited by the bound H_2O component).

The ion track etching mechanism can be discredited in terms of the relationship between $\bar{V}(h, N_2)$ and/or $\bar{V}(S, N_2)$ and $\bar{V}(m, N_2)$ for the dehydration experiments of Figure 13. If indeed the inner reaches of the induced "ink bottles" are excluded by bound water filling the narrow necks we would expect the increments of volume filling terms $\bar{V}(h, N_2)$ and $\bar{V}(S, N_2)$ to be much greater than the surface term $\bar{V}(m, N_2)$. Furthermore, a limited capacity for water $\bar{V}(S, H_2O)$ should be apparent and is not as noted in Figure 6. Such behavior should be sensed if the internal voids are equal to or less than ca 500 Å and are encased in a rigid framework. Conceptually it is difficult to envisage migration of the bulk entities through small orifices (< ca 30 Å) in either anhydrous molecular form (i.e., Al_2O_3 , SiO_2 , MgO , NaO) or hydrated form. If appreciable differential migration and deposition on the surface had occurred we would expect an appreciable change in the chemical and physical nature of the surface. Granted one has difficulty differentiating slit or ink bottle pores based solely on the nature of nitrogen hysteresis (Figure 9)⁽¹⁷⁾. However, one would expect water hysteresis (Figures 6 and 7) to be closely related to the nitrogen results for ink bottles in a rigid substrate, both in magnitude and partial pressure dependence. This is definitely not the case for this sample.

Considering the grain boundary mechanism we have some difficulty in explaining the experimental results. If water indeed penetrates these boundaries with release of the strain energy one would anticipate a folding open with the primary elements spreading to leave an open "V" shaped pore which would not give rise to hystereses in the water and nitrogen isotherms. The enhanced area should be accessible to both vapors in near equal amounts regardless of degree of hydration. However if the surface grains were to remain in contact in a very unique manner (i.e., cubes arranged in very ordered states such that all edges were in contact via a hydration layer) one would sense increased area and volume capacities as the bound water is removed. However, it is unlikely that such an array of macroscopic entities are present for they

should be discernible in electron microscopic analyses and have not been detected to our knowledge^(18,19).

The chemical hydration model is far superior in terms of explaining the experimental results. The hydration of anhydrous metallosilicates is a very thermodynamically favored reaction⁽²¹⁾ albeit generally a very slow process. However the strain energy and disorder⁽²⁾ in the surfaces of these material is quite large and probably tends to accelerate the reaction. The hydration mechanism for most common metallosilicates^(21,22) is akin to that noted for feldspar:



If we correlate the monolayer capacity, $\Gamma(m, H_2O)$ to the loosely bound molecular water of hydration (a constant fraction of n) and the bound water capacity $\Gamma(S, H_2O)$ to the hydroxyl complement and strongly bound molecular water, we find from Figure 8 that $\Gamma(m, H_2O)/\Gamma(S, H_2O) = 0.41-0.42$. This ratio is constant for the entire extent of hydration as one would expect for a stoichiometric process.

Furthermore, we can readily explain the enhanced water adsorption $\Gamma(S, H_2O)$ with respect to $\Gamma(S, N_2)$ for various degrees of hydration/dehydration. Apparently the metallosilicate laminae are free to expand under the capillary forces of condensed water virtually without limit. Conversely, nitrogen sorption at $-196^\circ C$ is limited to the external surface and/or only to the interlaminar channels that are voided by high temperature dehydroxylation. A detailed analysis of the nitrogen data (Figures 14 and 15) allow us to define more of the details. Apparently the leaflets or laminae are expanded to a very limited extent as observed by others^(22,23). Our data indicate that nitrogen forms a layer on both internal surfaces of the laminate, each which then accommodates another layer, with further adsorption limited to one layer between these. The desorption freely removes 2 of these N_2 layers and the "sandwich" layer retained hysteretically until the 0.6 P. is reached on desorption. This is evident in our data for nitrogen:

<u>Ratio (N₂)</u>	<u>Model</u>	<u>Experiment</u>
$\Gamma(n)/\Gamma(I)$	0.5	0.73-0.76 (Figure 13)
$\Gamma(S)/\Gamma(I)$	2.5	2.6-2.8 (Figure 15)
$\frac{\Gamma(S)-\Gamma(h)}{\Gamma(I)}$	2.00	2.00 (Figure 15)

A further interesting comparison can be made, utilizing the data of Figures 17 and 19, with respect to what one would anticipate for the

ink bottle or laminar surface configuration. In both cases the most labile surface species is probably the hydroxyls and hydrates on the external surface. Outgassing at lower temperatures will remove this complement initially (25 to 100°C) with a concurrent minor enhancement of $\bar{V}(m, N_2)$ due to increased roughness and/or energy of adsorption. Subsequently an ink bottle model would predict a very marked increase in $\bar{V}(m, N_2)$ and $\bar{V}(h, N_2)$ for a small increment of $\bar{V}(B, H_2O)$ (dehydration of restricted orifices) followed by a nearly constant, larger surface and volume capacity as the surfaces of the internal voids are dehydrated. Conversely the laminar model is more consistent with the experimental data. The surface capacity and volume capacity are increased in direct proportion to the amount of internal dehydration in the temperature realm of 100 to 300°C. This is the trend one would anticipate for interlaminar dehydration where accessibility is afforded by removal of the interlaminar water and/or hydroxyls. Their presence tenaciously binds the laminae to the substrate (especially at -19°C) by means of cross-linking hydrogen bonds. A similar conclusion, favoring the laminar model, evolves when the rehydration data of Figure 20 is considered.

Further credit for the laminar model is obtained in comparing our results to that of others. The total surface area enhancement due to dehydration can be calculated as the ratio of $\bar{V}(m, N_2)$ for 300°C outgassing to $\bar{V}(I, N_2)$ as 2.97 from the data of Figure 12 which is also semi-quantitatively the 400°C value of 3.05 (Figure 12). These values are virtually identical to the 3.0 fold increase in $\bar{V}(m, N_2)$ noted for dehydration of montmorillonite⁽²⁴⁾. In our case we can see that the hydration mechanism has not proceeded into the bulk appreciably. Apparently we are limited to the formation of a single laminar metallosilicate layer over the external surface of the particles. At this juncture we have encountered the prohibitively slow kinetics that involve geologic time scales of weathering⁽²⁵⁾. Our limiting case of hydration (Figures 17, 18 and 19) involves only 0.18 weight percent of the sample. Even then, it is doubtful that we have formed a contiguous laminate over the surface. Rather, the hydration layer is probably comprised of small leaflets which yield even to the rather weak forces involved in the interlaminar condensation of nitrogen.

Additional credence for the metallosilicate model is obtained by the similar analysis of volcanic sand which had been subjected to extensive percussive grinding⁽²⁾. This material behaved semi-quantitatively identical in virtually every respect to this and other lunar samples. Apparently the grinding process quite adequately simulates the meteoritic bombardment to produce fresh disordered surfaces. Temper this conclusion with the knowledge that ionic bombardment⁽²⁶⁾ of annealed lunar samples does appear to qualitatively regenerate some of the surface activity. However sample processing for the radiation experiment did involve some abrasion of the particles which assuredly disturbed (activated) surface layers. Moreover, heavy ion tracks are long in bulk material and the majority of lattice disruption occurs far below the crystal surface. In our experiment⁽²⁵⁾ the small particles (1 to

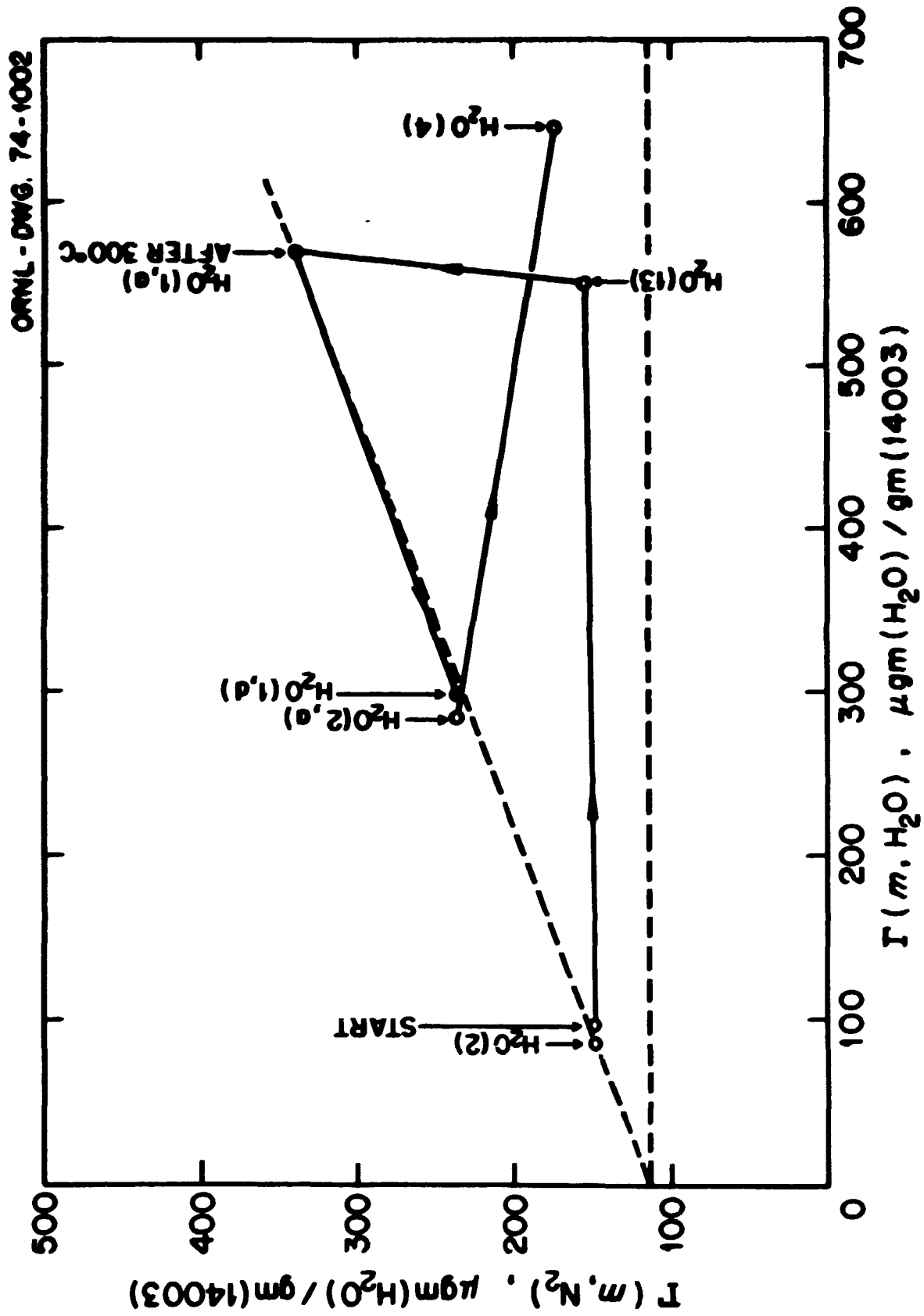


Fig. 20. Surface properties of 14003 (rehydration at 22.00°C).

10 μ m) were used. Thus the single particle sizes were less than the length required to slow the ions to allow momentum transfer (and simultaneous lattice disruption). We can be assured that some (if not most) of the incident ions dissipated their energy near the surface of the particles that made up the heterogeneous target.

Likewise, a large fraction of the macroscopically homogeneous ion beam (both in experiment and in the cosmic flux on the moon) will be slowed differentially in the bed of small particles (more in particle center and less near edges). This condition soon leads to a high degree of energy dispersion for lower layers of particles in a bed. All in all, it is difficult to envision ionic bombardment of small particles resulting in energy dissipation exclusively in classical ion tracks within the particles. If indeed this is the case we can readily explain the very small amount of reactivity⁽²⁶⁾ reinduced by experimental ion bombardment.

In view of the previous correlations of lunar samples to their terrestrial analogs it is informative to compare the temperature realms of stability as shown in Figure 21. Typically the lunar samples are a conglomerate of feldspathic, pyroxenic, amorphous, and/or glassy metasilicates of varying chemical and mineralogic composition. We have noted several characteristics of the hydrated products i.e., dehydration (reversible and irreversible), intraparticulate sintering, and sample loss by volatilization (1000°C and 10^{-7} torr). These phenomena can be correlated to relatively pure minerals as shown in Figure 21. Although there is considerable variation for the transition temperature of the clays (*) they generally collapse to form the three dimensional metasilicate structures in the temperature range (800-1200°K) noted for the heterogeneous lunar samples. Dehydration of the hydrated lunar sample generally occurs over a wide temperature range, akin to the illite, allophane, or vermiculite samples rather than at a very characteristic temperature (+) noted for singular compounds and other clays. Furthermore, the general temperature regions of dehydration are coincident. In addition, we can further substantiate our assumption⁽²⁾ that the 1000°C (10^{-7} torr) weight loss (Figure 16) is due to volatilization of low molecular weight oxides (Na_2O , K_2O , CaO , MgO , etc.). The noted vapor pressures (volatility) of representative alkali oxides and/or alkaline earth oxides are given in Figure 21.

E. SUMMARY

Water vapor reaction with lunar soil is closely related to the geochemical weathering of terrestrial primary metasilicates. The product is a hydrated laminar metasilicate comprised of a two-dimensional array such as clay minerals. The hydration process involves only the outermost complement of the particles which have been disordered by the ions of meteoritic impact and radiation damage in the lunar environ. Microgravimetric analyses prove to be very valuable in studying this weathering process in simulated arid climates (humidity fluctuations without solution transport). Alternate plausible mechanisms

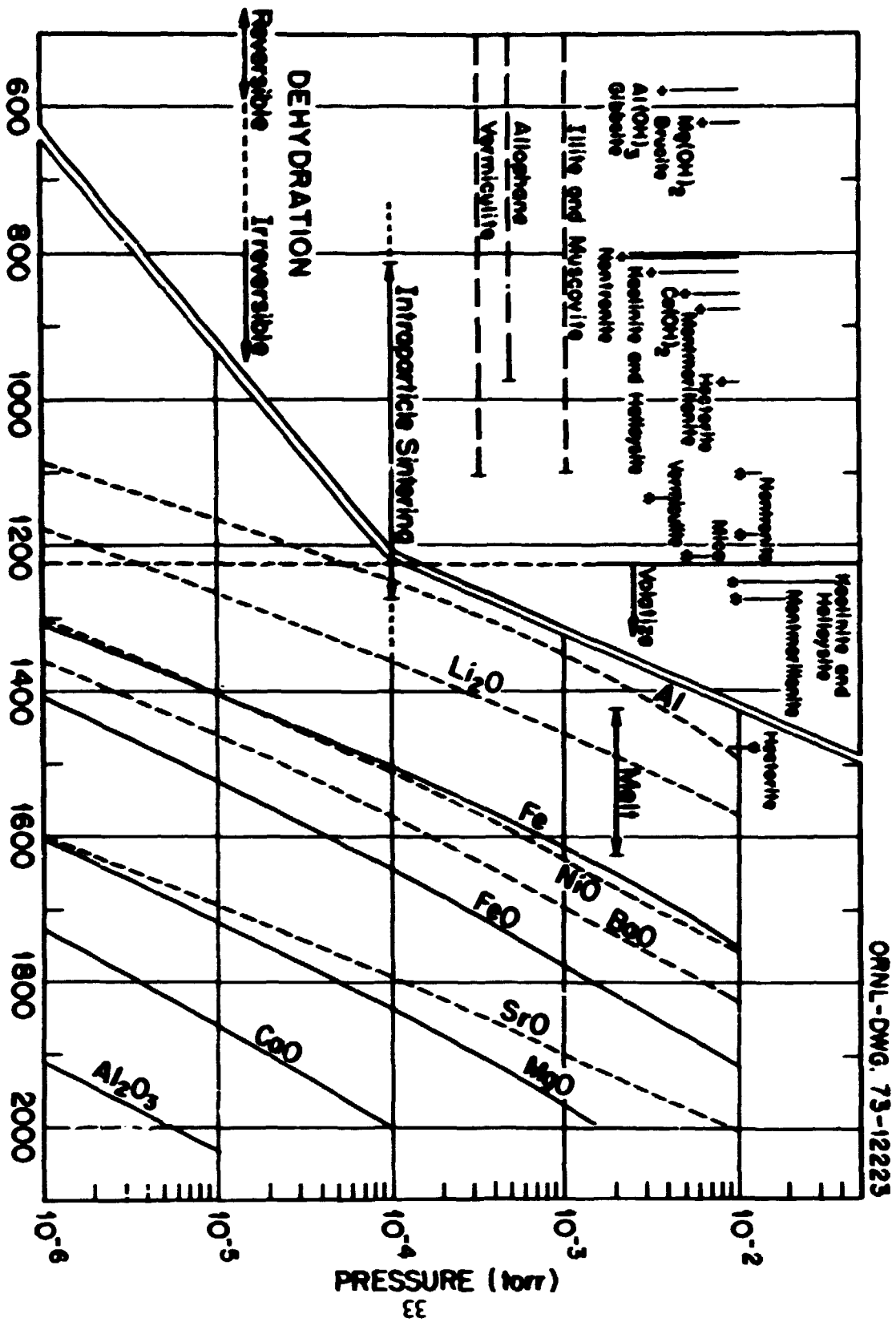


FIG. 21. Temperature effects for lunar and analogous materials.

ORNL-DWG. 75-12225

have been discredited as being minor contributions in terms of experimental results.

F. REFERENCES

1. E. L. Fuller, Jr., H. F. Holmes, R. B. Gamage and K. Becker, Proceedings of the Second Lunar Science Conference (Suppl. 2 Geochim. Cosmochim. Acta. Vol. 3, The MIT Press, p. 2009 (1971).
2. E. L. Fuller, Jr., J. Colloid and Interface Science, In Press.
3. D. A. Cadenhead, J. R. Stetter and W. G. Buerger, 47th National Colloid Conf., Ottawa (1973), J. Colloid Interface Science, 47,322 (1974).
4. E. L. Fuller, Jr., H. F. Holmes and C. H. Secoy, Vacuum Microbalance Techniques 4,109 (1964).
5. E. L. Fuller, Jr. and P. A. Agron, Progress in Vacuum Microbalance Techniques Vol. 4, Heyden and Sons, London (1976, In Press).
6. G. A. Samorjai, Principles of Surface Chemistry, Prentice Hall (1972).
7. S. Brunaur, P. H. Emmett and P. E. Teller, J. Am. Chem. Soc. 60,309 (1938).
8. J. D. Carruthers, D. A. Payne, K. S. W. Sing and L. J. Stryker, J. Colloid Interface Sci. 36,205 (1971), and A. L. McClellan and A. L. Harnsberger, J. Colloid Interface Sci. 23,577 (1967).
9. S. J. Gregg and K. S. W. Sing, Adsorption Surface Area and Porosity, Academic Press (1967).
10. J. H. deBoer, The Dynamical Character of Adsorption, Oxford (1968).
11. M. Polary, D. Phys. Ges. 18,55 (1916), and Zeit Electrochem. 26,370 (1920).
12. J. H. deBoer and C. Zwikker, Z. Physik. Chem. B3,407 (1929).
13. J. O. Hirschfelder, C. F. Curtiss and R. B. Bird, Molecular Theory of Gases and Liquids, John Wiley (1954).
14. J. Hagymassy, S. Brunaur and R. Sh. Mikhail, J. Colloid Interface Sci. 29,485 (1969).
15. P. A. Cutting, Vacuum Microbalance Techniques 7,71 (1974).
16. See citations in References 1 and 9.

17. J. H. deBoer, The Structure and Properties of Porous Materials, p. 68, Butterworth (1958).
18. R. B. Gammage, H. F. Holmes, E. L. Fuller, Jr., and D. R. Glasson, J. Colloid and Interface Sci. 47,350 (1974).
19. J. Borg, M. Maurette, L. Durrieu and C. Jouret, Proc. 2nd Lunar Sci. Conf., Geochim Cosmochim. Acta (Suppl. 2) 3,2027 (1971).
20. H. Ramberg, Chemical Thermodynamics in Mineral Studies, in Physics and Chemistry of the Earth (Vol. 5) p. 226, Pergamon Press (1964).
21. F. C. Loughnan, Chemical Weathering of the Silicate Minerals, American Elsevier (1969).
22. W. D. Keller in Soil Clay Mineralogy, University of North Carolina Press, edited by C. I. Rich and G. W. Kronze (1964).
23. F. Rouqueral, Thesis, Centre D'Etude Nucléaires de Saclay (1966).
24. J. deD.Lopez-Gonzalez and V. Dietz, J. Res. NBS 48,325 (1952).
25. R. M. Garrels, Rates of Geochemical Reactions at Low Temperatures and Pressures, in Researches in Geochemistry, (P. H. Abelson, editor), John Wiley (1959).
26. H. F. Holmes, P. A. Agron, E. Eichler and G. D. O'Kelly, Earth and Planetary Science Letters 28,33 (1975).
27. L. C. Northcliffe and R. F. Schilling, Range and Stopping Power Tables for Heavy Ions in Nuclear Data Tables, (K. Way, editor) Sec. A, Vol. 7, No. 3 and 4, Academic Press (1970).
28. J. L. Margrave, The Characterization of High Temperature Vapors, Wiley (1967).

PART II GEOCHEMICAL ASPECTS OF LUNAR SOIL WEATHERING

The lunar materials are of chemical and mineralogic composition quite similar to the feldspathic-pyroxinic primary rocks from which our secondary minerals are generated by chemical weathering. Keller⁽¹⁾ has treated the topic of the origin and alteration of clay minerals in an excellent comprehensive manner. Specifically, the knowledge of the hydrolyses, dissolution, hydration and oxidation of primary aluminosilicates is of interest. In view of the limited amount of water involved in our sorption experiments we can limit our correlations to the desert conditions found here on earth. That is, the multilayer sorption is akin to the condition wherein the amount of precipitation is not in excess of the evaporative losses. This condition is more nearly related to our "closed" system, in the sorption apparatus, than to a dissolution-precipitation "open" system where an excess and/or constant supply of fresh liquid water is available. The adsorbed films of water will be capable of hydrating surface species but with a minimal amount of differentiation which requires dissolution and reprecipitation. The surface hydration would probably allow very short range reorientation via rotation and/or interchange of adjacent molecular entities. This is in accord with the interfacial reactions occurring at the aluminosilicate/water interface:⁽¹⁾

1. Formation of an amorphous layer,
2. Formation of hydrated alumina minerals or primary bauxite,
3. Formation of kaolinite,
4. Formation of endelite,
- 5-7. A sequence of processes that occur in an open system where the reaction products are carried away from the substrate with the passage of time.

Step one in the normal argillation process occurs in natural rolling and/or in laboratory grinding processes⁽²⁾. Step two proceeds relatively rapidly on the new, disordered surfaces to form a thin layer of SiO_2 and $\text{Al}(\text{OH})_3$ around feldspathic grains when the reactive alkali and alkaline earth oxides are dissolved. The passivity of this layer is noted in that the inner alkali metals are not available until the aluminosilicate is removed either mechanically or chemically. In a semi-arid system (i.e., limited liquid water) "hydrolysis of the silicate occurs while it is wet, but as drying ensues, the solutions of cations originally dilute become saturated with respect to Mg, Ca, Fe, Na, etc., and their combination with O-Si-Al during drying can develop montmorillonite. Thus by utilization of the divalent ions in the ground water even granitic rocks (rich in K and Na, but typically in Ca) can alter to montmorillonite in a semi-arid climate, whereas if rainfall on them had exceeded evaporation they would have given rise to kaolinite"⁽¹⁾. In an aqueous

environ this amorphous hydrated layer formed to only a limited depth (ca 300 A for K-feldspar and ca 20 A for Na-feldspar).⁽¹⁾ If the leaching process proceeds, the ratio of Al:Si approaches that of kaolinitic clay minerals in the immobilized hydrated zone.

The rates of these processes are a function of "temperature, size of particles, and concentration of ions in solution."⁽¹⁾ To this we can include the degree of crystallinity retained in the abraded surfaces or, in other words, the amount of stored energy therein. We can be sure that the lunar silicates are as disordered as the laboratory samples. The prolonged exposure, in vacuo, to the bombardment by meteoritic ionic and electromagnetic species and the concomitant sputtering⁽³⁾ surely produces a surface which is much more strained and reactive than the Beilby layers normally associated with grinding. Furthermore the glassy component of lunar soil will be as, if not more, reactive than the volcanic glassy rocks found to be so reactive here on earth.^(4,5,6)

In general, the sorption induced processes will follow the process outlined by Tamura and Jackson⁽⁷⁾ and Fieldes⁽⁸⁾ with some qualification to apply to a closed system:⁽¹⁾

- "1. Hydrous alumina crystallizes to a gibbsite structure in which the aluminum is contained within octahedral sheets of hydroxyls and adjacent sheets are linked by hydrogen bonds.
- "2. Partial dehydration removes from the gibbsite some hydroxyls which are replaced by the oxygen atoms of the silica tetrahedra from solution. Silica is taken on at random, in this way cross-linking between octahedral sheets of alumina and forming a random structure full of channels but relatively rigid. This form of silicated alumina corresponds to allophane (allophane A of Fieldes).
- "3. When sufficient silica is available, under the influence of wetting and drying, silica reorients unidirectionally to form a hexagonal silicate sheet structure resulting in a kaolin type mineral."

The primary changes in the above scheme, when applied to closed systems, can be outlined quite easily. In step one one can conceive of Iron(II) and alkaline earth oxides, in their hydrous state, crystallizing to a trioctahedral brucite structure⁽⁹⁾ analogous to the dioctahedral gibbsite entity. In addition we are forced to conclude that the lateral dimensions of such sheets are quite short since the excess silica is not carried completely into solution, and back again to the substrate, in our sorption experiment. However, short range segregation does occur as the hydration-dehydration processes proceed. Thus we see an ideal opportunity for process two to occur simultaneously with the hydration of step one.

In step two, the "taking on of silica" can just as logically be viewed as a rearrangement of randomly positioned silica and alumina units, by inversion, to tend to form continuous octahedra facing tetrahedra.

In this context we can view the disordered surface region as a pot-pourri of tetrahedral and octahedral segments which are the primary building units of clays. This, in turn, lays the groundwork for the modifications apropos to step three. In a closed system we are restricted to the composition that is initially available. That is, there is limited differentiation which occurs when leaching is present. Such a condition limits us to a high alkali content and a relatively acid condition. Both of these restrictions favor the formation of smectites, illites and chlorites over the kaolinitic species that prevail when the alkali, alkaline earth, and acid are flushed away in an open system. The sorption system is even more restricted than the closed system of a solubility experiment where a relatively large excess of water is in contact with the solid, reacting, substrate primary aluminosilicate. Solubility experiments alter the composition of the amorphous region appreciably. As a consequence, we would not anticipate the residual kaolinitic behavior as Keller and Huang⁽¹⁰⁾ observed after ~ 0.15 wt % differential dissolution of a lunar sample. Granted, the hydration in multilayer and/or persorption of water will have some preferential association with the various entities, but the subsequent dehydration will leave all of the species in close juxtaposition. The net effect of a sorption-desorption cycle will be to permit the reorientation of the structural units to a more preferred and somewhat ordered state. All of these phenomena will undoubtedly be limited to the external reaches of the unit particles without the penetration much beyond a few angstroms (probably limited to one or two lattice dimensions of the resultant clay structure). DeVore⁽¹¹⁾ notes the sequence of hydrous alteration of feldspar to form a "series of temporarily metastable ionic groups--leading to Al-Si single chains having the feldspar Al-Si ratio. Without further cation transformation the derived chains can transform directly into ordered mica sheets. A simple transformation in these chains permits the kaolinite sheet structure to form. The close spacial relationship between the micaceous alteration products and parent feldspar are explained in part by the mica-like surface chemistry of the feldspar acting as nucleation sites for the micaceous minerals."

Correns⁽²⁾ has shown that a large number of primary silicates undergo a transformation wherein a hydrous amorphous boundary layer is formed quite readily. He rightly points out that the amount of such material formed is greater for larger specific surface area (small particle size) and consequentially the rate of decomposition (dissolution) is greater. However, he finds that olivine layers seem to be somewhat more pervious since the dissolution process does not vary for different size fractions.

All of this discussion has dealt with relatively pure primary silicate minerals and their weathering behavior in various degrees of disorder. The concepts need not be limited to single phases or to⁽²⁾ aluminosilicates solely. Considerable work has been done with basalts⁽²⁾ and alkaline earth⁽¹²⁾ silicate hydrolyses with qualitatively similar observations.

Direct analyses of the hydrated layers on these primary minerals is difficult. X-ray analyses are not fruitful due to the amorphous character, relative thinness, and profusion of characteristically intense diffraction peaks due to the crystalline substrate. Differential thermal analyses are also hampered because the active material is only a very small fraction of the analytical sample. Thermogravimetric analyses require high precision (i.e. microbalance analyses) but, even at best, reveals only a broad, diffuse weight loss characteristic of disordered clays.⁽¹³⁾ Furthermore, the asymmetric environ in which this epitaxial allophanic product resides⁽⁶⁾ will mask characteristic dehydration and/or dehydroxylation behavior.

Electron microscopic analyses⁽¹³⁾ may or may not be fruitful, for if the laminar clay-like material is formed, the characteristic leaflet structure⁽¹⁴⁾ may be observed only after repeated wetting-drying cycles. On the other hand the epitaxial forces emanating from the substrate may be strong enough to prevent the curling that permits definitive observation. At this writing we can only speculate concerning the curling of a single (or at most a few) laminae if heterogeneously attached to a primary silicate substrate. On the other hand, one may be able to observe the 55 Å allophanic⁽¹⁵⁾ entities, if sufficient relief resolution is available. A mixture of cations, such as present in our lunar samples, may enhance the formation of "bent" or "ruffled"⁽¹⁶⁾ intraplanar configurations.

Heats of immersion experiments show promise.⁽¹³⁾ However, caution must be exercised in such analyses. Although considerable data for clay immersion is available,⁽¹³⁾ much less is known about the primary silicates (especially as a function of the degrees of disorder therein). Such analyses could conceivably be helpful in elucidating the chemical weathering process as well as subsequently characterizing the intermediate and final surface states. Caution must be exercised to avoid mechanical (abrasive) removal of the hydrated layer if in situ characterization is desired. Also extensive dilution and simultaneous differentiation are to be avoided if one desires to characterize the initial reaction products that prevail in closed system reactions. Conversely, the system can be calorimetrically analyzed with various degrees of differentiation and approach the state that is of prime concern with respect to geological weathering in the open terrestrial environs. This is the pseudoequilibrium state that is the wellspring of material wherefrom the reserves of mineral-forming solutes are derived. This latter process involves the slow dissolution of alumina, silica, etc., from the differentiated layer and simultaneous release of the more mobile alkali and alkaline earth oxides from the interior.⁽²⁾ This very slow process dominates unless there is a mechanical or biological⁽¹³⁾ intervention to remove the passive hydrous layer or expose a fresh, anhydrous primary silicate layer. Calorimetry would also be useful in studying the energetics associated with the mechanical and/or radiative disorder comparative to that of a cleaned surface.

Cation exchange capacities (CEC) are often used⁽¹³⁾ to characterize clays. In the present analyses the author has neither the expertise

nor apparatus for such analyses. A cursory examination of the literature reveals little evidence for intermediate weathering products. The amount of hydrated material is small and the standard data is given in milliequivalents per 100 grams of sample. To distinguish between low CEC due to the absence of clays (or kaolinitic versus smectitic behavior) will require cautious analyses. However the picture may not be entirely one of gloom, for if, indeed, these feldspathic, olivinic surfaces have hydrated to a claylike material, the CEC capacity per unit area (internal and/or external) will allow one to ascribe kaolinitic or smectitic traits thereunto. Related to the CEC type of analyses is the general area of colloidal properties of clay soils.⁽¹⁷⁾ Here again the behavior is characteristic of clays per se not the initial weathering products adhering to the primary substrate. Infrared spectroscopy is quite a useful diagnostic tool⁽¹⁸⁾ for well crystallized clays where very characteristic absorption bands are noted for specific vibrational frequencies. However as the degree of disorder increases the bands broaden, weaken and overlap to yield much less distinctive spectra. Furthermore the opacity of the lunar samples is so great and the water content so low (even in the hydrated state) that transmission spectra are difficult to obtain.

Electron diffraction data may be useful. Attempts to obtain diffraction patterns from the amorphous layer of lunar fines⁽¹⁹⁾ have been fruitless since this region is virtually metamict. Not all of the lunar particles have the pronounced 200-1000 Å metamictized layer. If one could be assured that adequate precautions were taken, the hydration of one of these metamictized particles may progress deeply enough to allow meaningful data acquisition wherein a rudimentary clay diffraction could be observed. The problem lies in the statistics of assuring oneself that a metamictized particle was chosen for the hydration-diffraction analyses. This metamictized particle would also be a prime candidate to reveal the leaflet structure mentioned earlier. These electron beam analyses are not easy to perform without the expertise and high energy (1 Mev) equipment that are possessed only by the most advanced investigators.⁽¹⁹⁾

It would appear that the most promising definitive analysis is the sorption behavior which in turn can be compared to that observed for various clay materials. In general⁽¹³⁾ clays can be classed as swelling (smectites) and nonswelling (kaolinites, illites, chlorite) with respect to the interlaminal penetration of sorbed water. Water vapor is specifically considered here but many polar species are capable of intercalary penetration⁽¹⁷⁾ if the interlaminal forces can be overcome. The swelling phenomena is notably present in well crystallized montmorillonites wherein discrete undulations in the water sorption isotherm are noted. Corresponding incremental increases in the c (translaminal) lattice parameter are noted for each layer of interlaminal molecular water.^(20,21) More recently the variation of the intraplanar "b" dimension change associated with this imbibed water has been noted.⁽²⁰⁾ More commonly (and apropos to the current application), less crystalline smectites are characterized by a classical sigmoidal water isotherm. However the water uptake is excessive compared to nitrogen sorption since the latter, less reactive gas, is incapable of prizing the laminae apart and consequentially

is adsorbed only on the outer surface.⁽¹³⁾

On the other hand, the kaolinitic, two-layer structures (and the illitic and chloritic, three-layer structures) are not usually penetrated by sorbed water. In the case of well ordered "hard" kaolins the nitrogen and water sorption capacities are comparable and generally thought to be a good measure of the external area of such samples. However, the less ordered and smaller sized fractions of kaolinite do seem to possess considerable internal area, i.e. area or sites available to water but not nitrogen. Witness the increase of the "Hydrophylicity Index" from unity to 3 to 6 as the "Crystallinity Index" decreases from unity to zero⁽²³⁾ for natural kaolinite. Also the water vs nitrogen area ratio increases from unity to ca 3 as prolonged kaolinite grinding is carried out.⁽²⁴⁾ Furthermore the very existence of the halloysitic⁽¹³⁾ minerals (kaolinitic with interlaminar water layers) shows that the smaller particles of kaolin can, will, and do imbibe water. Temper this correlation with the observation that halloysites generally are not readily rehydrated⁽²⁵⁾ once the interlaminar water is expelled. Conversely, even the hard kaolins can be intercalated with agents stronger than water.⁽²⁶⁾ Here again we see that many of the generalities associated with clay types are based on ideal (well crystallized, highly pure, large particle size, etc.) samples not under the influence of the epitaxial forces of a primary silicate substrate. In the present context we should concern ourselves with work that has been done on the less well developed or "soft" clay samples, reserving the knowledge of "hard" clay behavior for the final product which most assuredly is formed only after much more reaction has occurred (on a geological time scale which we have not even approached).

Turning now to the sorption behavior of lunar soil, with respect to clay minerals of comparable chemical compositions, we note that, in a very general way, the lunar chemical composition is comparable to basalts, igneous rocks and tektites with one obvious difference (cf Ref. 10). The lunar material has only about one-tenth as much alkali metal (Na and K) oxide with respect to these other representative materials. Varying amounts of minerals are present (i.e., olivine, plagioclase, pyroxene, etc.). The mineralogic ratio varies markedly from one lunar site to another as does the percentage of glassy material. The general surface properties do not vary appreciably from sample to sample (5 at this writing) which is not too surprising in view of the observed reactivity of disordered terrestrial materials⁽²⁾ varying only slightly from mineral to mineral. It seems that the reactivity depends primarily on the particle size and the degree of disorder of the surface regions. That is to say, the degree of reaction and physical nature of the hydrated surface species depends primarily on the degree of disorder of the primary silicate, when viewed on a unit area basis. Chemical composition, i.e. the second component in the silicate mineral, is of secondary importance as far as the ensuing hydrated structure is concerned. The prime contribution, noted as stemming from chemical composition, is whether the brucite or gibbsite type of structure forms adjacent to the tetrahedral silica layer and/or the degree of intermixing of chemical entities within the octahedral and/or tetrahedral

sheets. The high concentration of mobile alkali metal cations favors the formation of the smectite structure and the iron content is sufficient to favor chlorite formation. All this is in context with the possibility and probability of isomorphous substitution (atomic proxying) within laminae. (27)

Turning now to the behavior of lunar materials we can analyze the sequence of events accompanying our treatment in the context of the favorability of the hydrolysis product assuming a laminar, clay-like configuration. The initial (22°C) H₂O exposure appears to be limited to the external surface until a duplex layer is formed whereupon the penetration phenomenon occurs as some slight shift of hydrated units (the hydrated gibbsite or brucite units of Correns⁽²⁾), occurs allowing further hydration of adjacent units just below this upper layer. Hydration of these domains or residual structural units proceeds relatively unhindered since the metamict region does not possess the strong, numerous, intermolecular binding forces inherent in the truly crystalline substrate. Desorption of H₂O at 22°C removes the vast preponderance of the water associated with this type of adsorption. This wetting-drying cycle seems to involve all of the available sites and the water binding forces are considerably greater than the interunit forces. Nothing much different occurs as the subsequent sorption-desorption (wetting-drying) cycles are carried out except a little more vacuum retention (hydroxylation?) and low pressure sorption occurs. However, when the more stringent drying and thermal activity is induced by the 100°C outgassing, we see that the surface structure has changed enough to allow unhindered access to the internal reaches of the surface region. This process continues virtually without limit through multilayer formation, which is behaviorally akin to the swelling of smectites.

Even more stringent drying (and thermal activation) at 300°C induces further changes. Subsequently, water vapor initially adsorbs on all of the sites (internal and external) up to a duplex capacity whereupon the sorption is limited to the external surface. Now the ordering sequence of the above processes can be viewed in the weathering sequence in two ways. One is the allophane-halloysite (8OH·2H₂O)-endelite (8OH·4H₂O) sequence and the second is along the allophane-kaolinite-smectite-illite sequence. Both sequences involve some conjectural assumptions but possess quite a degree of credibility.

The first model involves an initial formation of an allophanic (by definition, small particles of amorphous material with constituent chemical compositions of clays) phase. Due to the low temperature and pressures of the experiment, a minimum amount of structural character is to be anticipated. Such material is routinely characterized by weakly bound water, the major portion of which is removed below 110°C. (13) [Rather than burden the reader with numerous, more recent references most of the correlations will refer to reviews, i.e. Ref. 13, Grim (1968).] Adsorption on allophanic material is characteristic of the small particles (large specific surface area). Orchiston⁽²⁸⁾ observed disproportionately high amounts of adsorption which led him to note "that the amorphous clay allophane differs markedly in displaying a

specificity unknown to the crystalline clay minerals (in context, referring to kaolin, halloysite and montmorillonite) and from a comparison of the surface areas available to water vapor and nitrogen, that some allophanes may possess the equivalent of an internal surface." Such a speculation was justified and proven true by Aomine⁽²⁹⁾ wherein he did find a threefold greater water capacity (as well as for other polar molecules). We can compare the behavior of the water on our 100°C treated sample and find the 2.7-fold enhancement of water uptake. Furthermore, the nitrogen adsorption is limited only to the external surface initially, and on the hydrated surface of the lunar sample, but does sense a portion of the internal surface voided by the 100°C outgassing. It is conceivable that the silica tetrahedra and nearby octahedra (alumina, magnesia, Iron(II), etc.) become associated at 0.8 P₀ via a hydrogen bonding linkage with a minimal amount of mass transport at 22°C. The 100°C dehydration and activation probably permits more concerted rearrangement to somewhat longer range order (sheet growth) forming imogalite-kaolinitic, two-layer structure. Subsequent hydrolyses forms the hydroxyls of constitution (kaolinitic) and water of hydration (halloysite-2H₂O). These species will be retained⁽³⁰⁾ and the pressure dependence (reversible portion of the isotherm) corresponds, at least in part, to the halloysite-4H₂O in the classical monolayer formation. In this state, the multilayer formation occurs on both sides of the induced laminae without hindrance. The 300°C activation induces considerably more order into the planar dimensions wherein subsequent rehydroxylation and 2H₂O hydration is readily affected. However this stabilized structure now resists swelling beyond the extent of the 4H₂O state with multilayer formation limited solely to the external surface.

In this two-layer (kaolinitic) model we can relate our results to the sorbtive behavior noted by others. Here again we should reiterate that sorbtive behavior on well crystallized clay material bears only indirectly on the case at hand. The kaolinite conundrum⁽¹³⁾ has not been resolved. This involves a comparative study⁽¹³⁾ of clays where a disproportionately large uptake is noted for kaolin between 0.8 P₀ and 0.9 P₀, much akin to our initial isotherms (22.00°C). It seems that kaolinite per se does imbibe water, but only at a very much higher threshold relative pressure than the smectite minerals.⁽²⁰⁾ Here again we see the general concept, nonswelling-kaolinitic versus swelling-smectitic delineation, may be only relative. Jackson's⁽³²⁾ nitrogen isotherm after a 110°C outgas of halloysite to a "disordered kaolinite" bears a marked resemblance to that of the 100°C outgassing of the hydrated lunar sample. Bear in mind that 100°C to 300°C outgassing of a nonhydrated lunar sample has very little effect on the nitrogen adsorptive behavior. The internal area is not present in the material prior to hydration. This is to assure the reader that there is virtually no inherent porosity prior to the water penetration phenomena associated with the 0.7 to 0.9 P₀. Halloysite in the free state is kaolinitic with an interlaminal layer of water, and the structure collapses from ca 10 Å to 7 upon dehydration.⁽³³⁾ In this free state rehydration is not easily affected⁽¹³⁾ since the pseudo (or disordered⁽³²⁾) kaolinitic 7 Å structure is quite stable. However we can

suspect that, "While meeting the general definition of an allophane it is certain that whatever relics of ordered arrangements persist, special qualities pertaining to them will be conferred upon attached amorphous material."⁽⁶⁾ Such perturbations from "free" behavior would undoubtedly be retained in the allophanic to halloysitic transition akin to that proposed by Wada.⁽³⁴⁾ Even "hard" kaolin (Peerless) does show a slight amount of desorption hysteresis,⁽³⁵⁾ the nature being somewhat dependent upon the exchangeable cation present. This is in addition to the retentive excess that is noted for prolonged degassing at 100°C outgassing⁽³⁶⁾ much akin to the rehydroxylation step noted for the lunar material. The dehydroxylation of kaolin has been studied extensively and in general is found to proceed at about 550°C⁽¹³⁾ with a relatively large endothermic collapse of the 7.1 Å structure.⁽³⁷⁾ In the kaolin itself this process is accompanied by some intralaminar shift⁽³⁸⁾ as adjacent hydroxyls coalesce to form molecular water which escapes. The residual hydroxyls are so separated (isolated) that the hydrogen is released in molecular form between 550 and 700°C⁽³⁹⁾ via a proton migration mechanism. The very last residual protonic release occurs exothermically at ca 900°C⁽⁴⁰⁾ when an anhydrous primary silicate is again formed. The dehydroxylation process has been found to involve some 51 kcal/mole in vacuo⁽⁴¹⁾ (41.0 kcal/mole⁽⁴²⁾) as an activation energy accompanying a rate of release "depending on a partial coverage of the dehydroxylating surface by chemisorbed water molecules."⁽⁴¹⁾

This two-layer, kaolinitic model seems to have considerable merit in view of the similar sorption behavior that has been noted for analogous disordered clays. The major merit of this concept, in contrast to that of the much more ordered three- and four-layer clay structures, is that a minimum amount of ordering (mass transport) is required. That is to say, only the interchange of tetrahedral with octahedral units is required to have a certain degree of continuity without a random alteration of these species.

However, the high concentration and relatively high mobility⁽⁴³⁾ of the alkali earth metals would favor their transport to a two-layer structure and thence epitaxially form the additional layers. Such a process can readily be noted as the Correns⁽²⁾ mechanism progresses. In this context we can visualize the initial adsorption as forming only very small domains of kaolinitic material (characterized by the 0.7-0.9 P₀ penetrating hydration with very little hysteresis). The 100°C drying brings some order into the chaos as a three-layer smectitic structure evolves (characterized by the swelling of this single sheet virtually unhindered). This is to be compared to data for free smectite clays which are generally intercalated with free swelling.⁽¹³⁾ Recall that minimal consideration is to be given to the behavior of ideally ordered structures⁽²⁸⁾ and that our primary concern is with the less ordered substrate material more akin to the results obtained by Orchiston⁽⁴⁴⁾ where the discreet undulations are not noted in the smectite water isotherms. Water is adsorbed on most montmorillonites to give a relatively classical sigmoidal isotherm. The sodium and potassium forms are somewhat unique in this respect⁽⁴⁴⁾ but since our stoichiometry is generally low in alkali we can turn to the calcium

magnesium and hydrogen forms with a good degree of confidence. In the free state the degree of penetration is quite large. The water is taken up by a mechanism that approaches the $\text{ca } 800 \text{ m}^2/\text{gm}$ of theoretical surface (if all planes are exfoliated). The energy of adsorption is generally related to the hydration energy of the exchangeable inter-laminar cation. ⁽⁴⁴⁾ In our case the adhering hydrous layer, where the reaction has proceeded only a single (or at most a few) layers deep, we sense only a 3 (2.7) fold increase in area as the reacted layer is virtually floated up from the primary substrate. This is in contrast to the $\text{ca } 50$ ⁽²⁰⁾ fold factor for ideal montmorillonite. Orchiston notes variation where the external area amounts to 10-15% of the total area ⁽³¹⁾ of montmorillonite. Such information is based on comparing H_2O sorption on the original material with that after 600°C sintering. This concept involves the assumption of complete structural irreversible collapse after 600°C which also eliminates all internal sites with a minimum of interparticle fusion. In our case this temperature does not seem to be adequate in that $\text{ca } 800^\circ\text{C}$ is required to close up all of the internal avenues in the hydrated lunar samples.

Smectites in general lose the interlaminar water of hydration gradually to $\text{ca } 300^\circ\text{C}$ and dehydroxylate between 450 and 700°C (depending on the specific composition). The nature of the exchangeable cation and amount of trioctahedral substitution plays an important role in water retention in smectites. ⁽¹³⁾ Smectites rehydrate readily if the dehydration temperature has not exceeded $\text{ca } 500^\circ\text{C}$ ⁽¹³⁾ which is identical to the rehydration we have noted for the hydrated lunar material. Out-gassing at 600°C forms a smectite substrate that accepts limited rehydration very slowly. ⁽¹³⁾ Further heating of smectites usually results in an endothermic transition around 800 to 900°C to various anhydrous silicates. ⁽¹³⁾

As more ordering of the lunar material is brought about by wetting-drying and heating to 300°C we would anticipate translaminar growth to occur to the illitic (where tetrahedral silicons are partially replaced by aluminum) under the influence of the appearance of the alkali and alkaline earth species from the adjacent substrate. This process increases the concentration of charge balancing cations in the inter-laminar regions. This illitic material now adsorbs water much akin to natural illites with limited H_2O uptake (corresponding to interlaminar layer formation). ⁽¹³⁾ Natural illites have area ratios ranging from 1.50 ⁽⁴⁵⁾ ($\text{H}_2\text{O}/\text{N}_2$) to 1.75 ($25^\circ\text{C}/600^\circ\text{C}$). In view of the low ratios compared to the lunar value of 2.72 and the large amount of mass transport required for the smectite to illite transformation it is doubtful if such a mechanism is in play. Quite likely we have observed the phenomena to which Van Olphen (Ref. 17, p. 71) alludes: "Potassium montmorillonites do have a tendency to become nonexpanding after moderate heating, particularly after repeated drying and wetting (collapse) (sic). The potassium ions in a montmorillonite are said to become fixed [his italics] by heating, since the loss of expansion involves a decrease in exchange capacity. Consequently, the distinction between the two groups of three-layer minerals becomes somewhat arbitrary." In either case, whether there is material transport to the

laminar structure or within the structure, the sorptive properties will be similar. The free swelling⁽⁴⁷⁾ character will be lost. Rehydration is now limited to rigid structural duplex hydration on each of the surfaces, with multilayer formation occurring only on the external surface. This would involve a swelling up to the stable condition where each clay surface accepts the two hydration layers of water molecules which are epitaxially oriented thereunto.⁽⁴⁸⁾ This stable state (in the absence of free interlaminar cations) does not yield to allow additional water to be imbibed.

In view of the high alkaline earth concentration in our substrate we should examine the behavior of the vermiculitic minerals. These are composed of "trioctahedral sheets of mica or talc separated by layers of water occupying a definite space (4.98 Å) which is about the thickness of two water molecules. In the natural state, therefore, the mineral consists of an alternation of mica and double water layers. On heating vermiculite to as high as 500°C the water is driven out from between the mica layers, but the mineral quickly rehydrates on exposure to water vapor at room temperature. The mineral, therefore, has an expanding lattice, but the expansion is restricted to about 4.98 Å, or two water layers. If the mineral is heated to 700°C there is no expansion again. In such material the 14 Å line and higher orders of it disappear, and a new line at 9.3 Å with other new mica lines appears on the diffraction pattern."⁽¹³⁾ This structure is quite similar to that of the chlorites⁽¹³⁾ (which are also favored by high alkaline earth and/or Iron(II) concentrations). The latter are generally found to be "noncollapsing" due to the additional interlaminar brucite type of layering. In well ordered samples there is no swelling; however, the more disordered "swelling" chlorites are considered to have a discontinuous brucite layer. Often natural clays can be described as mixed layer structures with relatively regular stratification of chlorite and vermiculite units. Here again the effect on sorptive properties is similar for the less well ordered structures and we can rely on the ideal behavior as a limiting condition which we have yet to achieve.

In concluding, the consideration of the probability of transformation to a 3 or 4 layer laminar species we should turn to the work concerning the dehydroxylation of montmorillonite. This collapsing, swelling mineral behaves in a very interesting manner when subjected to dehydroxylation. The bulk structure undoubtedly does collapse. However, there is definite similarity between the internal and external area as the hydroxyls are removed.⁽⁴⁹⁾ There is a threefold increase in nitrogen capacity which accompanies the dehydration, compared to the 2.7 fold for the dehydration of the hydrated lunar material. It is interesting to speculate that the external laminae on this smectite are loosely bound to the collapsed compact substrate, due to the inherent force imbalance at the interface. It seems that the cooperative interlaminar forces are required to bring about collapse. In both cases this very external layer is readily separated from the substrate by the relatively weak action of the nitrogen molecules. Alternatively, the heterogeneities on the surface do not allow the leaflets^(14,50) to

adhere and they are already available as surface sites for nitrogen. This is akin to the "bocking" effect that is often noted for very disordered and/or small particle clays. (26)

Although much of the preceding discussion is, by convention, modeled by the alumina/silica analogies, similar behavior is noted for other systems. Dicalcium silicate hydrolyzes relatively quickly to similar surface texture, i.e. an area ratio (H_2O/H_2) of 2.0. (12) Note also the dehydroxylation behavior of the magnesium analogue, serpentine (51) being virtually identical to kaolin. The literature for the analogues is too voluminous to burden the reader. Just let us note here that all of the substrate primary minerals found in lunar soil can and do transform into a hydrated ternary or quaternary species when exposed to water. The amorphous character of these lunar surfaces is probably more akin to volcanic ash than to most any other primary silicates found on earth. Numerous field studies have been carried out and the results show a remarkably rapid rate of weathering (5,6) of volcanic debris. Laboratory preparations of zeolites from synthetic and natural glasses (52) also attest to the reactivity of disordered primary silicates through an intermediate "gel" phase. This is not to say that the products are the same as we have, but that there exists a surface phase in each case that is in general a hydration product of the substrate (differentiated in both normal weathering and chemical attack). It does not seem necessary that liquid water per se must contact the substrate. Witness the presence of some clay material, albeit only a small percentage, in the antarctic soil that has been in permafrost zones virtually since its original deposition. (53)

An interesting corollary can be drawn involving this hydrated zone. If the true dissolution does occur differentially through such a membrane (the composition of which is composed of the less soluble components) the "solubility" of the material would be strictly a function of the surface area and the size of the beaker (water to solids ratio). This is the basis of a "ranking correlation" proposed by Hughes and Poster. (54) They note that the moisture content of their clays is also a function of the specific surface area (assumedly the area measured by water), so consequently they find a direct, near linear, correlation between moisture content and extent of dissolution (percent of sample). If we use the solubility data of Keller (10) and the water content of our lunar samples we find virtually the same correlation for magnitudes of nearly one one-hundredth of that of the reference data. (54) Again this is to be taken as indirect evidence that the hydrated layer on the lunar materials behaves much as if it were a clay.

We can summarize the conclusions of these comparative analyses to say that sorbed water reacts with the surfaces of lunar materials in much the same manner that it does in the initial stages of terrestrial weathering of primary silicates. A hydrated surface region is formed which possesses much of the character of the clays which are the product of such aqueous weathering. Further conclusions at this writing involve some conjecture. The mild conditions of sorption at ambient temperature favor the formation of kaolinitic-halloysitic bilaminar structures with

their inherent simplicity. On the other hand, the high concentration of alkaline earth and Iron(II) species, in the absence of long range differentiation, favors the more demanding formation of smectitic, illitic or chloritic multilaminar structures. With only sorption analyses available at present, it is difficult to say which form predominates in the hydrated state. This decision is to be made in the light of the smectite-halloysite⁽¹³⁾ and the smectite-illite⁽¹⁷⁾ similarities noted by others when studying sorption on these materials. However, we can favor the multilaminar hydration product in view of field studies where high alkaline earth concentrations prevail.⁽⁵⁵⁾ The main intrigue of this study is to note that these lunar samples have allowed us the unique opportunity to study the very initial stages of the weathering process. The NASA procedure has kept the reaction to a minimum so that excessive water sorption has not occurred nor "For example, when meteorites pick up bacteria more quickly than collectors can recover them in sterile bags, in the weathering process, by activity of the microbiosphere."⁽⁵⁶⁾ In addition, we can envision the production of useful entities (i.e. zeolites⁽⁵⁷⁾) from the anhydrous raw material, via the clay intermediate form, for direct extraterrestrial application.

REFERENCES

1. W. D. Keller, in Soil Clay Mineralogy, The University of North Carolina Press, Chapel Hill, edited by C. I. Rich and G. W. Kranze (1964).
2. C. W. Correns, "Experiments on the Decomposition and Discussion of Chemical Weathering," in Clays and Clay Minerals, 10th Conf., Pergamon Press, New York (1963).
3. B. W. Hapke, W. A. Cassidy, and E. N. Wells, "Analysis of Optical Coatings on Apollo Fines," Second Lunar Sci. Conf., M.I.T. Press (1971).
4. W. D. Keller, "Dissolved products of artificially pulverized silicate minerals and rocks," J. Sediment. Petrology 33, 191 (1963).
5. M. Fieldes and R. J. Furkart, "The Nature of Allophanes in Soils. Part 2. Differences in Composition," N. Z. Jl. Sci. 9, 608 (1966).
- 5a. C. E. Marshall, The Physical Chemistry and Mineralogy of Soils, John Wiley (1964).
6. W. D. Keller, "Hydrothermal kaolinization (endellization) of volcanic rock." In Clay and Clay Minerals, 10th Conf., Pergamon Press, New York, p. 333 (1963).
7. T. Tamura and M. L. Jackson, "Structural and energy relationships in the formation of iron and aluminum oxides, hydroxides, and silicates," Science 117, 381 (1955).

8. M. Fieldes, "Clay Mineralogy of New Zealand Soils, Part II. Allophane and related mineral colloids," N. Z. J. Sci. and Tech. 37, 336 (1955).
9. R. W. Grimshaw, The Chemistry and Physics of Clays, Ernest Benn, Ltd., London (1971).
10. W. D. Keller and W. H. Huang, "Response of Apollo 12 lunar dust to reagents simulative of those in the weathering environment of Earth," Proc. Second Lunar Sci. Conf., M.I.T. Press (1971), p. 973.
11. G. W. De Vore, "The surface chemistry of feldspars as an influence on their decomposition products," Clays and Clay Minerals, Sixth Conf. (1958).
12. J. Odler and P. Skaling, "Pore structure of hydrated calcium silicates," J. Colloid and Interface Sci. 36, 293 (1971).
13. R. E. Grim, Clay Mineralogy, McGraw-Hill (1968).
14. R. L. Borst and W. D. Keller, "Scanning electron micrographs of API reference clay minerals and other selected samples," International Clay Conference (1969), p. 871.
15. Y. Kitagawa, "The 'unit particle' of allophane," Amer. Mineralogist 56, 465 (1971).
16. Von F. Liebau, "Ein Beitrag zur Krystalchemie der Schichtsilikate," Acta Cryst. B24, 690 (1968).
17. H. van Olphen, An Introduction to Clay Colloid Chemistry, Interscience Pub., New York (1963).
18. V. C. Farmer and J. D. Russell, "The infrared spectra of layer silicates," Spectrochim. Acta 20, 1149 (1964); see also: Yu. I. Tarasenich and F. D. Ovcharenko, Koll. Zhur. 31, 753 (1969).
19. J. Borg, L. Durrien, J. C. Dran, C. Jaret, and M. Maurette, "Irradiation, texture and habit histories of the lunar dirt," Second Lunar Sci. Conf., M.I.T. Press (1971) et seq.
20. H. van Olphen, "Thermodynamics of adsorption of water in clays. I. Sodium vermiculite," J. Coll. Sci. 20, 822 (1965).
21. R. M. Barrer and D. M. Macleod, "Intercalation and sorption by montmorillonite," Trans. Faraday Soc. 70, 980 (1954); see also: W. H. Slabaugh, J. Phys. Chem. 63, 436 (1959).
22. I. Ravina and P. F. Low, "Relation between swelling, water properties and b-dimensions in the montmorillonite-water systems," Clay and Clay Minerals 20, 109 (1972); see also: ibid. 18, 325 (1970);

and Nature 226, 445 (1970).

23. M. K. Lloyd and R. F. Conley, "Adsorption studies on kaolinites," Clay and Clay Minerals 18, 37 (1970); see also: ibid. 19, 273 (1971); J. Coll. and Interface Sci. 37, 186 (1971); R. W. Mooney, A. G. Keenan, and L. A. Wood, J. Amer. Chem. Soc. 74, 1367 (1952) and J. Phys. and Coll. Chem. 55, 1462 (1951).

24. S. J. Gregg, K. J. Hill, and T. W. Parker, "The grinding of kaolin: I. Preliminary study," J. Appl. Chem. 4, 631 (1954); see also ibid. 3, 169 (1953); ibid. 4, 666 (1954); and J. G. Miller and T. D. Oulton, "Prototropy in kaolinite during percussive grinding," Clay and Clay Minerals 18, 313 (1970).

25. W. F. Bradley, "Diagnostic criteria for clay minerals," Amer. Mineralogist 30, 704 (1945).

26. A. W. Weiss, B. R. Thielepape, W. Ritter, H. Shafer, and G. Goring, "Kaolinit-Einlagerungs-Verbindungen," Int. Clay Conf., Stockholm 1, 287 (1963).

27. See Ref. 9, p. 84, and L. Pauling, J. Am. Chem. Soc. 51, 1010 (1929).

28. H. D. Orchiston, "Adsorption of water vapor: 7. Allophane and some clay mixtures at 25°C," Soil Sci. 88, 159 (1959).

29. S. Aomine and H. Otsuka, "Surface of soil allophanic clays," International Congress of Soil Science, Adelaide, Austr., Vol. 3, p. 731 (1968).

30. See Ref. 13, p. 310-313.

31. H. D. Orchiston, "Adsorption of water vapor: II. Clays at 25°C," Soil Sci. 78, 463 (1954).

32. B. L. J. Jackson, A. Metcalfe, and R. J. Wilcock, "Adsorption hysteresis on disordered kaolinite," Trans. Faraday Soc. 67, 2137 (1971).

33. G. J. Churchman, L. P. Aldridge, and R. M. Carr, "The relationship between the hydrated and dehydrated states of an halloysite," Clay and Clay Minerals 20, 241 (1972); see also: Amer. Mineralogist 57, 914 (1972).

34. K. Wada, "A structural scheme of soil allophane," Amer. Mineralogist 52, 690 (1967).

35. R. T. Martin, "Water vapor sorption on kaolinite: Hysteresis," Clay and Clay Minerals, Sixth Conf., p. 259 (1958); see also: Eighth Conf., p. 259 (1960) and Tenth Conf., p. 133 (1962).

36. J. J. Jurinak, "The effect of pretreatment on the adsorption and desorption of water vapor by lithium and calcium kaolinite," J. Phys. Chem. 65, 1853 (1961).
37. J. L. McAtee, Jr., "Simultaneous X-ray diffraction - DTA," Clay and Clay Minerals 18, 223 (1970).
38. G. B. Mitra and S. Bhattacharjee, "X-ray diffraction studies of the transformation of kaolinite into metakaolin," Acta Cryst. B26, 2124 (1970) and references therein.
39. Von F. Freund and H. Gentsch, "Loss of H₂ during the dehydration of Mg(OH)₂, Al(OH)₃ and single crystals of kaolinite," Ber. Dtsch. Keram. Ges. 44, 51 (1967).
40. K. J. D. MacKenzie, "The effect of electric fields on the 980°C exotherm of kaolinite," Proc. Brit. Ceram. Soc. 20, 209 (1972).
41. G. W. Brindley, J. H. Sharp, J. H. Patterson, and B. N. Narahari, "Kinetics and mechanism of dehydroxylation processes: I. Temperature and pressure dependence of dehydroxylation of kaolinite," Amer. Mineralogist 52, 201 (1967); see also: Air Force Report No. AFRL-65-606.
42. H. B. Johnson and F. Kessler, "Kaolinite dehydroxylation kinetics," J. Amer. Chem. Soc. 52, 199 (1969).
43. W. Chesworth, "The residual system of chemical weathering: A model for the breakdown of silicate rocks at the surface of the Earth," J. Soil Sci. 24, 69 (1973).
44. H. D. Orchiston, "Adsorption of water vapor: III. Homoionic montmorillonites at 25°C," Soil Sci. 79, 71 (1955).
45. R. T. Johansen and H. N. Dunning, "Water vapor adsorption on clays," Clay and Clay Minerals, Sixth Conf., p. 249 (1959).
46. H. D. Orchiston, "Adsorption of water vapor: V. Homoionic illites at 25°C," Soil Sci. 87, 276 (1959).
47. D. H. Fink, C. I. Rich, and G. W. Thomas, "Determination of internal surface area, external water and amount of montmorillonite in clay-water systems," Soil Sci. 105, 71 (1968).
48. K. Norrish, "The swelling of montmorillonite," Disc. Faraday Soc. 18, 120 (1954); see also: D. H. Fink and H. Nakayama, Soil Sci. 114, 355 (1972).
49. J. de D. Lopez-Gonzalez and V. Dietz, "Surface changes in an original and activated bentonite," J. Res. NBS 48, 325 (1952).
50. N. R. O'Brien, "Fabric of kaolinite and illite flocules," Clay and Clay Minerals 19, 353 (1971).

51. G. W. Brindey and H. Ryoso, "Kinetics and mechanism of dehydration and recrystallization of serpentine I," Clay and Clay Minerals, Twelfth Conf., p. 35 (1964).
52. R. Aiello, C. Collela, and R. Sersale, "Zeolite formation from synthetic and natural glasses," in Molecular Sieve Zeolites, edited by E. M. Flanigan and L. B. Sand, Amer. Chem. Soc. (1971), p. 51.
53. F. C. Ugolini and D. M. Anderson, "Ionic migration and weathering in frozen Antarctic soils," Soil Sci. 115, 461 (1973).
54. I. R. Hughes and P. K. Foster, "The ranking of halloysites and kaolinites by moisture content measurements," N. Z. Jl. Sci. 13, 89 (1970).
55. W. D. Keller, "Environmental aspects of clay minerals," J. Sediment. Petrology 40, 788 (1970).
56. W. D. Keller, unpublished results, Geological Society of America, Dallas, November 1973.
57. H. Takahashi and Y. Kishimura, "Formation of zeolite type A from halloysite and allophane," Clay and Clay Minerals, Fourteenth Conf., p. 185 (1966).

PART III SIMULATED WEATHERING OF VOLCANIC SOIL

Vacuum microbalances are very useful as a means of studying sorptive properties.^(1,2,3) We have recently undertaken a study of the interaction of gases with lunar materials.^(4,5,6) This report is a summary of some of our efforts to assure ourselves that our results are accurate and free from systematic errors. Most of our samples are designated as "lunar fines" which are the fraction of the lunar soils which pass through 1 mm openings in a sieve screen. Optical microscopic examination reveals that the vast preponderance of the particles is in the range of 0.5 - 10 μ m. The specific surface areas of these samples range from 0.2 to 1.5 m^2/g . Sample aliquots available to us have been limited to 0.1 to 1.0 g; hence we must deal with low surface areas (0.1 to 1.0 $m^2/sample$). For those of us still acquainted with the English system of measurements, 0.1 m^2 is approximately one square foot. A nitrogen monolayer on such a surface is ca 30 μ g, which can be accurately determined with modern microbalances. However, we felt that the optimum results could be obtained only after extensive evaluation of the balance systems per se. To this end we present the following results.

Various vapors were introduced into the system with a 312 mg pellet of aluminum metal on the microbalance. Aluminum metal was chosen as a blank here to closely approximate the density (2.72 g/cc) and weight of the lunar samples. The pellet was formed from the molten metal and is free of internal area and/or excessive roughness. The results as given in Figure 1 are just what one would expect for buoyant displacement of the vapors by the suspended sample and quartz pan at -196°C. Within experimental accuracy the slopes of the lines of Figure 1 adhere to the ideal gas behavior of the gases. There is no sign of adsorption phenomena on the small amount of area (ca 0.0008 m^2). There is very little contribution due to the thermomolecular flow (TMF) effects^(2,7) in the higher pressure range. Concurrently we acquired additional data for each of these gases in the lower pressure regions (10^{-6} to 10 torr) to more accurately evaluate the TMF effects and their reproducibility. The results are entirely consistent with those reported earlier in Ref. 2.

The higher pressure data of Figure 1 are subject to the "convection"^(8,9) effects as shown in Figure 2. We find, as do others, that there is a threshold (200 to 300 torr) pressure for the appearance, and disappearance, of the "noise". The magnitude of the "noise" rises from the \pm 0.2 μ g due to the inherent electronic effects to a near-constant \pm 4-5 μ g. The threshold pressure can be increased appreciably by minimizing the amount of shock induced into the system (i.e., introducing the vapors through a small orifice). The magnitude and threshold pressure do not depend on the height of the bath above the sample (\pm 3 cm) nor on the stirring rate (nitrogen flow) of the liquid nitrogen bath. Thus we conclude that the effect is due to flow past the hangdown wire (not the sample pan) and is not due to temperature fluctuations of the

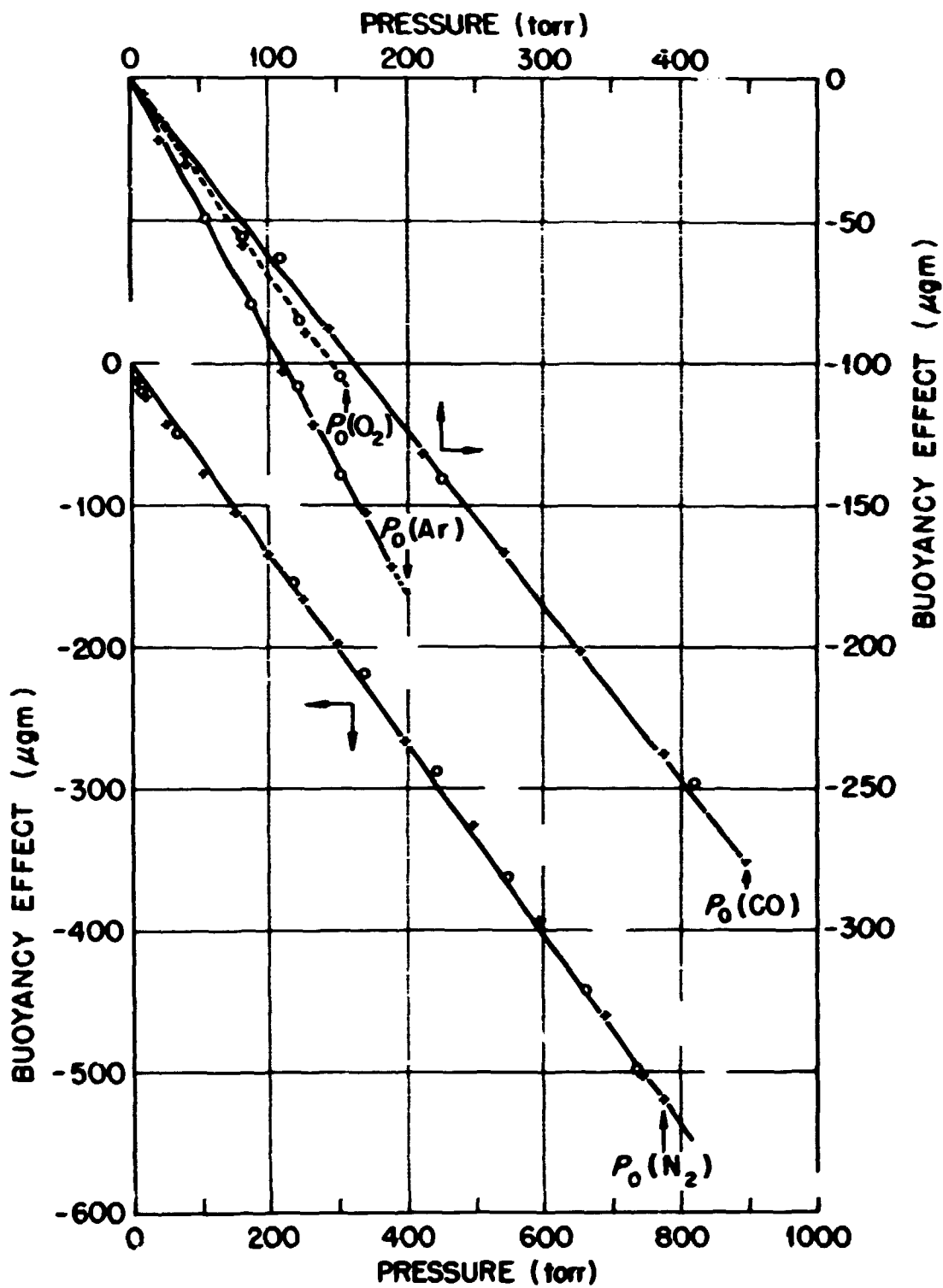


Fig. 1. Vapor displacement by aluminum billet.

bath. Closer examinations of the chart records (Figure 2) show that in the early (moderate) levels the perturbations are of a periodic nature. Helium vapor displacement (Figure 3) results show no sign of the convection effect over the entire pressure range, whereas each of the other vapors exhibit the effect at and above 200-250 torr. Furthermore the noise level shows a negative effect for each gas. This is shown in Figure 2 where the dashed lines are the nitrogen effect one would anticipate for ideal gas behavior with respect to the helium results. The most accurate representation of the buoyancy effect seems to be obtained by utilizing the uppermost data in each case. These data also lead us to conclude that these convection effects are due to an upward flow of gas past the hangdown wire at or near the temperature gradient (at or near the liquid nitrogen - air interface). The periodic momentum transfer occurs at 1-2 minute intervals with more frequent (and possibly stronger) impulses being delivered at higher pressures. The limiting case arises where the number of such impulses increases to yield a "random", saturated noise condition.

At this writing we have chosen to use the upper (heavier) peak noise level as truly representative of the apparent mass of the sample. We would surely alter the TMF calibration curves if we were to install a restricted tubulation at the liquid nitrogen - air interface as was reported in Ref. 10. The other alternative means of eliminating the effect is to use a symmetrical system where the tare pan and weight are also at -196°C (liquid nitrogen bath).⁽¹¹⁾ This method ostensibly decreases the magnitude of the TMF effect and may be utilized in the future.

These studies with the aluminum pellet have shown conclusively that the microbalance system is capable of acquiring excellent sorption data. There does not seem to be any appreciable sorption by the balance system per se and there are no detectable hydrostatic effects due to stress or strain in the mounting system. Furthermore there is very good "zero" stability in both the long and short term as sensed by virtually no apparent mass change (at given temperature and pressure) over a time span of several months.

In addition, we feel that we have shown that one can evaluate the buoyancy effect using a non-reactive vapor and the specific sorbate of interest. To this end we present the data of Figure 3 and 4 as being exemplary. The helium does not interact with the samples as noted in the linearity and "zero intercept" of the data.

This technique of in situ determination avoids several complications. Lunar materials are mixtures of minerals (i.e., glass, iron, plagioclase, pyroxene, olivine, etc.). Independent determinations⁽²⁾ of densities have been made on many of the samples, usually by the liquid density gradient method. We hope we can avoid problems associated with variations in aliquots of a given sample and/or discrepancies due to the media used to evaluate the density. The use of an independently determined density in estimating buoyancy effects must be supplemented by in situ determinations of buoyancy effects due to asymmetric beam

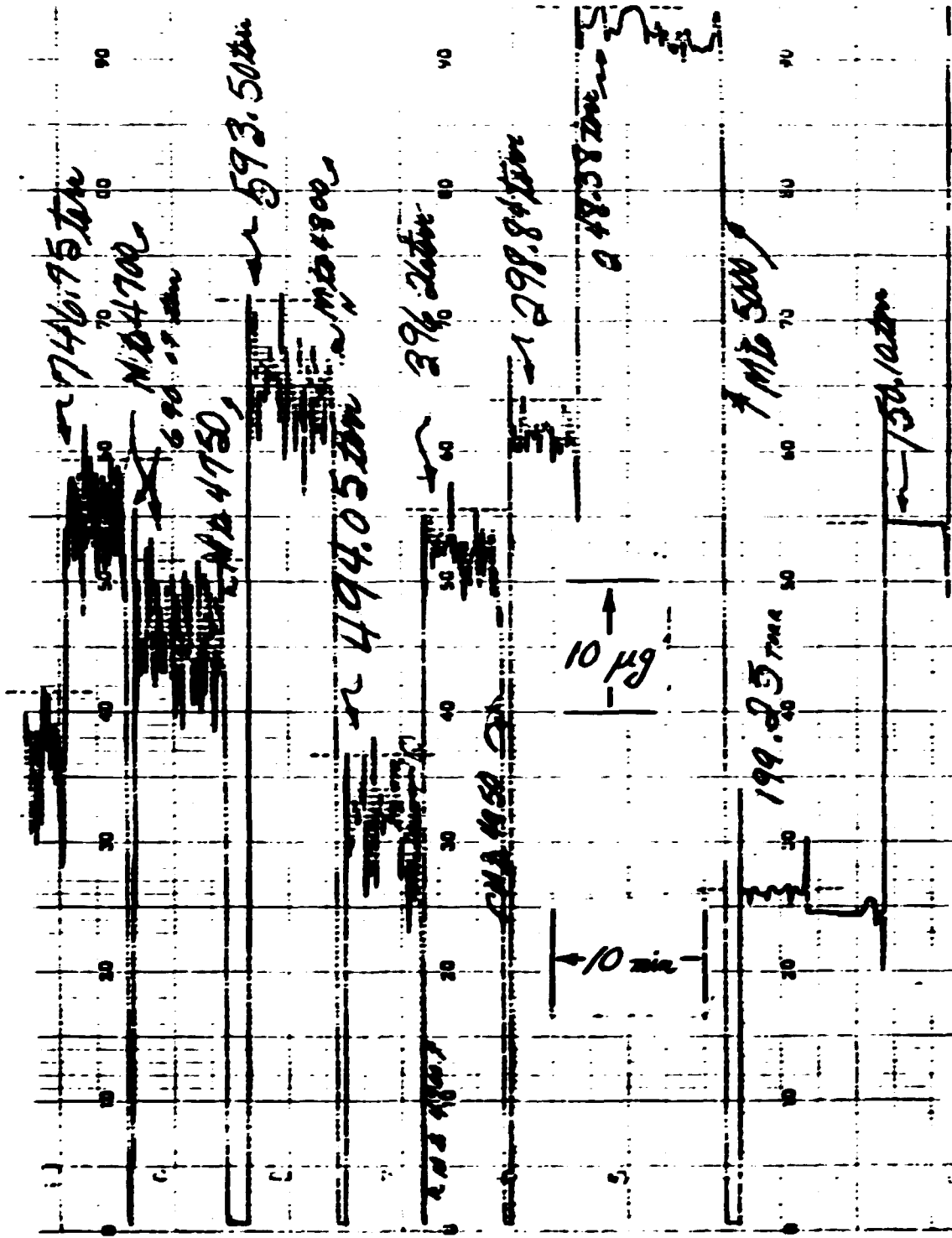


Fig. 2. Nitrogen on aluminum pellet.

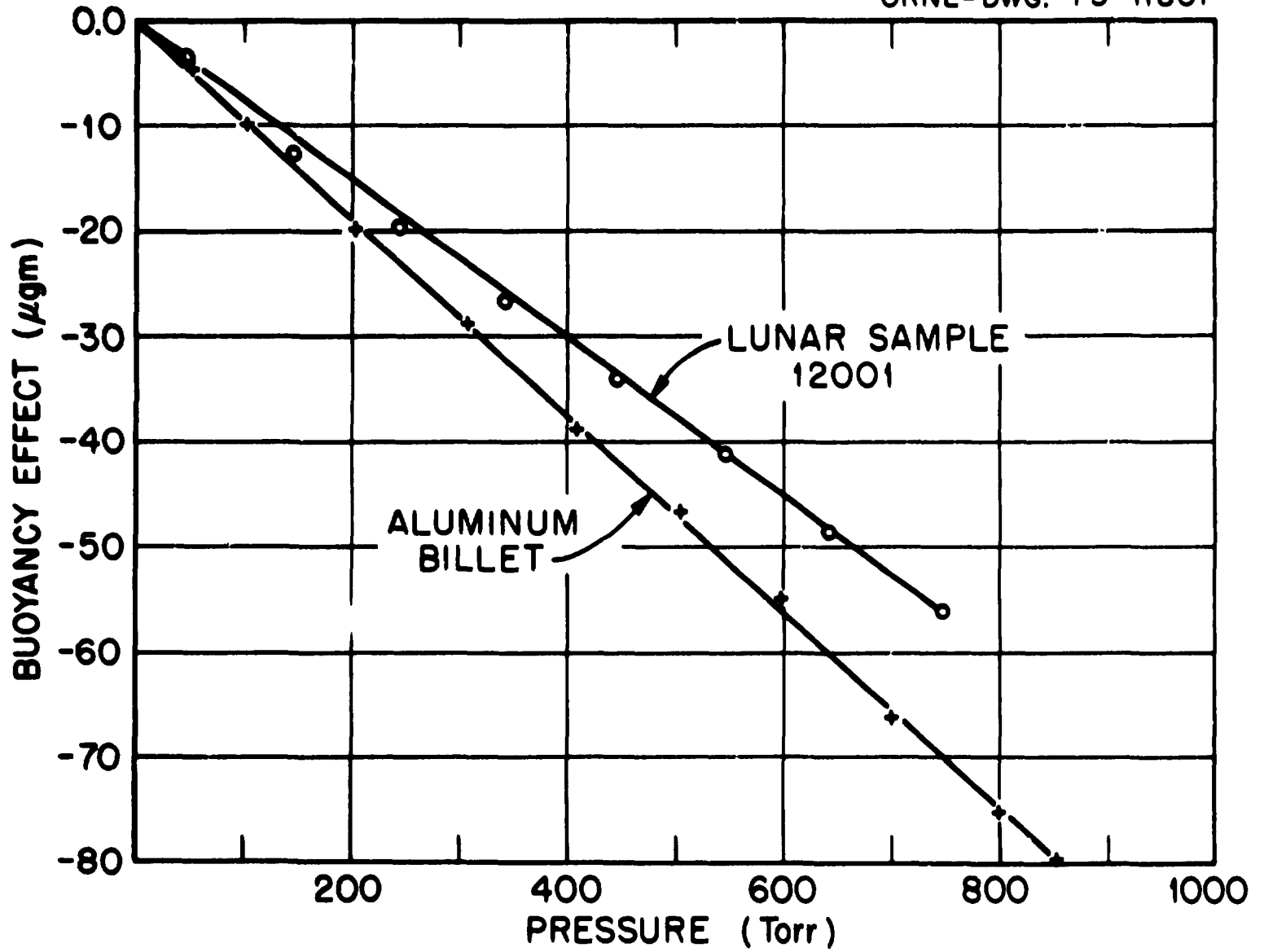


Fig. 3. Helium displacement.

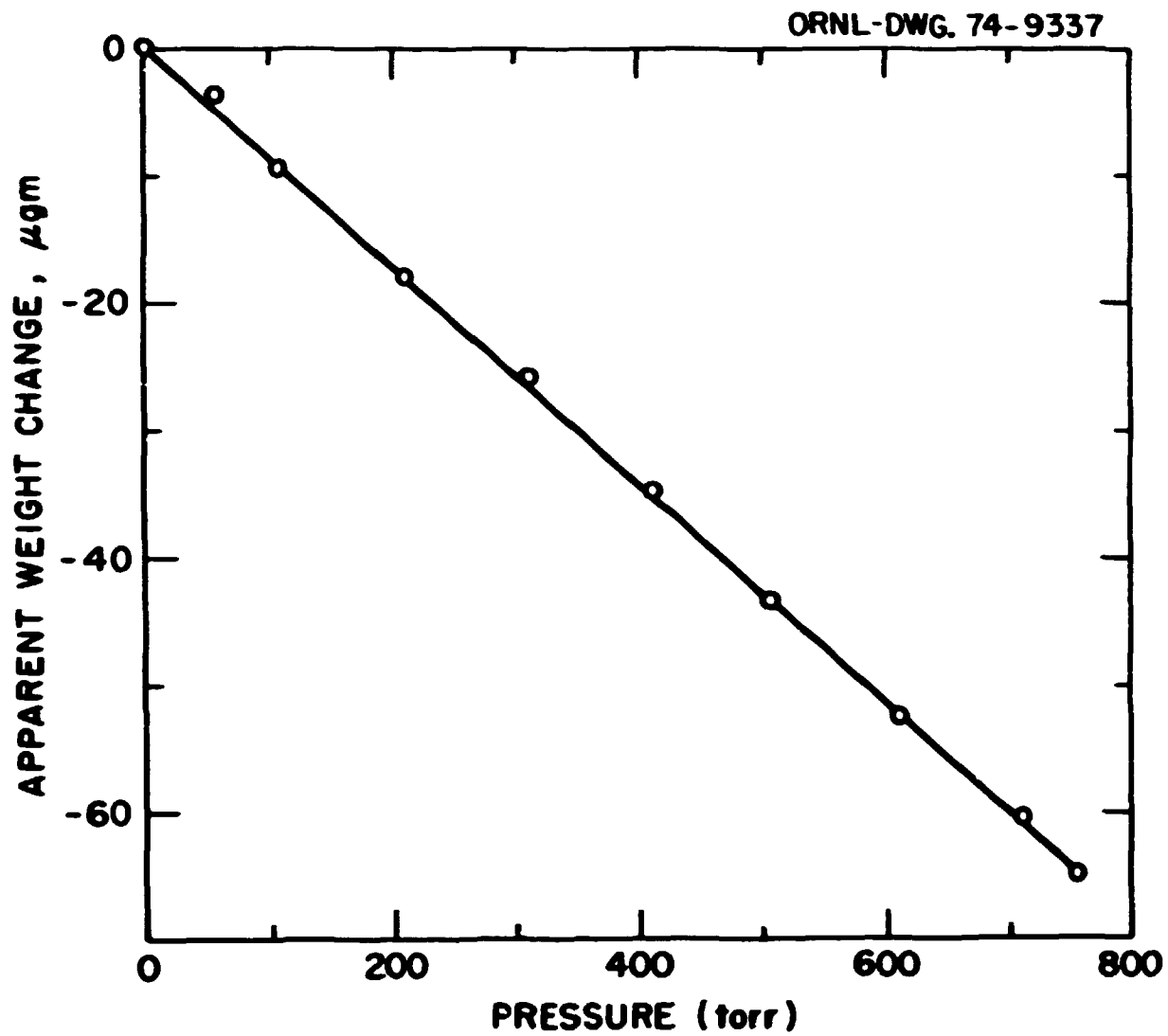


Fig. 4. Helium on BSG33 at -196°C .

effects and effects due to sample pan, tare pan and tare weights. The direct method outlined here simplifies the procedure and assures us of equal or better accuracy.

Figure 5 is characteristic of the results we obtain. Progressing chronologically, we see the precision with which the apparent mass is determined both without and with the convection noise. The dashed lines are the calculated mass change (from the preceding steady state) due to buoyancy effects alone for each pressure increment (based on helium data). We see that 5 to 10 minutes are adequate to dissipate the heat released in the exothermic sorption process. Furthermore the crude extrapolation of the sorption curves to "zero" time is entirely consistent, albeit less accurate, with the helium data. Here again we see the merit of using the maximum of the "noise" band in the convective region. If a mean value had been chosen (either visually, electronically, or statistically) we would conclude that there is little, if any, sorptive increments in this pressure region. The 5X scale expansion is presented here to show that electronic damping was not (nor should not) be employed to decrease the "noise" level. Such action often, in the extreme cases, shows spurious negative adsorption with respect to the buoyancy effect.

Figure 6 is a presentation of characteristic results. The sample we designate as BSG33 was employed as a terrestrial analog of the lunar fines. It is a mixture of minerals (plagioclase, olivine, etc.) obtained initially from the "Black Sand Beach" of Hawaii. The original material was washed extensively with distilled water and then subjected to extensive percussive grinding. We note that nitrogen sorption occurs. The initial marked uptake of monolayer formation at lower pressures approaches the somewhat linear behavior at intermediate pressures. The high pressure "hook" is due to extensive multilayer adsorption. Appreciable hysteresis is noted on desorption due to condensation in restricted capillaries. When the appropriate buoyancy and TMF corrections are applied to the data of Figure 6, we obtain the sorption isotherms as presented in Figure 7.

Several features of the isotherms of Figure 7 are informative. The original sample has a low surface area (BET analysis) as shown by the mark at ca $0.09 P_0$ corresponding to $0.59_2 \text{ m}^2/\text{g}$. The classical sigmoidal shape is characteristic of monolayer-multilayer formation culminating in asymptotic sorption at saturation. Water adsorbs on and reacts with this sample to increase the apparent monolayer and alter the hysteretic behavior with a shift to lower pressures (smaller capillaries?). Removal of bound species by outgassing enhances the sorptive capacity over the entire pressure range (see curve C). The emptying/filling process is reversible to the extent that the hydration/dehydration cycles of B through E are noted. The second hydration shows some further reaction to show that an over-all twofold enhancement in the uptake in the monolayer region (curve E with respect to A). A summary of the results is given in Figure 8. Concurrent with the monolayer enhancement is the enhanced hysteresis. A crude measure of the hysteretic retention is obtained by measuring the maximum disparity between the desorption and

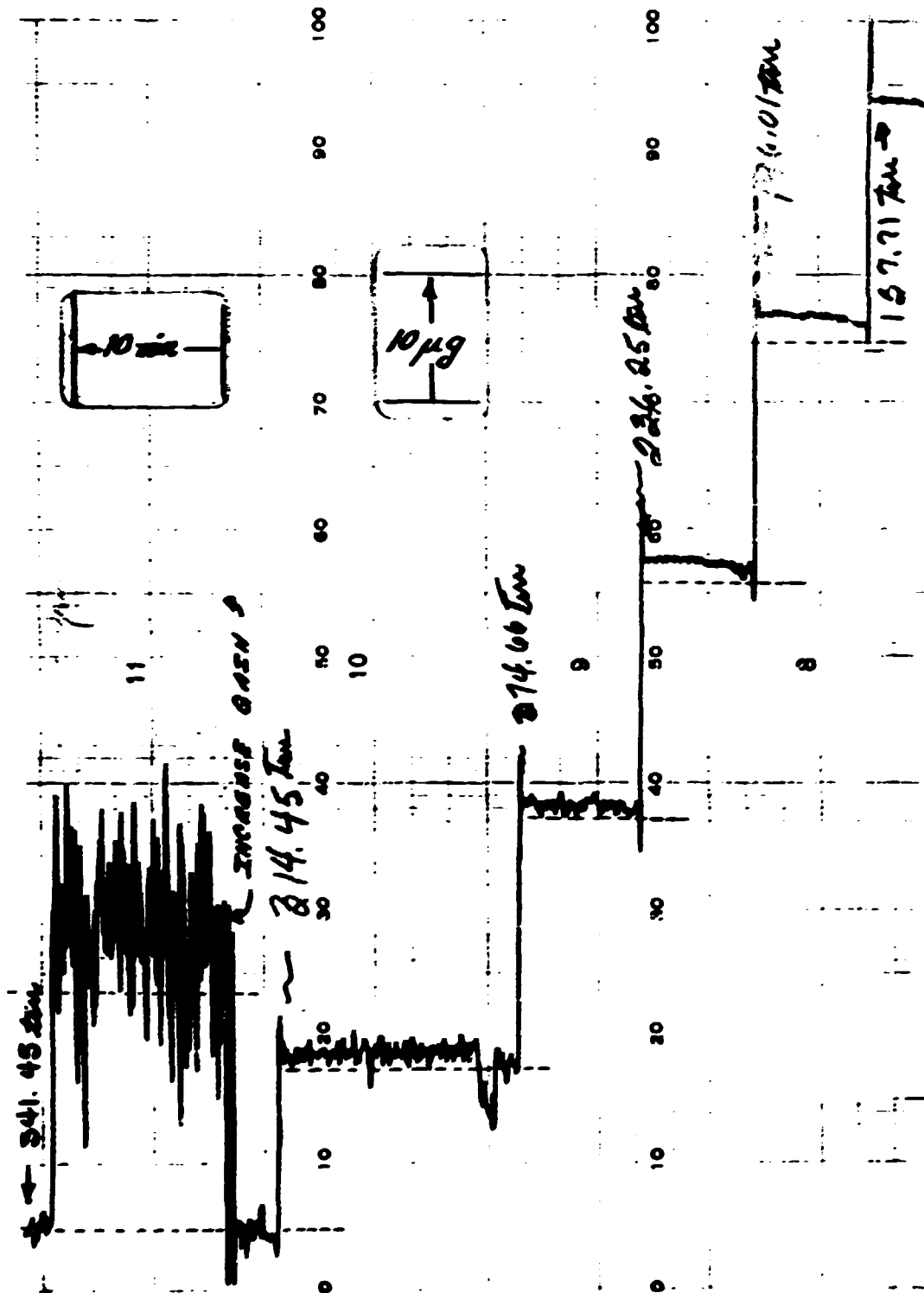


Fig. 5. Nitrogen vapor on 63321 at -196°C .

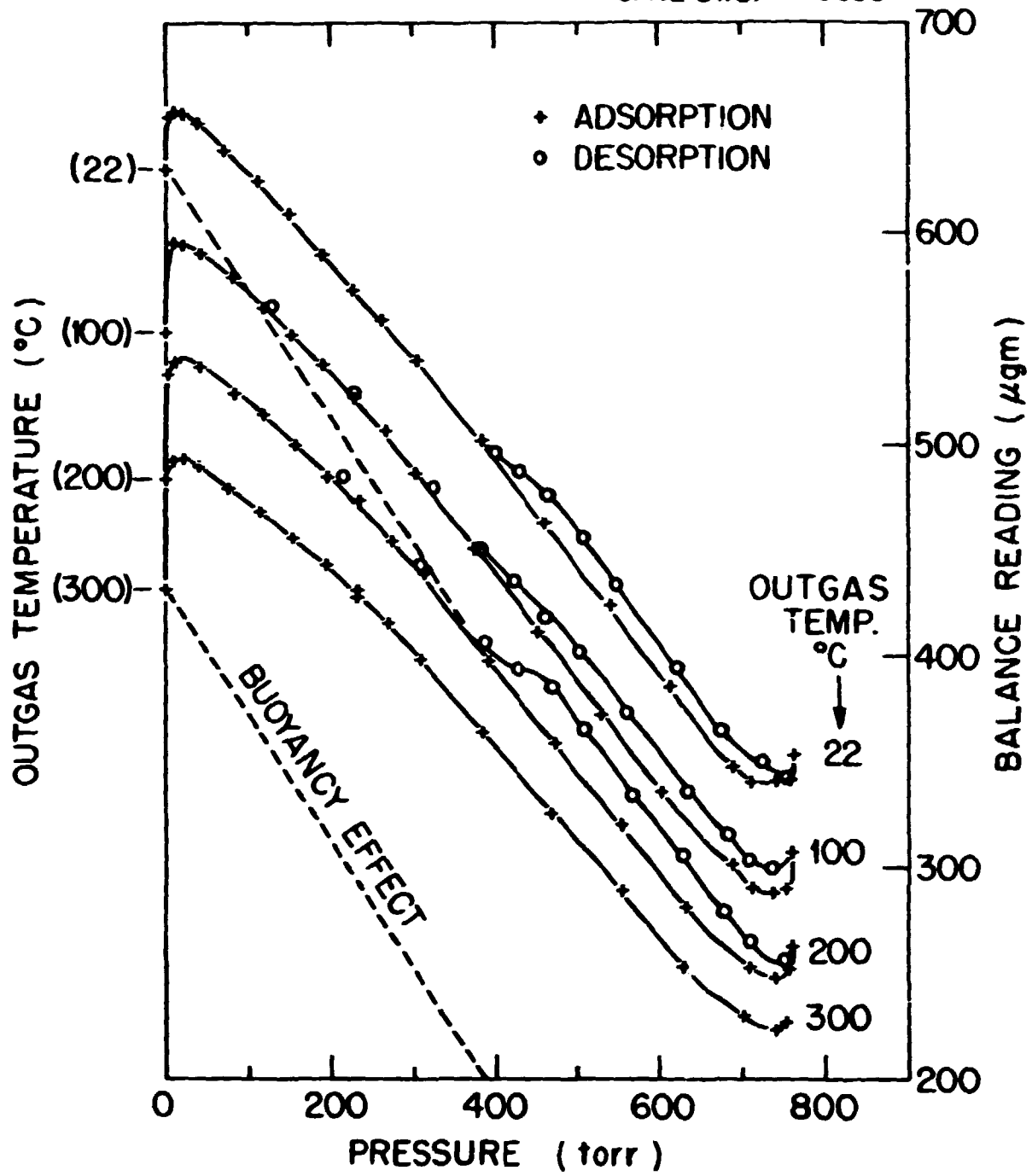


Fig. 6. Nitrogen interaction with BSG33 at -196°C (after H_2O).

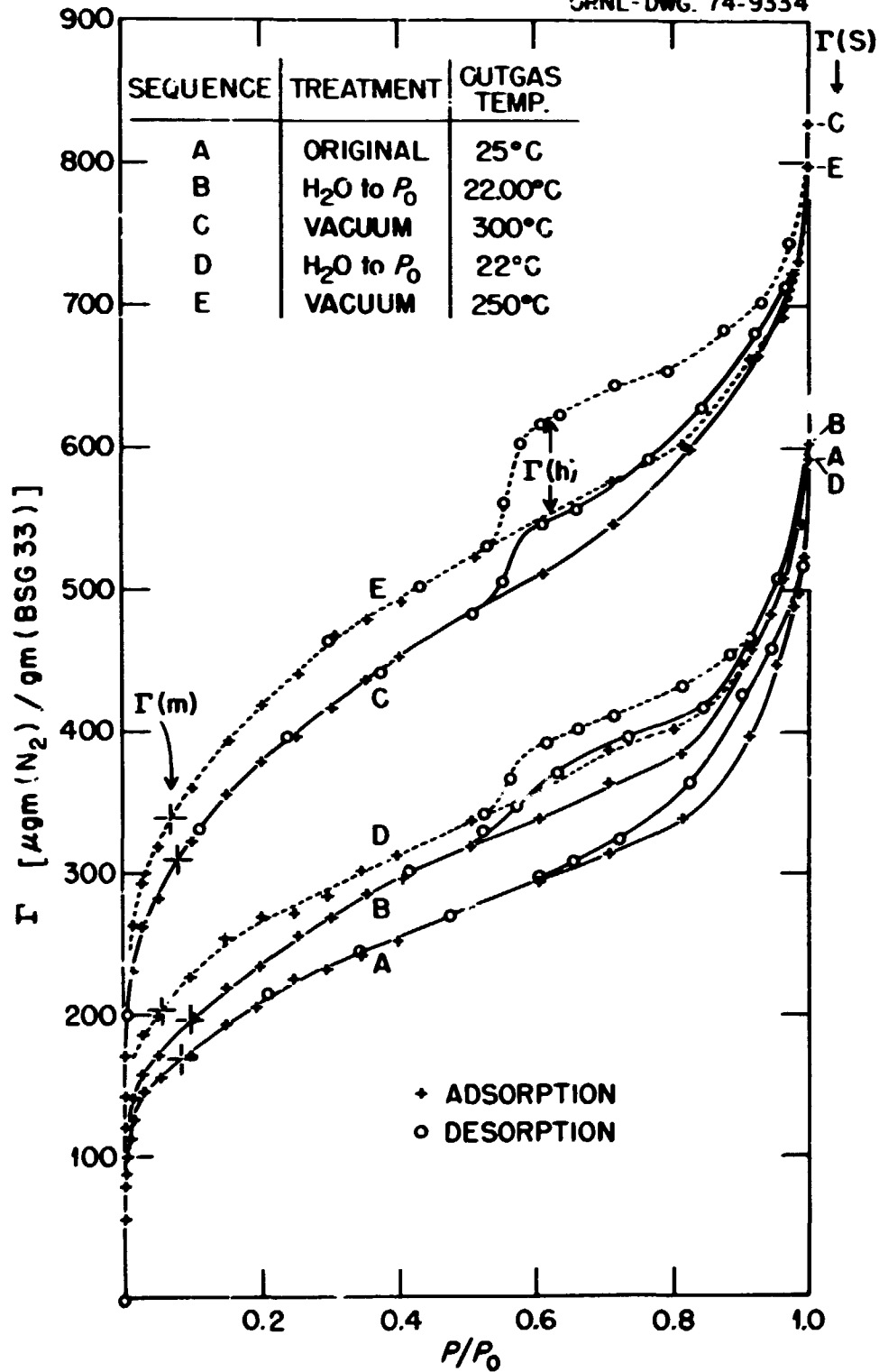


Fig. 7. Nitrogen sorption by BSG33 at -196°C .

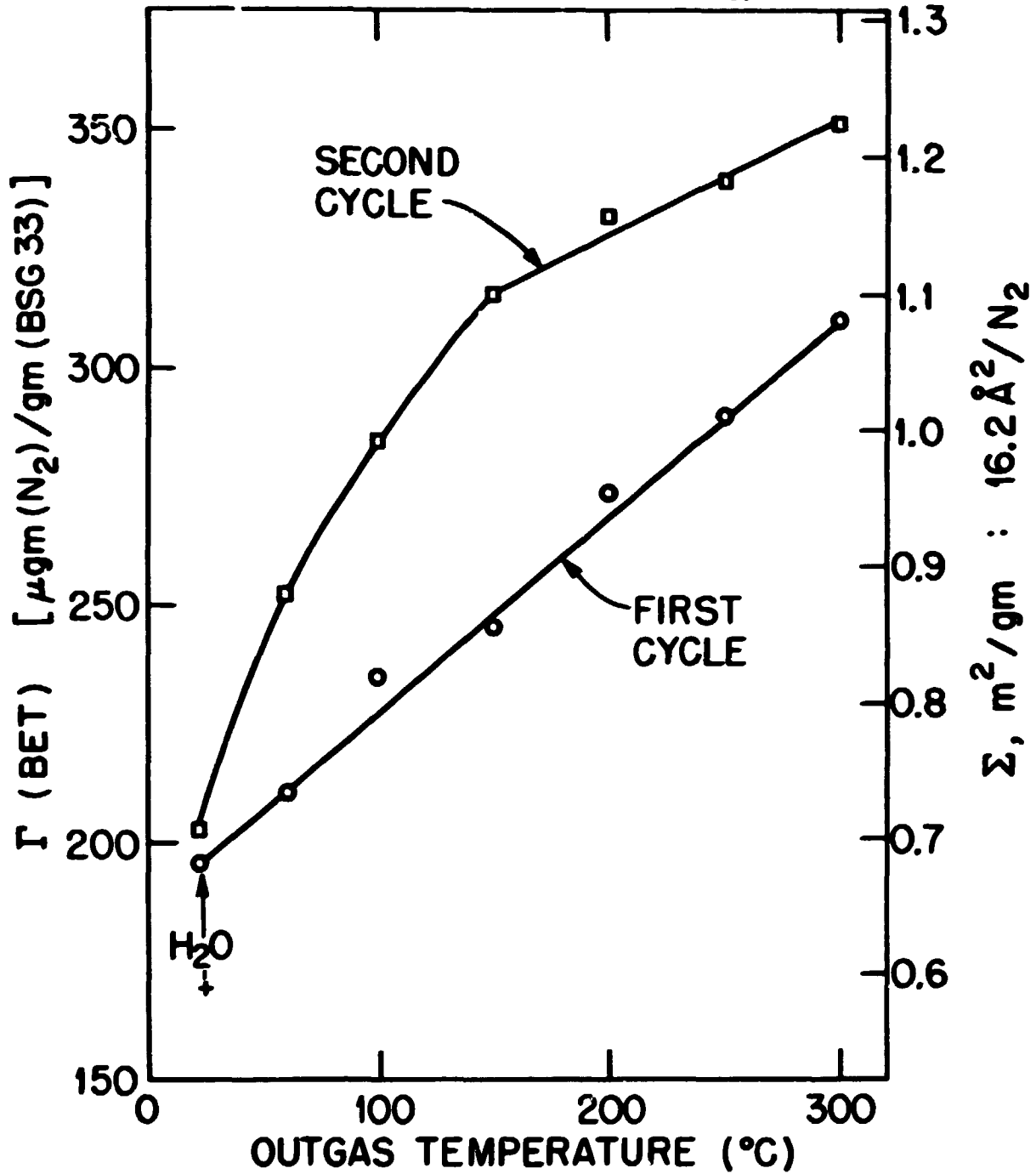


Fig. 8. Nitrogen adsorption on BSG33 at -196°C .

adsorption branches. In general, this maximum prevails at ca $0.6 P_0$ (except for the original material, A). Hysteresis generally is associated with pores whose openings are equal to or less than the internal dimensions. The absence of hysteresis can assuredly be taken to mean the absence of such "internal" surface. Thus we see that our data is consistent with the existence of an external surface adsorbing ca $136 \mu\text{g } (N_2)/\text{g}(\text{BSG33})$ for the apparent monolayer capacity $[\Gamma (\text{BET}) \text{ or } \Gamma (m, N_2)]$. The general linear relation of the hysteretic capacity $[\Gamma (h, N_2)]$ is depicted in Figure 9 with respect to the corresponding $\Gamma (m, N_2)$.

The high pressure ($0.9-1.0 P_0$) regions of the nitrogen isotherms are worth of note. As in Figure 7, our data show the classical behavior of the asymptotic approach to "infinite uptake" at saturation pressure. This is in contrast to the work of others⁽¹¹⁾ who find the microbalance sorption to be less than that observed for the volumetric technique and their anticipation of finite slope at $P/P_0 = 1$. Our data do seem to indicate that there is finite sorption at our measured $P/P_0 = 1$. We note that there is a virtually infinite slope on the isotherms as we approach P_0 . Incremental doses of nitrogen show apparent mass increases as P is increased above P_0 . However, this is a transient effect and is most probably due to mass flow downward past the sample and wire as the excess nitrogen condenses on the walls of the hangdown tube. Additional doses of nitrogen (corresponding to ca $0.02 P_0$ for each) lead to the transient excursion and return to the same sample weight. If indeed the sample is warmed appreciably by radiative transfer from the ca 298°C upper regions, the amount of heat (and hence the sample temperature) should depend on the solid angle of incidence. When we lower the bath 5-6 cm the solid angle due to the circular opening at the liquid bath surface approximately doubles. Such an operation has no effect on the saturation uptake $[\Gamma (S, N_2)]$. An interesting correlation evolves when we consider the relationship of $\Gamma (S, N_2)$ to the corresponding internal area $\{\Gamma (m, N_2) - 136.5\}$ as shown in Figure 10.

The versatility of the microbalance is further noted as one considers the additional data obtained in the outgassing experiments. More stringent (higher temperature) outgassing leads to further loss of bound species from the sample as seen in Figure 11. This data represents steady state conditions attained after about 4-6 hours at the given temperature (and verified by 16 to 96 hours) at ca 10^{-6} torr. The enhanced nitrogen sorption for more complete outgassing (Figure 8) is related directly to the amount of bound species as shown in Figure 12.

At this point it is interesting to examine the water vapor sorption isotherms. The techniques and corrections applied to this data have been described earlier.⁽²⁾ Experiments with the aluminum pellet showed that the previous background correction curves⁽²⁾ are still valid. Figure 13 is characteristic of the results obtained for the BSG33 sample. In general the incremental mass changes for each pressure increment

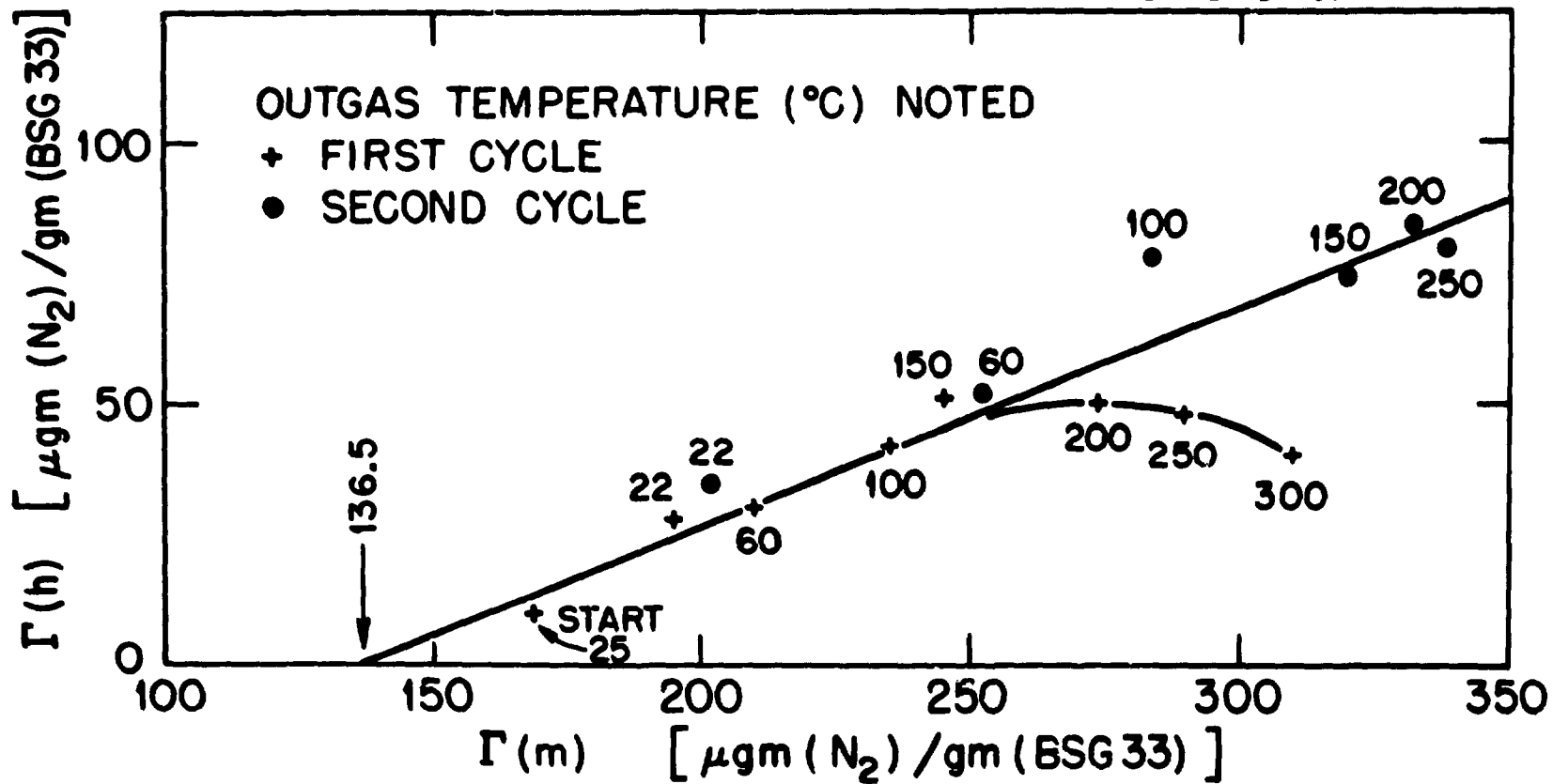


Fig. 9. Nitrogen sorption by BSG33.

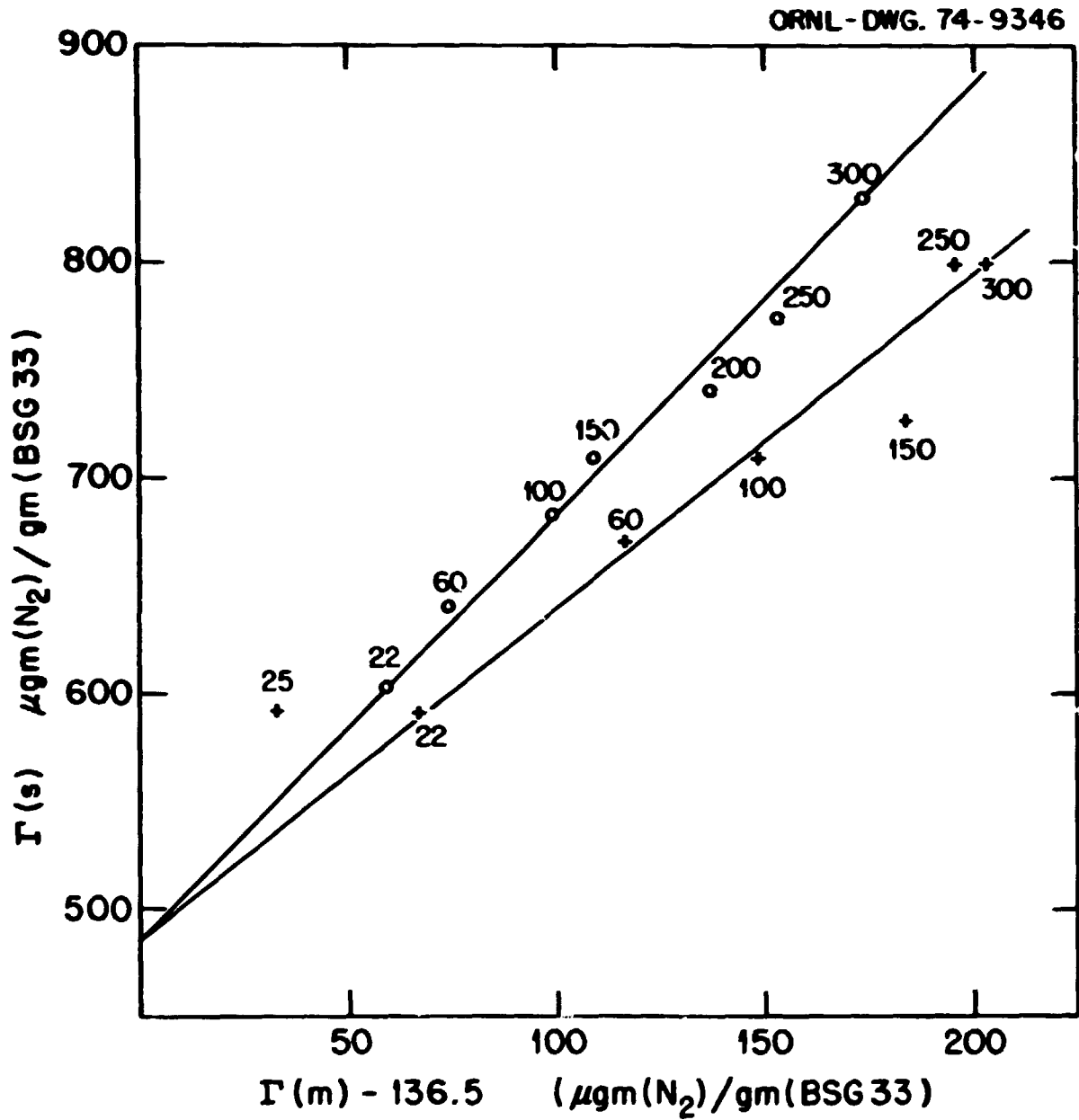


Fig. 10. Nitrogen sorption on BSG33.

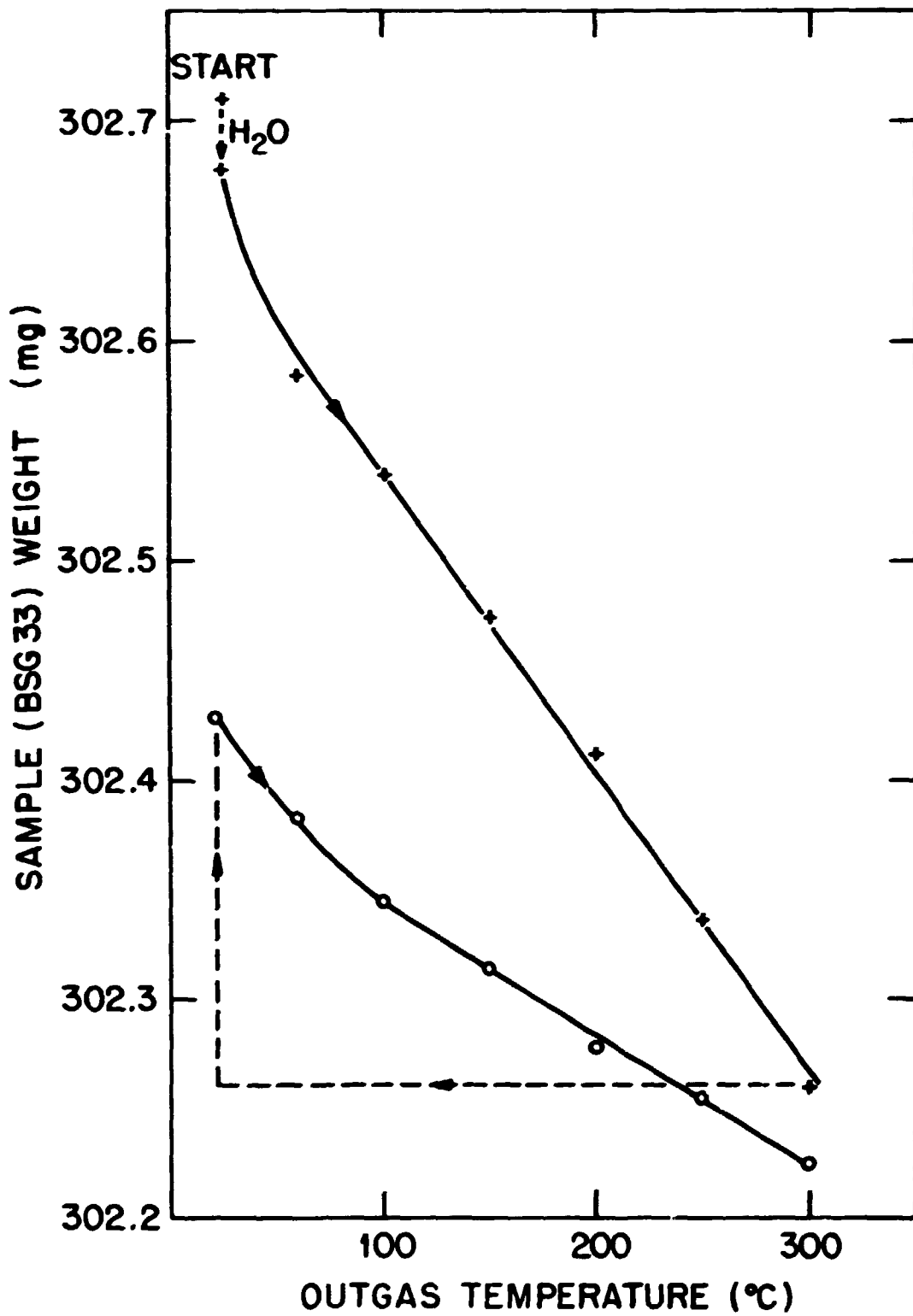


Fig. 11. Steady state vacuum weight of PGG 33.

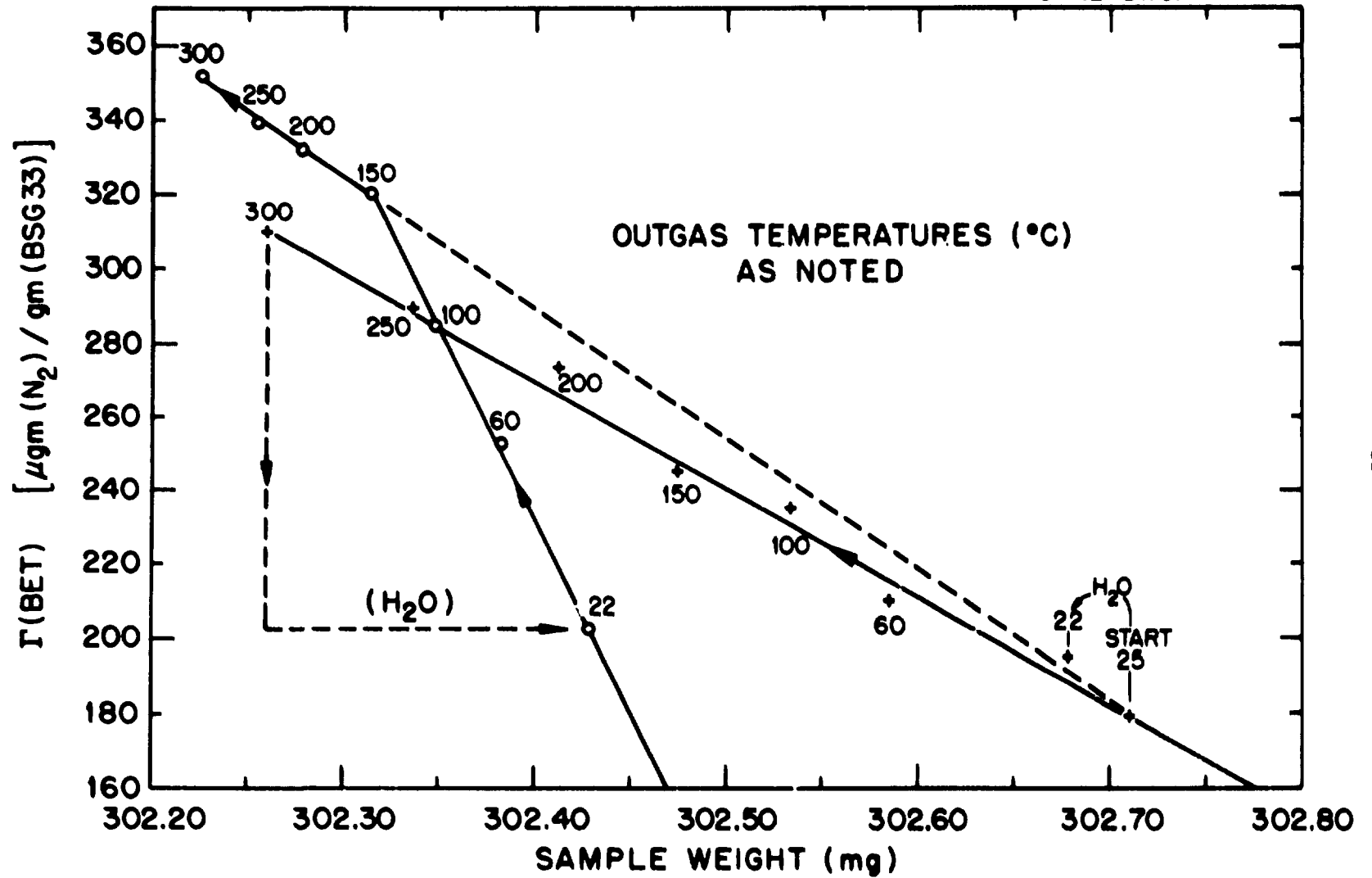


Fig. 12. Sorptive properties of BSG33.

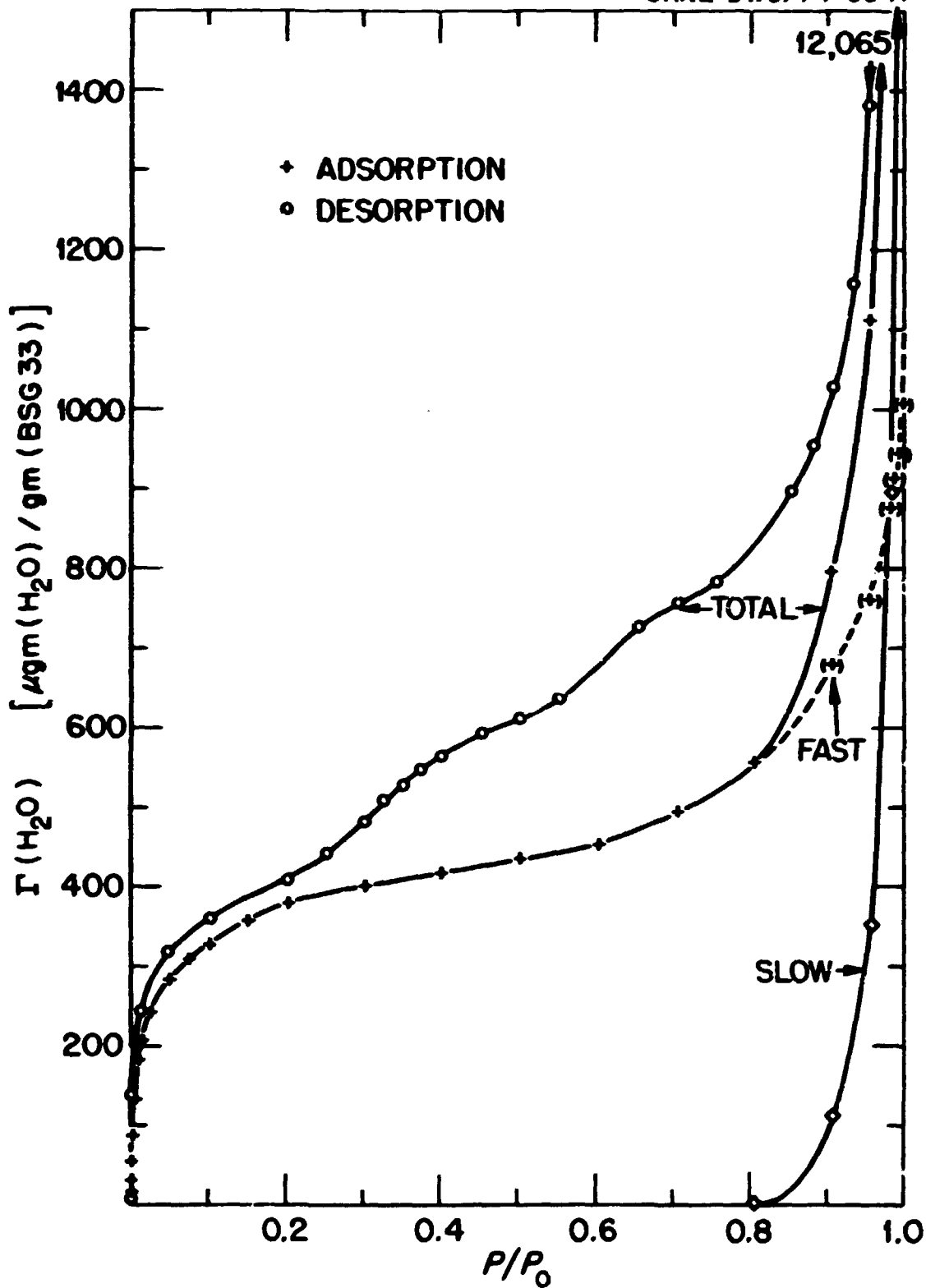


Fig. 13. H_2O (No. 11) on BSG33 at 22.00°C.

were complete in 3 to 5 minutes. Here again the steady state condition was verified by 16-96 hours at fixed pressure (± 0.005 torr or $\pm 2.5 \times 10^{-5} P_0$) and temperature ($\pm 0.001^\circ\text{C}$). In the course of construction of the adsorption isotherm, this rapid equilibration prevailed until the pressure reached that corresponding to ca $0.9 P_0$ whereupon more and more time was required to achieve steady state conditions. These latter states were achieved by first order kinetics, where the rate of approach to steady state depends inversely on the amount mass deficit below the steady state mass. The kinetic behavior is depicted in Figure 14 for the annotated pressure changes. The total mass involved in these slow processes is noted in the "zero time" intercepts of each of the lines. The cumulative effect of these slow processes is depicted in Figure 13. When the slow component is deducted from the steady state conditions we are able to construct the isotherm for the amount of adsorption for the "fast" states (external surface?).

The first order rate constants (proportional to the slopes of the lines of Figure 14) show marked decrease for increasing pressure as noted in Figure 15. Here we see that there are two phenomena involved which must be considered in data acquisition. Not only does the amount of adsorption increase rapidly with pressure, but the rate of achieving steady state conditions also becomes ever more slow.

Desorption of water from these hydrated states shows a marked hysteresis in the capillary condensation (0.3 to $1.0 P_0$) region. Also there is an appreciable amount of desorptive excess in the monolayer ($0.0 P_0$ to $0.2 P_0$) region and vacuum retention (10^{-6} torr). This vacuum retention (bound) component is the material involved in the nitrogen exclusion described previously.

Much of the aforementioned results point out the striking changes wrought by the reaction with water vapor. The question of the absolute accuracy of such data can best be answered by independent measurements on a specific sample in a specific state (degree of hydration). To this end we have volumetric krypton adsorption data⁽¹³⁾ for the following lunar samples:

Sample	Specific Surface Area (m^2/g)	
	N_2 , Gravimetric	Kr, Volumetric
10087	1.15	1.16
12001	0.33	0.37
12070	0.56	0.55

Such correlations assure us that the nitrogen data are quite accurate, at least in the region of ca $0.05 P_0$ to $0.35 P_0$, with respect to similar materials.⁽¹⁴⁾ The water vapor sorption generally is interpretable in terms of micropore and capillary condensation perturbations as shown in Reference 4.

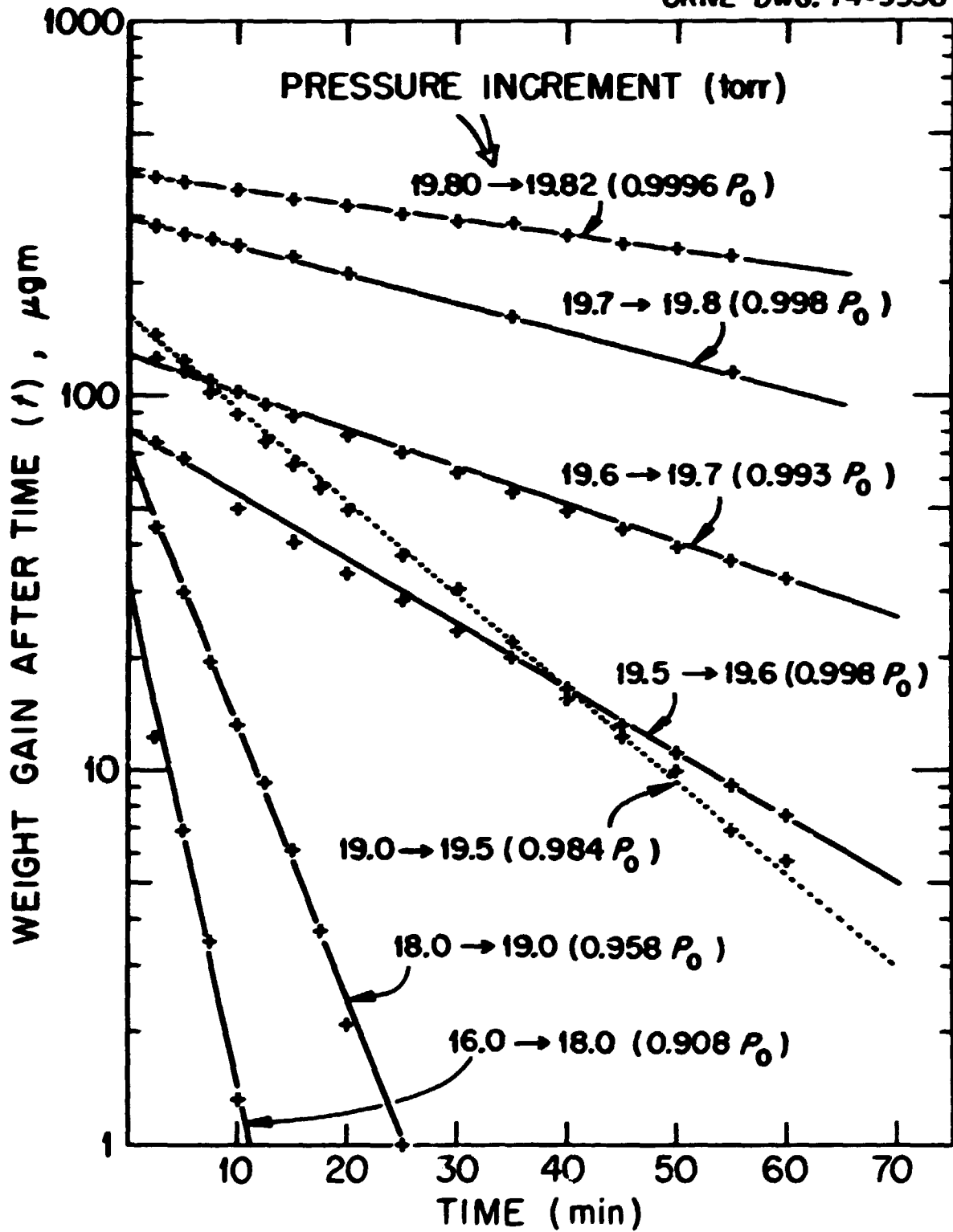


Fig. 14. Slow sorption of H_2O by BSG33 at 22.00°C .

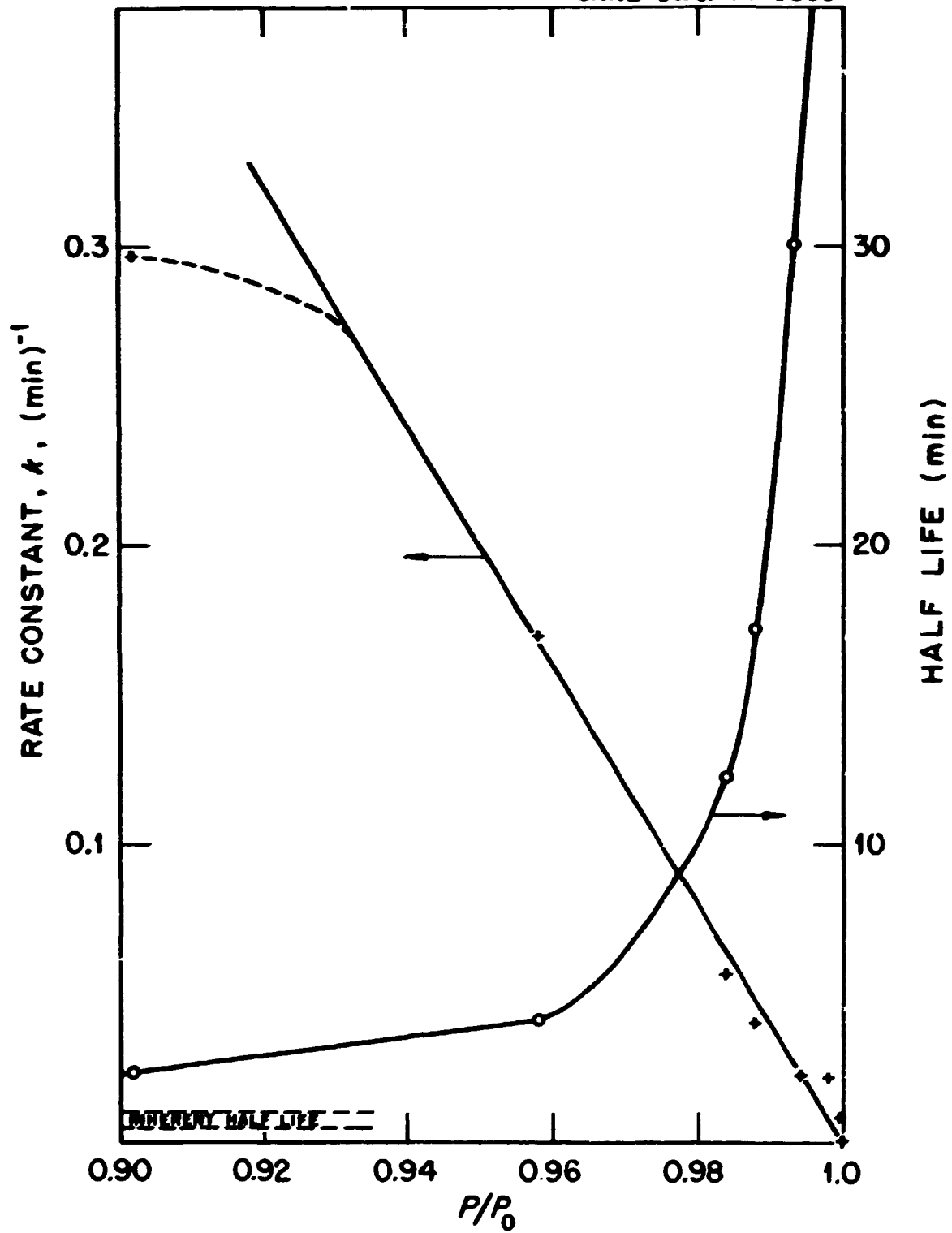


Fig. 15. Kinetic parameters for water sorption on BSG33.

REFERENCES

1. A. W. Czanderna, in Ultra Micro Weight Determination in Controlled Environments, S. P. Wolsky and E. J. Zdanuk, editors, Interscience Publishers, New York, 1969, p. 399.
2. E. L. Fuller, Jr., H. F. Holmes and C. H. Secoy, Vacuum Microbalance Tech. 4, 109 (1964).
3. E. L. Fuller, Jr., H. F. Holmes and R. B. Gamage, Progress in Vacuum Microbalance Techniques, Vol. 1, T. Gast and E. Robens, editors, Heyden and Sons, London, 1972, p. 265.
4. E. L. Fuller, Jr., H. F. Holmes, R. B. Gamage, and K. Becker, Proceedings of the Second Lunar Science Conference (Suppl. 2 Geochim. Cosmochim. Acta), Vol. 3, The M.I.T. Press, 1971, p. 2009.
5. H. F. Holmes, E. L. Fuller, Jr., and R. B. Gamage, Proceedings of the Fourth Lunar Science Conference (Suppl. 4, Geochim. Cosmochim. Acta), Vol. 3, 1974, p. 2413.
6. R. B. Gamage, H. F. Holmes, E. L. Fuller, Jr., and D. R. Glasson, J. Colloid and Interface Sci. 47, 350 (1974).
7. C. H. Massen, B. Pelupessy, J. M. Thomas and J. A. Poulis, Vac. Microbal. Tech. 5, 1 (1966).
8. A. W. Czanderna, Ultramicro Weight Determination in Controlled Environments, S. P. Wolsky and E. J. Zdanuk, editors, Interscience, 1969, p. 41.
9. E. Robens, G. Sandstede, G. Walter, and G. Wurzbacher, Vac. Microbal. Tech. 7, 195 (1970).
10. H. P. Boehm and R. Sappak, Prog. Vac. Microbal. Tech. 1, 247 (1972).
11. A. W. Czanderna, personal communication.
12. F. A. Cutting, Vac. Microbal. Tech. 7, 71 (1974).
13. W. R. Laing et al., Analytical Chemistry Division, Oak Ridge National Laboratory.
14. S. J. Gregg and K. S. W. Sing, Adsorption, Surface Area and Porosity, Academic Press, 1967.

ACKNOWLEDGEMENTS

The author is deeply indebted to several people for assistance in this work: H. F. Holmes and R. B. Gamage who served as principle investigator and coinvestigator, respectively, for the program during the period of NASA funding; P. A. Agron, G. D. Brunton, and T. Tamura of ORNL whose helpful suggestions were invaluable; W. D. Keller of the University of Missouri for learned discussions pertaining to the geochemical facets of the problem; and the administration of the ORNL Chemistry Division for establishing an atmosphere conducive to exploratory research.